

ความแตกต่างของอินฟราเรดสเปกตรัมของพอลิเมอร์ผสมของ

พอลิสไตรีนโคอะครีโลไนไตรล์และพอลิเมทิลเมทาครีเลต

ในสภาวะที่เข้ากันได้และในสภาวะแยกเฟส



นาย สงเคราะห์ ผาสุนิรันต์

วิทยานิพนธ์นี้เป็นส่วนหนึ่งของการศึกษาตามหลักสูตรปริญญาวิศวกรรมศาสตรมหาบัณฑิต

สาขาวิชาวิศวกรรมเคมี ภาควิชาวิศวกรรมเคมี

คณะวิศวกรรมศาสตร์ จุฬาลงกรณ์มหาวิทยาลัย

ปีการศึกษา 2545

ISBN 974-17-2162-5

ลิขสิทธิ์ของจุฬาลงกรณ์มหาวิทยาลัย

DIFFERENCES IN FTIR SPECTRUM OF MISCIBLE AND PHASE
SEPARATED POLYMER BLEND OF POLYSTYRENE ACRYLONITRILE
COPOLYMER(SAN) AND POLY(METHYL METHACRYLATE) (PMMA)



Mr. Songkroh Pasuknirant

A Thesis Submitted in Partial Fulfillment of the Requirements
for the Degree of Master of Engineering in Chemical Engineering

Department of Chemical Engineering

Faculty of Engineering

Chulalongkorn University

Academic Year 2002

ISBN 974-17-2162-5

Thesis Title DIFFERENCES IN FTIR SPECTRUM OF MISCIBLE AND
 PHASE SEPARATED POLYMER BLEND OF POLYSTYRENE
 ACRYLONITRILE COPOLYMER (SAN) AND POLY (METHYL
 METHACRYLATE) (PMMA)

By Mr. Songkroh Pasuknirant

Field of Study Chemical Engineering

Thesis Advisor Assistant Professor M.L. Supakanok Thongyai, Ph.D.

Accepted by the Faculty of Engineering, Chulalongkorn University in Partial
Fulfillment of the Requirements for the Master's Degree

-----Dean of Faculty of Engineering
(Professor Somsak Panyakeow, D.Eng.)

THESIS COMMITTEE

-----Chairman
(Professor Piyasan Prasertdam, Dr. Ing)

-----Thesis Advisor
(Assistant Professor M.L. Supakanok Thongyai, Ph.D.)

-----Member
(Assistant Professor Seeroong Prichanont, Ph.D.)

-----Member
(Wit Soontaranun, Ph.D.)

สงเคราะห์ ผาสุขนิรันดร์ : ความแตกต่างของอินฟราเรดสเปกตรัมของพอลิเมอร์ผสมของ พอลิสไตรีนโคอะคริโลไนไตรล์และพอลิเมทิลเมทาคริเลตในสภาวะที่เข้ากันได้และใน สภาวะแยกเฟส (Differences in FTIR spectrum of miscible and phase separated polymer blend of polystyrene acrylonitrile copolymer (SAN) and poly(methy methacrylate) (PMMA). อ. ที่ปรึกษา: ผศ.ดร.มล. ศุภกนก ทองใหญ่, 136 หน้า. ISBN 974-17-2162-5

งานวิจัยนี้เกี่ยวข้องกับการศึกษาวิธีการเตรียมตัวอย่างที่เหมาะสมสำหรับการวิเคราะห์เชิงปริมาณ (Quantitative Analysis) การศึกษาผลของการแยกเฟส (phase separation) และการทำนายสัดส่วนของการผสมของพอลิเมอร์ผสมที่ไม่ทราบความเข้มข้นระหว่างโคพอลิเมอร์ของสไตรีนและอะคริโลไนไตรล์ (SAN) และ พอลิเมทิลเมทาคริเลต (PMMA) ที่อัตราส่วนโดยน้ำหนักของ SAN เท่ากับ 30, 40, 50, 60, 70, 80, 90% โดย เครื่องฟูรีเยร์ ทรานสฟอร์มอินฟราเรดสเปกโตรมิเตอร์ (FTIR) พอลิเมอร์ผสมของ SAN และ PMMA ถูกเตรียม โดยวิธีหลอมเหลวด้วยความร้อน (melt Mixing) ในส่วนของการศึกษาวิธีการเตรียมตัวอย่างที่เหมาะสมสำหรับการ วิเคราะห์เชิงปริมาณโดยใช้ FTIR พบว่าการเตรียมตัวอย่างเป็นแผ่นฟิล์มเป็นวิธีที่เหมาะสมที่สุด เนื่องจากไม่มี ปัญหาด้านการกระจายตัวของตัวอย่าง และการดูดซับน้ำในอากาศ

ในส่วนของการศึกษาผลของการแยกเฟสของพอลิเมอร์ผสมของ SAN และ PMMA พบว่า อินฟราเรดสเปกตรัม ของพอลิเมอร์ผสมของ SAN และ PMMA ที่เป็นเนื้อเดียวกัน (Miscible) และ ที่เกิดการ แยกเฟส (phase separation) พบว่าพีคคาร์บอนิล (Carbonyl Peak) ของ PMMA ที่เลขคลื่น(Wavenumber) 1732 cm^{-1} ของพอลิเมอร์ผสมที่เป็นเนื้อเดียวกัน และที่เกิดการแยกเฟส ประกอบขึ้นจากห้าพีคย่อยที่เลขคลื่น $1720, 1726, 1732, 1738$ และ 1747 cm^{-1} ตามลำดับที่ทุกอัตราส่วนการผสม และเมื่อเปรียบเทียบอัตราส่วนของ พื้นที่ใต้พีคย่อยแต่ละพีคต่อพื้นที่ใต้พีคของอะคริโลไนไตรล์ (Acrylonitrile) พบว่าอัตราส่วนของพื้นที่ใต้ของพีค ย่อยที่เลขคลื่น $1720, 1726,$ และ 1738 cm^{-1} ต่อพื้นที่ใต้ของพีคอะคริโลไนไตรล์ มีแนวโน้มเดียวกัน คืออัตรา ส่วนของพื้นที่ใต้ของพีคย่อย ต่อพื้นที่ใต้ของพีคอะคริโลไนไตรล์ ระหว่างพอลิเมอร์ผสมที่เป็นเนื้อเดียวกัน มีค่า มากกว่า อัตราส่วนของพอลิเมอร์ที่เกิดการแยกเฟส และพบว่าอัตราส่วนของพื้นที่ใต้ของพีคย่อย ต่อพื้นที่ใต้ของพี คอะคริโลไนไตรล์นั้น แปรตามปริมาณของ PMMA ในพอลิเมอร์ผสม ยิ่งปริมาณ PMMA มากอัตราส่วนจะมาก ตาม

ในส่วนของทำนายอัตราส่วนการผสมของพอลิเมอร์ผสมที่ไม่ทราบความเข้มข้นระหว่าง SAN และ PMMA เราสามารถทำนายได้จากการสร้างกราฟมาตรฐานระหว่างอัตราส่วนของพื้นที่ใต้พีคคาร์บอนิลต่อพื้นที่ใต้ พีคของ พีคของหมู่แทนที่ของ SAN ที่เลขคลื่น 702 cm^{-1} กับอัตราส่วนโดยน้ำหนักของ SAN ในพอลิเมอร์ผสม

ภาควิชา.....วิศวกรรมเคมี..... ลายมือชื่ออนิลิต.....

สาขาวิชา.....วิศวกรรมเคมี..... ลายมือชื่ออาจารย์ที่ปรึกษา.....

ปีการศึกษา.....2545.....

4270571821: MAJOR CHEMICAL ENGINEERING

KEY WORD: BLEND/ PHASE SEPARATION/ POLY(METHYL METHACRYLATE)/
STYRENE-ACRYLONITRILE COPOLYMER/ QUANTITATIVE ANALYSIS/ FTIR

SONGKROH PASUKNIRANT: DIFFERENCES IN FTIR SPECTRUM OF
MISCIBLE AND PHASE SEPARATED POLYMER BLEND OF POLY STYRENE
ACRYLONITRILE COPOLYMER (SAN) AND POLY (METHYL
METHACRYLATE) (PMMA), THESIS ADVISOR: ASSISTANT PROFESSOR
M.L. SUPAKANOK THONGYAI, Ph.D. 136 pp. ISBN 974-17-2162-5

This work involved the studies of searching the suitable sampling preparation for quantitative analysis, the studies of the effects of phase separation and the prediction of the blending composition of unknown between styrene acrylonitrile copolymer (SAN) and poly (methyl methacrylate) (PMMA) at the weigh percent of SAN: 30, 40, 50, 60, 70, 80, 90 by using Fourier transform infrared spectrometer (FTIR). This polymer blend were prepared by melt mixing method. For the studies of searching the suitable sampling preparation for quantitative analysis by using FTIR. It was found that the film preparation method was the suitable method because It's no effects from dispersing of sample and absorbing of moisture in air.

For the studies of the effects of phase separation on the IR spectra of SAN / PMMA blends. It's found that the IR spectra of carbonyl peak of PMMA at wavenumber 1732 cm^{-1} of miscible samples and phase separated samples were composed from five hidden peak at wavenumber 1720, 1726, 1732, 1738 and 1747 cm^{-1} respectively at any composition of blending. When comparing the ratio of area under each hidden peaks to area under acrylonitrile peaks, it's found that the ratio of area under hidden peaks at wavenumber 1720, 1726 and 1738 cm^{-1} to area under acrylonitrile peaks had the same trend. That was the ratio of area under hidden peaks to area under acrylonitrile peaks of miscible samples were higher than those of phase separated samples and found that the ratio of area under hidden peaks to area under acrylonitrile peaks were depend on the quantities of PMMA in blends, if PMMA in blend were higher these ratio were higher too.

For the studies of the prediction of the blending composition of unknown between SAN and PMMA the prediction can proceed from the standard curve that plotted between the ratio of area under carbonyl peaks to area under mono-substitution group in SAN at wavenumber 702 cm^{-1} and weight percent of SAN in blends.

Department... Chemical Engineering.... Student's signature.....

Field of study..Chemical Engineering... Advisor's signature.....

Academic year.....2002.....

ACKNOWLEDGEMENTS

The author would like to express his deeply gratitude to his advisor: Assistant Professor Dr. M.L. Supakanok Thongyai, who supervised and encourage him through out this course, He is also grateful to Professor Dr. Piyasarn Prasertdam, Assistant Professor Seeroong Prichanont and Dr. Wit Soontaranun as Chairman, members of the thesis committee, respectively.

Thanks for the financial support are due to Department of Chemical Engineering and Graduate School, Chulalongkorn University.

The author wish to thank Assistant Professor Sanong Ekgasit, Department of Chemistry, Faculty of Science, Chulalongkorn University, for their help with the FTIR spectrometer and the valuable advice and constructive comment.

The author wish to thank Assistant Professor Somchai Puajindanetr and Mr. Juggaparn, Department of Industrial Engineering, Chulalongkorn University, for their help with the hydraulic hotpress. It is his honour to receive a first priority during his experiment.

Sincerely thanks to all member of the Polymer Engineering Research laboratory at Department of Chemical Engineering, Chulalongkorn University as well, who always build up such a joyful ambience in the lab and bring up such an interesting subject to discuss, particular P' Ta for the samples of polymer blend and the valuable advice. And he also would like to thank all member of Spectroscopy Research laboratory at Department of Chemistry, Chulalongkorn University, particular Patcharin, Nopparat, Tasimon, Joe, P' Pim and everyone whose name may not mention here for their assistance.

Finally, the author would like to dedicate this thesis to his family, who generously supported and encouraged his through the years spent on this study and understand him not only today but also tomorrow.

CONTENTS

	PAGE
ABSTRACT (IN THAI)	iv
ABSTRACT (IN ENGLISH)	v
ACKNOWLEDGEMENTS	vi
CONTENTS	vii
LIST OF TABLES	xii
LIST OF FIGURES	xv
CHAPTER	
I. INTRODUCTION	1
1.1 The Objectives of the Present Study.....	2
1.2 The Scope of the Present Study.....	3
II. LITERATURE REVIEW	4
III. THEORY	7
3.1 Styrene-Acrylonitrile Copolymer (SAN).....	7
3.2 Poly(methyl methacrylate) (PMMA).....	8
3.3 Polymer blend.....	10
3.3.1 The Preparation of the Polymer Blends.....	10
3.3.1.1 Melt Mixing.....	10
3.3.1.2 Solvent Casting.....	11
3.3.1.3 Freeze Drying.....	12
3.3.1.4 Emulsions.....	12
3.3.1.5 Mixing via Reaction.....	13

CONTENTS(continued)

	PAGE
3.4 Miscibility Characteristics of the Blends.....	13
3.4.1 Thermodynamics of Mixing.....	14
3.4.2 The Phase Diagrams of Polymer Blends.....	16
3.5 Phase Separation Phenomena.....	18
3.5.1 Mechanisms of Phase Separation.....	19
3.5.1.1 Nucleation and Growth (NG).....	20
3.5.1.2 Spinodal Decomposition (SD).....	21
3.6 Infrared Spectroscopy.....	22
3.6.1 Introduction.....	22
3.6.2 Theory of FTIR.....	22
3.6.3 Instrumentation.....	26
3.6.4 Sample Techniques.....	28
3.6.4.1 Gas Sample.....	29
3.6.4.2 Liquid Sample.....	29
3.6.4.3 Solid Sample.....	29
3.6.5 Interpreting The Spectrum.....	30
3.6.6 FTIR for Quantitative Analysis.....	31
3.6.7 Consider for Solid Polymer Sample.....	33
3.6.7.1 Mull Technique and KBr Technique.....	33
3.6.7.1.1 Sample Alterations.....	33
3.6.7.1.2 Uniformity.....	34
3.6.7.2 Film Technique.....	34
3.6.7.2.1 Uniformity of Film Technique.....	35
3.6.7.2.2 Pressure and Temperature Effects of Film Technique.....	35
IV. EXPERIMENTS.....	36
4.1 Materials.....	36
4.1.1 Styrene-Acrylonitrile Copolymer (SAN).....	36
4.1.2 Poly(methyl methacrylate) (PMMA).....	37

CONTENTS(continued)

	PAGE
4.2 Equipment.....	37
4.2.1 Digital Hot Plate Stirer.....	37
4.2.2 Automatic Hydraulic Hot Press.....	38
4.2.3 Surface Temperature Probe & Digital Thermometer.....	38
4.2.4 Fourier Transform Infrared Spectrometer.....	39
4.3 FTIR Studies.....	41
4.3.1 Sample Blending Preparation.....	41
4.3.2 Sample Preparation methods for FTIR Quantitative Analysis.....	41
4.3.2.1 KBr Disc.....	41
4.3.2.2 KBr Cubic.....	43
4.3.2.3 Film Preparation.....	44
4.3.3 Determine of Homogeneity in Three Preparation Method by FTIR.....	45
4.3.3.1 KBr Disc	45
4.3.3.2 KBr Cubic.....	45
4.3.3.3 Film Preparation.....	45
4.3.4 The Studies of Phase separated Effect.....	46
4.3.4.1 Sample Preparation.....	46
4.3.4.2 Second Derivative Method.....	46
4.3.4.3 Curve Fitting Technique and Detecting Area under Interesting peak.....	48
V. RESULT & DISCUSSIONS.....	50
5.1 The Finding of The Suitable Sample preparation Method For FTIR Quantitative Analysis.....	52
5.1.1 Discussions.....	52

CONTENTS(continued)

	PAGE
5.2 The Difference in Spectra of the Miscible Samples and Phase Separated Samples at various Compositions by FTIR.....	61
5.2.1 Discussions.....	62
5.3 The Prediction of Unknown Blend Samples of SAN/PMMA.....	108
5.3.1 Discussions.....	108
VI. CONCLUSIONS AND RECOMMENDATIONS.....	111
6.1 Conclusions.....	111
6.2 Recommendations for further Studies.....	113
REFERENCES.....	114
APPENDIX.....	118
VITA.....	136


 สถาบันวิทยบริการ
 จุฬาลงกรณ์มหาวิทยาลัย

LIST OF TABLES

TABLE	PAGE
A.1 The area under peak at wavenumber 2237 cm^{-1} (cyanide peak) of miscible samples.....	118
A.2a The area under peak at wavenumber 1720 cm^{-1} of miscible samples.....	119
A.2b The area ratio between peak at wavenumber 1720 cm^{-1} and peak at wavenumber 2237 cm^{-1} of miscible samples.....	119
A.3a The area under peak at wavenumber 1726 cm^{-1} of miscible samples.....	120
A.3b The area ratio between peak at wavenumber 1726 cm^{-1} and peak at wavenumber 2237 cm^{-1} of miscible samples.....	120
A.4a The area under peak at wavenumber 1732 cm^{-1} of miscible samples.....	121
A.4b The area ratio between peak at wavenumber 1732 cm^{-1} and peak at wavenumber 2237 cm^{-1} of miscible samples.....	121
A.5a The area under peak at wavenumber 1738 cm^{-1} of miscible samples.....	122
A.5b The area ratio between peak at wavenumber 1738 cm^{-1} and peak at wavenumber 2237 cm^{-1} of miscible samples.....	122
A.6a The area under peak at wavenumber 1747 cm^{-1} of miscible samples.....	123
A.6b The area ratio between peak at wavenumber 1747 cm^{-1} and peak at wavenumber 2237 cm^{-1} of miscible samples.....	123
A.7 The area under peak at wavenumber 2237 cm^{-1} (cyanide peak) of phase separated samples.....	124

LIST OF TABLES (continued)

TABLE	PAGE
A.8a	The area under peak at wavenumber 1720 cm^{-1} of phase separated samples.....125
A.8b	The area ratio between peak at wavenumber 1720 cm^{-1} and peak at wavenumber 2237 cm^{-1} of phase separated samples.....125
A.9a	The area under peak at wavenumber 1726 cm^{-1} of phase separated samples.....126
A.9b	The area ratio between peak at wavenumber 1726 cm^{-1} and peak at wavenumber 2237 cm^{-1} of phase separated samples.....126
A.10a	The area under peak at wavenumber 1732 cm^{-1} of phase separated samples.....127
A.10b	The area ratio between peak at wavenumber 1732 cm^{-1} and peak at wavenumber 2237 cm^{-1} of phase separated samples.....127
A.11a	The area under peak at wavenumber 1738 cm^{-1} of phase separated samples.....128
A.11b	The area ratio between peak at wavenumber 1738 cm^{-1} and peak at wavenumber 2237 cm^{-1} of phase separated samples.....128
A.12a	The area under peak at wavenumber 1747 cm^{-1} of phase separated samples.....129
A.12b	The area ratio between peak at wavenumber 1747 cm^{-1} and peak at wavenumber 2237 cm^{-1} of phase separated samples.....129
B.1	The area under carbonyl peak of miscible samples.....130
B.2	The area under carbonyl peak of phase separated samples.....130
B.3	The area under mono-substitution of aromatic in SAN of miscible samples.....131
B.4	The area under mono-substitution of aromatic in SAN of phase separated samples.....131

LIST OF TABLES (continued)

TABLE		PAGE
B.5	The area ratio between carbonyl peak and mono-substitution of aromatic in SAN at wavenumber 700 cm^{-1} of miscible samples.....	132
B.6	The area ratio between carbonyl peak and mono-substitution of aromatic in SAN at wavenumber 700 cm^{-1} of phase separated samples.....	132
B.7	The area ratio between carbonyl peak and cyanide peak at wavenumber 2237 cm^{-1} of miscible samples.....	133
B.8	The area ratio between carbonyl peak and cyanide peak at wavenumber 2237 cm^{-1} of phase separated samples.....	133



 สถาบันวิทยบริการ
 จุฬาลงกรณ์มหาวิทยาลัย

LIST OF FIGURES

FIGURE	PAGE
3.1 The repeating units of styrene and acrylonitrile.....	7
3.2 The repeating units of Poly (methyl methacrylate).....	8
3.3 The illustrations of the criteria for miscibility.....	15
3.4 Schematic representation of six possible phase equilibrium diagrams for binary mixtures.....	17
3.5 The LSCT phase diagram of blend with the spinodal and the binodal phase boundaries.....	19
3.6 Schematic illustration of a phase separation by the nucleation and growth mechanism.....	20
3.7 Schematic illustration of a phase separation by the spinodal Decomposition mechanism.....	21
3.8 Procedure of transmission.....	24
3.9 The stretching vibration of molecule.....	25
3.10 The bending vibration of molecule.....	26
3.11 The schematic of the Michelson interferometer.....	27
3.12 The absorption of bonds.....	31
4.1 The repeating units of styrene and arylonitrile.....	36
4.2 The repeating units of poly (methy methacrylate).....	37
4.3 Automatic Hydraulic Hotpress LP-50.....	38
4.4 A schematic diagram of an FTIR spectrometer.....	40
4.5 A FTIR-Bruker spectrometer.....	40
4.6 The powder sample of SAN/PMMA at blending ratio 5:5.....	42
4.7 The equipment for preparing KBr disc.....	42
4.8 The smoothness cubic KBr(A); thesandwich cubics KBr (B).....	43
4.9 The set of apparatus for compressing film.....	44
4.10 The example of second derivative technque.....	47
4.11 An example of an initial a guess at a set of bands to be used in a curvefit.....	49

LIST OF FIGURES (continued)

FIGURE	PAGE
5.1 The water absorption effect in KBr Disc method.....	55
5.2 The effect from size of ground samples in KBr Disc method.....	56
5.3 The non-linearity effect in KBr Disc method.....	57
5.4 The quality of KBr cubics in KBr cubic method.....	58
5.5 The nonlinearity effect in KBr cubic method.....	59
5.6 The suitable spectra for quantitative analysis by film preparation method.....	60
5.7 The IR spectra of miscible samples between SAN/PMMA blends prepared by film preparation method.....	64
5.8 The IR spectra of phase separated samples between SAN/PMMA blends prepared by film preparation method.....	65
5.9 Detecting homogeneity of the IR spectra of miscible samples at composition ratio of blending 30% weight of SAN.....	66
5.10 Detecting homogeneity of the IR spectra of miscible samples at composition ratio of blending 40% weight of SAN.....	67
5.11 Detecting homogeneity of the IR spectra of miscible samples at composition ratio of blending 50% weight of SAN.....	68
5.12 Detecting homogeneity of the IR spectra of miscible samples at composition ratio of blending 60% weight of SAN.....	69
5.13 Detecting homogeneity of the IR spectra of miscible samples at composition ratio of blending 70% weight of SAN.....	70
5.14 Detecting homogeneity of the IR spectra of miscible samples at composition ratio of blending 80% weight of SAN.....	71
5.15 Detecting homogeneity of the IR spectra of miscible samples at composition ratio of blending 90% weight of SAN.....	72
5.16 Detecting homogeneity of the IR spectra of phase separated samples at Composition ratio of blending 30% weight of SAN.....	73

LIST OF FIGURES (continued)

FIGURE	PAGE
5.17 Detecting homogeneity of the IR spectra of phase separated samples at Composition ratio of blending 40% weight of SAN.....	74
5.18 Detecting homogeneity of the IR spectra of phase separated samples at Composition ratio of blending 50% weight of SAN.....	75
5.19 Detecting homogeneity of the IR spectra of phase separated samples at Composition ratio of blending 60% weight of SAN.....	76
5.20 Detecting homogeneity of the IR spectra of phase separated samples at Composition ratio of blending 70% weight of SAN.....	77
5.21 Detecting homogeneity of the IR spectra of phase separated samples at Composition ratio of blending 80% weight of SAN.....	78
5.22 Detecting homogeneity of the IR spectra of phase separated samples at Composition ratio of blending 90% weight of SAN.....	79
5.23 Comparing the second derivative of carbonyl peak at composition ratio of blending 30% weight of SAN.....	80
5.24 Comparing the second derivative of carbonyl peak at composition ratio of blending 40% weight of SAN.....	81
5.25 Comparing the second derivative of carbonyl peak at composition ratio of blending 50% weight of SAN.....	82
5.26 Comparing the second derivative of carbonyl peak at composition ratio of blending 60% weight of SAN.....	83
5.27 Comparing the second derivative of carbonyl peak at composition ratio of blending 70% weight of SAN.....	84
5.28 Comparing the second derivative of carbonyl peak at composition ratio of blending 80% weight of SAN.....	85
5.29 Comparing the second derivative of carbonyl peak at composition ratio of blending 90% weight of SAN.....	86
5.30 Comparing the simulated carbonyl peak from four hidden peaks with real carbonyl peak from the experiment.....	87

LIST OF FIGURES (continued)

FIGURE	PAGE
5.31 Comparing the simulated carbonyl peak from five hidden peaks with real carbonyl peak from the experiment.....	88
5.32 Comparing real spectra and simulated spectra of miscible samples at composition of blending 30% weight of SAN.....	89
5.33 Comparing real spectra and simulated spectra of miscible samples at composition of blending 40% weight of SAN.....	90
5.34 Comparing real spectra and simulated spectra of miscible samples at composition of blending 50% weight of SAN.....	91
5.35 Comparing real spectra and simulated spectra of miscible samples at composition of blending 60% weight of SAN.....	92
5.36 Comparing real spectra and simulated spectra of miscible samples at composition of blending 70% weight of SAN.....	93
5.37 Comparing real spectra and simulated spectra of miscible samples at composition of blending 80% weight of SAN.....	94
5.38 Comparing real spectra and simulated spectra of miscible samples at composition of blending 90% weight of SAN.....	95
5.39 Comparing real spectra and simulated spectra of phase separated samples at composition of blending 30% weight of SAN.....	96
5.40 Comparing real spectra and simulated spectra of phase separated samples at composition of blending 40% weight of SAN.....	97
5.41 Comparing real spectra and simulated spectra of phase separated samples at composition of blending 50% weight of SAN.....	98
5.42 Comparing real spectra and simulated spectra of phase separated samples at composition of blending 60% weight of SAN.....	99
5.43 Comparing real spectra and simulated spectra of phase separated samples at composition of blending 70% weight of SAN.....	100

LIST OF FIGURES (continued)

FIGURE	PAGE
5.44 Comparing real spectra and simulated spectra of phase separated samples at composition of blending 80% weight of SAN.....	101
5.45 Comparing real spectra and simulated spectra of phase separated samples at composition of blending 90% weight of SAN.....	102
5.46 Comparing ratio of area under peak 1720 cm^{-1} and area under peak 2237 cm^{-1} with weight percent of SAN.....	103
5.47 Comparing ratio of area under peak 1726 cm^{-1} and area under peak 2237 cm^{-1} with weight percent of SAN.....	104
5.48 Comparing ratio of area under peak 1732 cm^{-1} and area under peak 2237 cm^{-1} with weight percent of SAN.....	105
5.49 Comparing ratio of area under peak 1738 cm^{-1} and area under peak 2237 cm^{-1} with weight percent of SAN.....	106
5.50 Comparing ratio of area under peak 1747 cm^{-1} and area under peak 2237 cm^{-1} with weight percent of SAN.....	107
5.51 Prediction the ratio of unknown composition of SAN/PMMA.....	109
5.52 Prediction the type of unknown composition of SAN/PMMA.....	110

สถาบันวิทยบริการ
 จุฬาลงกรณ์มหาวิทยาลัย

CHAPTER I

INTRODUCTION

Nowadays the polymeric material can be considered to be one of the essential components in varieties of products, for example, household appliances, toys, electric and electronic equipment, automobiles. These products require different physical, chemical, electrical, mechanical and other properties from the polymer materials. The ability to improve these properties of the polymeric materials to meet the current and future demand is still the importance reach and development activities in both academic and industrial sectors.

New properties of polymeric materials can be obtained in several ways [Brydson, 1995]. The synthesizations of new types of homopolymers and copolymers are always an option. However, the costs and time needed are quite substantial. Another way is to use proper additives to improve the processing and service properties of the polymeric materials. Still another way is to form polymer blends by blending or mixing existing polymeric materials, either homopolymer or copolymer or both, together to obtain new properties. Polymer blends have enjoyed wide spread interests from both academic and industrial sectors in the past few decades because of their relatively minor capital investment and shorter period of time needed with respect to synthesization. In addition, polymer blends can fill the deficiencies in prices or performances of the existing homopolymers and copolymers [Paul and Newman, 1978].

There are several methods for preparing polymer blend such as melt mixing, solvent casting, freeze drying. Each of method has its own advantage and disadvantage and can influence the resulting properties of polymer blend [Wash, 1985]. When two polymer or more are mixed together, for miscible polymer blend, the interaction bond in blend occurs. There are several interactions between two polymers such as hydrogen bonding, ion-dipole interaction. Fourier transform infrared spectroscopy (FTIR) can be used to detect interaction bond in polymer blend. The hydrogen bond can easily be detected by FTIR because of strong absorption [Coleman, 1987; Painter, 1991; Cesteros, 1993; Radmard, 2000.] In this work, the miscible blend containing this polymers: styrene acrylonitrile copolymer (SAN) and poly (methyl methacrylate) were prepared by melt mixing method in order to study actually interaction between this polymer blend.

1.1 THE OBJECTIVES OF THE PRESENT STUDY

- 1.1.1 To find the suitable sampling preparation method for FTIR quantitative analysis.
- 1.1.2 To study the effects of phase separation on the IR spectra of the SAN/PMMA blend by using FTIR spectrometer
- 1.1.3 To predict the blending composition ratio of unknown of the SAN/PMMA blend by using FTIR spectrometer

1.2 THE SCOPE OF THE PRESENT STUDY

The polymer blends of styrene-acrylonitrile copolymer (SAN) and poly (methyl methacrylate) (PMMA) at various composition (30, 40, 50, 60, 70, 80, 90 wt% of SAN) were prepared from melt mixing method by using twin screw extruder. This blending samples were used for FTIR quantitative analysis, three samples preparing methods: KBr Disc, KBr cubic and film preparation were studied to find the suitable sampling preparation method for FTIR quantitative analysis. The suitable sampling preparation method was used for preparing the FTIR spectra of miscible samples. The spectra of phase separation samples were also obtained. Both miscible spectra and phase separation spectra were compared by using second derivative method and curve fitting method in order to study the effect of phase separation and predict the composition of this polymer blend. The condition of FTIR spectrometer was setted at resolution 4 cm^{-1} and number of scan 1000 cycle.



สถาบันวิทยบริการ
จุฬาลงกรณ์มหาวิทยาลัย

CHAPTER II

LITERATURE REVIEW

Interaction between two miscible blend have been widely studied in academic for a long time. Fourier transform infrared spectrometer was used to detect hydrogen interaction. The primary purpose of using the FTIR was used for detecting the functional group of organic samples, interaction peaks such as hydrogen bond, ion-dipole interaction between two polymers in polymer blend reducing peak from degradation of polymer. In this chapter, the literatures on the studies of interaction between on the two polymers that compose of the blend and quantitative analysis by using FTIR were presented.

Coleman, Michal M; Skrovanek [1988] used infrared spectroscopy quantitatively to measure the fractions of hydrogen-bonded groups in polyamide and polyurethane. The mixing of the simple amorphous polyurethane with a polyether was considered. This system were chosen because of its relevance to the more complicated segmented polyurethane and its essentials in focus upon the spectroscopic characteristics of the interaction of urethane N-H bond with ether functional groups.

Janathanan, V and Karasz, F.E.; Macknight, W.J. [1993] studied specific interactions as functions of copolymer composition and blend ratio of poly (p-caprolatone)(PCL) and styrene-co-acrylonitrile (SAN) by using Fourier transform infrared spectroscopy (FTIR). It was shown that miscibility occurred within a certain range of copolymer compositions because the presence of PCL reduced the thermodynamically unfavorable repulsion between styrene and acrylonitrile segments in the random copolymer. This effect of PCL to copolymer were observed in terms of shift to higher frequencies in the 700cm^{-1} Y-CH out of plane deformation vibration absorption of styrene and in the approximately 2236 cm^{-1} C equivalent N stretching frequency band in acrylonitrile segment. Specific intermolecular interaction between SAN and PCL were not observed in this study.

Lim, Jong-Chul [1994] used FTIR to examine the specific interactions contributing to the partial miscibility in blend of styrene-sodium methyl methacrylate copolymer (S-NaMA) and poly(ethylene oxide) (PEO). From the shifts of carboxylate ion and ether group stretching bands, the important specific interactions were found which involving ion-dipole bonding between the ionic group in styrene ionomer and the ether group in PEO. The asymmetric stretching vibration frequency of the carboxylate ion group increases as the fractional amount of PEO in the blend is increased, while symmetric stretching frequency is decreased. The transition value of the fraction of PEO, above which both vibration frequencies of the carboxylate ion mentioned above remained almost unchanged, but increases as the concentration of ionic groups in ionomer is increased. The ether group stretching band shifts to higher frequencies as the PEO content in the ionomer/PEO blend increases. From the differential scanning calorimetry (DSC) and FTIR studies, it was found that the ion-dipole interaction is the important mechanism that determines the miscibility of S-NaMA/PEO blends.

Ha, Chang-Sik; Cho Young-Wook [1996] use Fourier transform infrared spectroscopy (FTIR) to reveal the nature of specific interactions between PP-g-MAH, polypropylene (PP) grafted with maleic anhydride (MAH), and Zn-S-EPDM, ethylene-propylene-diene-terpolymer (EPDM) sulfonated and neutralized with bivalent cation zinc. Results of the FTIR spectra of the blends showed that the peak of the carbonyl group shifts to lower wavenumber and specific interactions were made between carbonyl group in PP-g-MAH and ZnSEPDM. Results also showed that the supposed mechanism of this dipole-ion interactions appeared and the dipole-ion interactions between PP-g-MAH and ZnSEPDM played significant role in improving their miscibility.

K. C. Cole, Y. Thomas, E. Pellerin, M. M. Dumoulin and R. M. Paroli [1996] proposed the new treatment for quantitative analysis of two-component polymer systems by infrared spectroscopy. It is based on a ratio of two peak's in the same spectrum. The relationship between such a ratio and the concentration of a given polymer was inherently nonlinear. It was shown

that this nonlinearity can be well described by a simple equation derived from the laws of optical transmission. This equation has the form $x_1 = \frac{m_1 + m_2 R}{1 + m_3 R}$, where x_1 is the weight fraction of polymer 1, the m_i are adjustable coefficients, and the ratio R is equal to $A_a / (A_a + A_b)$. The quantitative A_a and A_b are the absorbances (peak height or areas) at two frequencies a and b of which the first is associated mainly with polymer 1 and the second with polymer 2. This equation has been applied to various peak combinations in spectra of miscible blends of poly (phenylene ether) with styrene and immiscible blends of polypropylene with polyethylene. It was shown that the equation is valid in all cases, covering the full concentration range from 0 to 100% even when the peaks used for the analysis involved the absorption by both polymers. It is therefore believed to be of a general useful method for the rough analysis of polymer blends and copolymers.

Rudiger Schafer, Jorg Zimmermann, Jorg Kressler and Rolf Moulhaupt [1996] show that Fourier transform infrared (FTIR) microscopy is able to monitor the phase morphology in blends of poly (methyl methacrylate) and poly(styrene-co-acrylonitrile). This is carried out by the spatially resolved detection of the absorbances of the C=O stretching vibration of the ester group of poly(methyl methacrylate) at 1732 cm^{-1} and the C≡N stretching vibration of (polystyrene-co-acrylonitrile) at 2238 cm^{-1} . The most serious restriction for FTIR microscope is the large spot size, which limits the spatial resolution of the detectable morphologies. An enormous advantage of FTIR microscopy compared to optical microscopy is its ability to provide quantitative information on the chemical composition of the phase. These data taken at different annealing temperatures can be used to obtain the phase diagram of blends showing lower critical solution temperature behavior. Larger deviations of data points measured by FTIR microscopy compared to cloud point measurements are observed at the poly(methyl methacrylate) rich side of the phase diagram, where also the error of the FTIR microscopic determinations of the phase composition is larger for the blend system under investigation.

CHAPTER III

THEORY

3.1 Styrene-Acrylonitrile Copolymer (SAN)

Styrene-acrylonitrile copolymer (~ 20-30 wt% acrylonitrile content) have been commercially available for a number of years [Brydson, 1995] and are usually produced by emulsion or suspension polymerization. The repeating units of styrene and acrylonitrile in styrene-acrylonitrile copolymers are shown as in Figure 3.1.

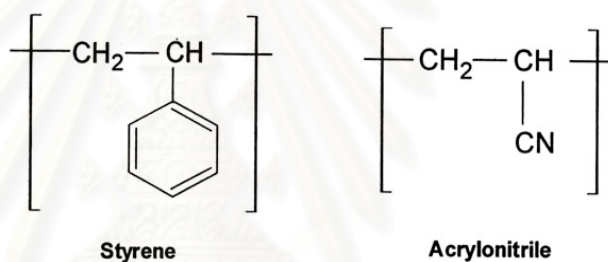


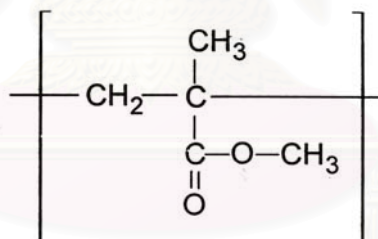
Figure 3.1 The repeating units of styrene and acrylonitrile.

Because the acrylonitrile molecules have the polar nature, so these copolymers have better resistance to hydrocarbons, oils and greases than polystyrene [Brydson, 1995]. They also have a higher softening point, a much better resistance to stress cracking, crazing enhanced impact strength and yet retained the transparency of the homopolymer [Brydson, 1995]. The higher the acrylonitrile content the greater the toughness and chemical resistance but the greater the difficulty in moulding and the greater the yellowness of the resin. So it is useful to add blue tint to counteract the yellowish tint.

The important features of rigidity and transparency make the material competitive with polystyrene and poly (methyl methacrylate) for a number of applications. However, it does not have such a high transparency or such good weathering properties as poly(methyl methacrylate). As a result of these considerations the styrene-acrylonitrile copolymers have found applications for dials, knobs and covers for domestic applications, electrical equipments and car equipments, for picnicwares and housewares, and for a number of other industrial and domestic applications. They are also widely used for transparent medical products and for meter or light lenses.

3.2 Poly(methyl methacrylate) (PMMA)

Poly(methyl methacrylate) is a clear, colorless, hard rigid and transparent material. The general chemical structure of poly(methyl methacrylate) is shown in Figure 3.2.



Methyl methacrylate

Figure 3.2 The chemical structure of poly(methyl methacrylate).

Poly(methyl methacrylate) is available as cast sheets, rods, and tubes, in extruded sheet and film form, and as compounds for the various fabricating processes. Poly(methyl methacrylate) compounds for molding or extrusion are made by bulk or suspension polymerization. The production of cast sheets, rods, and tubes is carried by bulk polymerization. The commercial poly(methyl methacrylate) is available in both atactic and syndiotactic structures. The glass transition temperatures (T_g) of the atactic and syndiotactic poly(methyl methacrylate) are approximately 104 °C and 115 °C, respectively. In consequence of a T_g of 104 °C with its amorphous nature, commercial poly(methyl methacrylate) is thus a hard transparent plastic material in normal conditions of usage [Brydson, 1995].

Poly(methyl methacrylate) is resistant to many aqueous inorganic reagents, including dilute alkalis and acids [Charrier,1991]. The outstanding property of poly(methyl methacrylate) is its excellent transparency [Charrier,1991]. Coupled with its unusually good outdoor weathering behavior, its transparency makes it highly useful in all applications where light transmission is important.

The mechanical properties of the polymer are suitable for short-term loading, but for long-term service the tensile strength must be limited to 31,000 kPa (1,500 psi) to avoid crazing or surface cracking [Rosato, 1991]. Electrical properties are good but not outstanding. A limitation to the optical uses of the material is its poor abrasion resistance compared to glass.

Many applications of poly(methyl methacrylate) are found as hard contact lenses, automobile tail-light lenses, reflective devices, skylights, aircraft cabin window, instrument and appliance covers, and home furnishing. It is also used as optical fibers [Charrier,1991].

3.3 Polymer Blends

A polymer blend is a mixture of at least two polymers or copolymers [Utracki, 1990]. The first polymer blend performed is not exactly known, but the first patent of polymer blend which was a blend between natural rubber and gutta percha was done in 1846 whereas the first patent on thermoplastic polymer blends, which was a blend of polyvinyl chloride (PVC) and acrylonitrile rubber (NBR), was performed in 1942 [Utracki, 1990]. The main purpose of blending polymers is to design new properties of polymeric material that different from those of the pure polymers without synthesizing a new polymer. The results of blending have many benefits such as not requiring more money, time and efforts than synthesizing the new polymer.

3.3.1 The Preparation of the Blends

There are many ways to prepare the new polymer blends such as by using heat, by using solvent or by mixing via reaction, etc.

3.3.1.1 Melt Mixing

Melt mixing of thermoplastic polymer is performed by mixing the polymers in the molten state under shear in the mixing equipment. This method is the choice for the preparation of polymer blends in a commercial scale because of its simplicity, speed of mixing and the advantage of being free from foreign components (e.g. solvents) in the result blends. A number of devices are available for laboratory-scale mixing such as Brabender mixer, electrically heated two-roll mill, extruder, rotational rheometer.

The primary disadvantage of this method is that both components must be in the molten state. It means that the temperature may be high to cause degradation. The secondly, melt mixing is difficult to mix in some pairs of polymers due to difference in the melt viscosity of the components. Beside, the cost of the equipment is another disadvantage of melt mixing. Finally, this method only works well with large amounts of material, e.g. at least 50 grams is required for even laboratory-size mixing equipment. If mixing of quantities of less than 1 g is required, melt mixing is usually not feasible.

3.3.1.2 Solvent Casting

This method is done by dissolving polymers into a suitable solvent. Solution of polymer blend is then cast on a glass plate into thin films and the removal of solvent from films is performed by evaporating at ambient or elevated temperature. Solvent casting is the simplest mixing method available and is widely practised in academic studies. Finally, this method is suitable and easy for very small quantities of experimental polymers.

The most severe problem with solvent casting is the influence of the solvent and the casting history on the resulting product. In spite of the fact that the most of the solvent can be removed from a cast film, the nature of the film depends strongly on the solvent and the conditions used during casting. Casting is best done in thin films, normally not exceeding 0.1 mm in thickness [Thongyai, 1990], with slow solvent removal to avoid concentration and temperature gradients during the removal of solvent.

To remove traces of solvent from the casting polymer films, the condition of high temperature is invariably needed, and protection of the polymer in case of degradation is essential. Flowing inert gas or

vacuums are typically used. In the vacuum conditions, the vapor pressure can be reduced and thus allows the solvents to evaporate more easily. However, too fast evaporation rate of solvent will result in the bubble in the final films produced.

3.3.1.3 Freeze Drying

In the freeze drying process, a solution of the two polymers is quenched down to a very low temperature and solvent is frozen. Solvent is then removed from the frozen solution by sublimation at a very low temperature and pressure. Dilute solutions must be used and the solution volume must be kept low for good heat transfer.

An advantage of this method is that resulting blend will be independent of the solvent, if the solution is single phase before freezing and the freezing occurs rapidly. However there are many limitations of this method. Freeze drying seems to work best with solvents having high symmetry, i.e. benzene, dioxane, naphthalene, etc. The powdery form of the blend after solvent removal is usually not very useful and further shaping must be performed. Freeze drying does require a good vacuum system for low-boiling solvents and it is not a fast blending method.

3.3.1.4 Emulsions

The handling of polymers as emulsion has as many advantages as the use of solvent casting. Films can be cast; mixing requires neither expensive equipment nor high temperature. However, emulsions of polymers are not always available or easy to make. While emulsion polymerization is highly advanced, it is not applicable to all monomers.

3.3.1.5 Mixing via Reaction

Co-crosslinking and interpenetrating polymer networks (IPN) formation are specially methods for forming blends. The idea of these methods is to force a degree of miscibility by reactions between the polymers. Other methods involve the polymerization of a monomer in the presence of a polymer and the introduction of groups onto the polymer chain.

3.4 Miscibility Characteristics of the Blends

Mixing is the process that produces blends by putting several components together so that the blend becomes homogeneous or heterogeneous with small domain sizes. Miscibility of the blends can be classified into three categories [Thongyai, 1990] as follows:

1. Miscibility

Miscibility is the state of a single phase where the level of molecular mixing is adequate to yield macroscopic properties expected of single phase material [Olabishi, 1979].

2. Partial Miscibility

Partial miscibility exhibits at least two miscible phase where each phase may comprise a high concentration of one component with a smaller dissolved portion of the other.

3. Immiscibility

Immiscibility is a state of two phases in which each phase comprises of the individual component and exhibits both macroscopic and/or microscopic properties of that component.

Miscibility characteristics of polymer blends depend on the conditions and methods of blend preparation such as compositions, temperature, pressure or shear rate .

3.4.1 Thermodynamic of Mixing

The basic and very useful thermodynamic equation that will be able to describe the miscibility of two polymers is the Gibbs free energy equation.

$$\Delta G_m = \Delta H_m - T\Delta S_m \quad (3.4.1)$$

where ΔG_m is the Gibbs free energy
 ΔH_m is the enthalpy of mixing
 ΔS_m is the entropy of mixing
 T is the temperature in Kelvin

Equation 3.4.1 apparently can predict whether a blend is miscible, immiscible, or partially miscible by taking into account the sign of ΔG_m as seen in figure 3.4.1. With the positive sign of Gibbs free energy, the blend is immiscible , whereas the negative can be seen in a miscible blend. Nevertheless, some can exhibit partially miscible, even with the negative sign of ΔG_m . Thus, the second derivative of Gibbs free energy is required to specify the difference between partially miscibility and miscibility as seen in equation 3.4.2. System always exhibit miscibility if they satisfy this following condition:

$$\frac{\partial^2 \Delta G_m}{\partial \phi_i^2} > 0 \quad (3.4.2)$$

The concept behind the criteria for miscibility can be demonstrated by the approximate illustrations [Thongyai, 1990] as below:

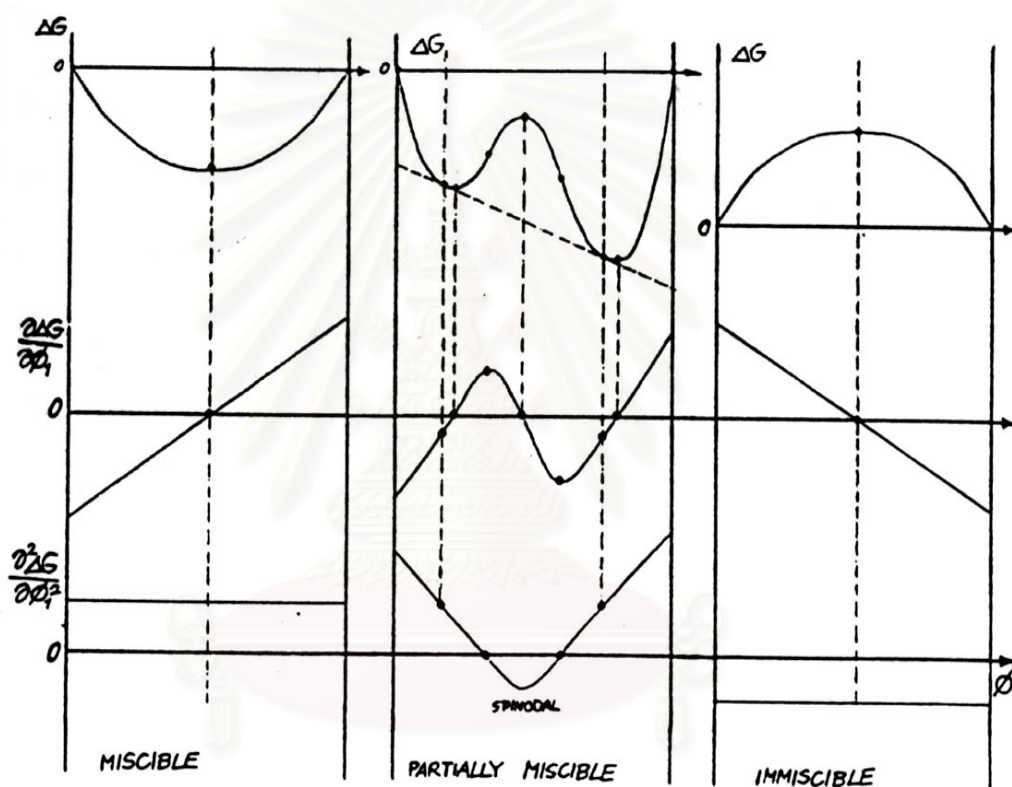


Figure 3.3 The illustrations of the criteria for miscibility [Thongyai, 1990].

3.4.2 The Phase Diagrams of polymer Blends

A phase is a “uniform” piece of matter with “reproducible”, “stable” properties depending only on thermodynamic variables. A certain amount of nonuniformity, such as small concentration and density fluctuations can change the behavior of phase [Olabishi, 1979]. For general usage, if the phase separation curves are available, the working conditions and the processing parameters of the blend can be properly determined. The phase separation curve can be obtained from the diagram called “Phase Diagram” which usually is a plot of temperature versus composition of the blend. Pressure and other process parameters also have some effects on phase separation, but these parameters hardly change in normal ambient conditions. In real polymer blend systems, many types of phase diagrams can be found as shown in Figure 3.4 [Kroschwitz, 1990]. The shade area in Figure 3.4 represents phase separation. The unshaded area in Figure 3.4 represents homogeneous region.

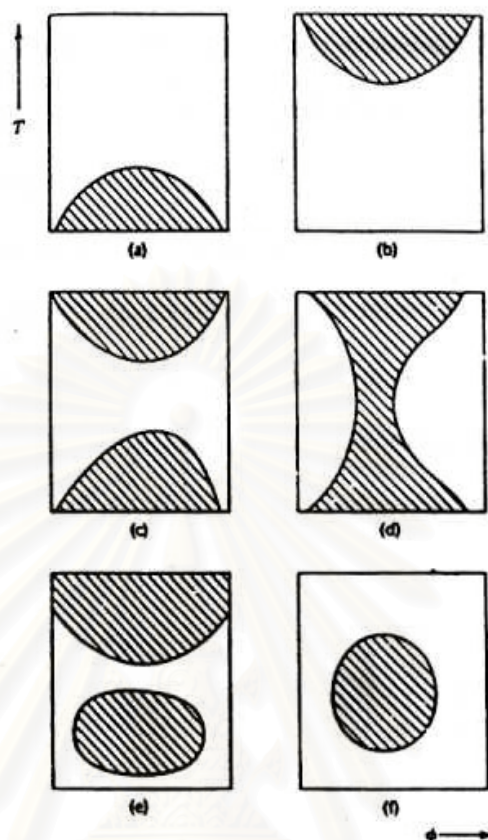


Figure 3.4 Schematic representation of six possible phase equilibria diagrams for binary mixtures in which the shade areas represent phase separation [Kroschwitz, 1990].

In the figure 3.4a shows the upper critical solution temperature (UCST) behavior of a typical polymer blends in which an initially homogeneous mixture undergoes phase separation upon lowering of temperature. The UCST behavior is a characteristic of low molecular weight system.

When the blend undergoes phase separation as the temperature is raised the lower critical solution temperature (LCST) behavior is called. This behavior is in contrast to the UCST behavior and is shown in Figure 3.4b. The main behavior observed in miscible polymer blends of high molecular weight belongs to this type of phase behavior.

Figure 3.4c illustrates the combination of both upper and lower critical solution phase boundaries, seen most commonly in nonpolar polymer solutions [Kroschwitz, 1990].

Figure 3.4d shows the convergence of upper and lower critical boundaries for an immiscible system to form an hourglass-shaped phase boundary. This type of phase diagram is the common phase diagram for the commercial polymer alloys [Thongyai, 1990].

Figure 3.4e illustrates the existence of upper, lower, and quasilower critical phase boundaries. This type of phase diagram can be observed in polar polymer solutions, e.g. poly(acrylic acid)-dioxane [Kroschwitz, 1990].

Figure 3.4f shows the immiscibility loop with upper and lower critical phase boundaries inverted. The examples of this type of system are nicotine-water and poly(vinyl alcohol)-water [Kroschwitz, 1990].

3. 5 Phase separation Phenomena

The kinetic aspect of phase separation in binary mixtures is considered to be important because mixtures of different morphologies can result from different decomposition mechanisms. This affords a possibility of enhancing the properties of compatible systems by phase separation [Paul and Newman, 1978]. Phase separation in a miscible system is brought about by temperature, pressure and/or composition variations. To explain more about the phase separation phenomena in a polymer blend, the lower critical solution temperature (LCST) phase diagram which is a characteristic of most polymer systems is considered. The LCST phase diagram as shown in Figure 3.4b is incomplete. In reality, there are two different phase boundaries in the diagram: the spinodal and the binodal. These phase boundaries are shown in Figure 3.5.

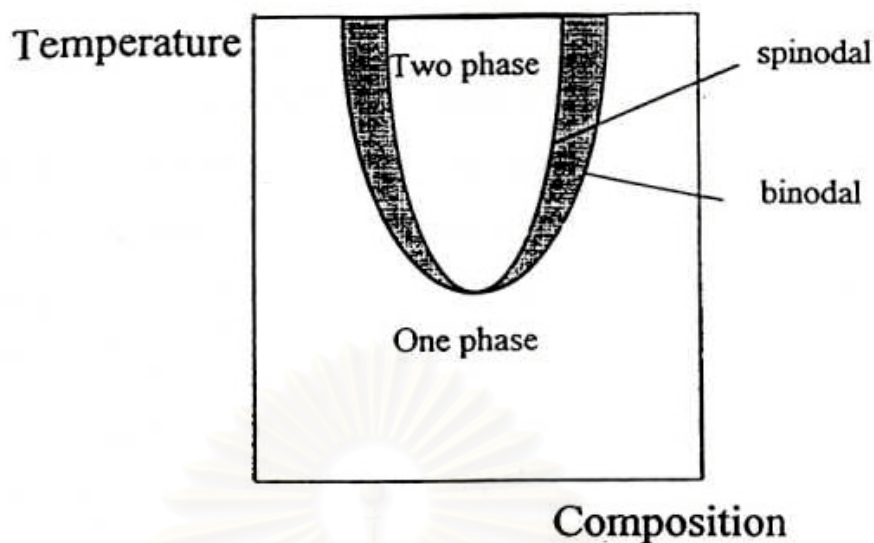


Figure 3.5 The LCST phase diagram of blend with the spinodal and the binodal phase boundaries [Oiarzabal, 1993].

These phase boundaries define three different zones in the phase diagram of the polymer mixture: Stable or one-phase, metastable, and unstable or two-phase regions. The main difference between the spinodal and the binodal boundaries is the mechanism of the phase separation. In the metastable region, between the spinodal and the binodal, phase separation occurs by nucleation and growth (NG) while in the two-phase region, a spinodal decomposition (SD) mechanism is followed.

3.5.1 Mechanisms of Phase Separation

Two major mechanisms of phase separation which are responsible for phase separation in the metastable and unstable regions are as follows:

3.5.1.1 Nucleation and Growth (NG)

The process by which initial fragments of a new, more stable phase are generated from within a metastable mother phase is known as nucleation. The initial fragments are the nuclei and the formation requires an increase in free energy, this excess free energy can be referred to as the work of forming a fluid of a different phase within another homogeneous one. As the nuclei grow by diffusion of macromolecules into that domain. This is a downhill type diffusion as the nucleated area will be surrounded by a matrix poor in one of the polymers. A large number of nuclei will be growing at the same time and therefore a dispersed two phase system will appear. As the droplets grow they will start to coarsen and, eventually, two individual phase will be reached. The composition of these two phase is defined by the binodal. The growth process as well as the corresponding phase structure is shown in Figure 3.6.

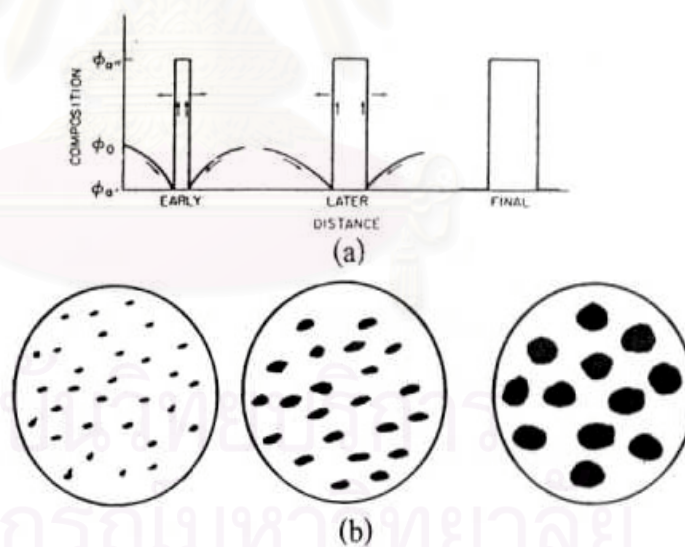


Figure 3.6 Schematic illustration of a phase separation by the nucleation and growth mechanism (a) one-dimension evolution of composition profiles: (b) two-dimension picture of the resultant phase structure [Olabishi, 1979].

3.5.1.2 Spinodal Decomposition (SD)

The kinetic process of creating a continuous growth of a more stable phase from within an unstable mother phase is referred to as spinodal decomposition. Inside the spinodal boundary, phase separation occurs spontaneously. Concentration fluctuations are unstable and create a new phase by an uphill diffusion of like molecules against the direction of the concentration gradient. In the early stage, The size scale of the phase separation is constant and the concentration change with time. In the intermediate stage, both the concentration and size of the phase change. Finally in the late stage the concentration is constant and the size of the phases increases because of the coalescence of smaller phases. The interconnected structure and the corresponding growth process are shown in Figure 3.7.

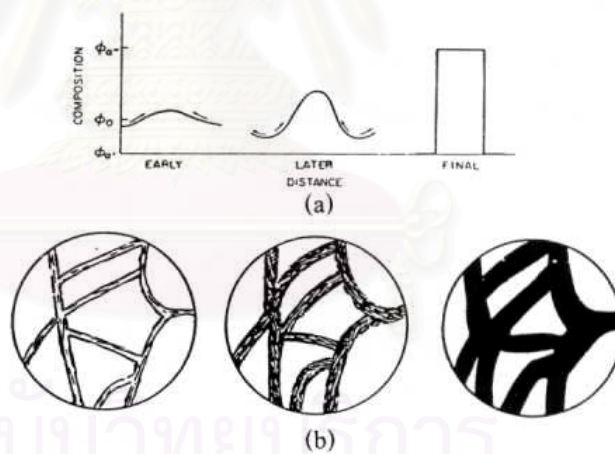


Figure 3.7 Schematic illustration of a phase separation by the spinodal decomposition mechanism: (a) one-dimensional evolution of composition profiles: (b) two-dimension picture of the resultant phase structure [Olabishi, 1979].

3.6 Infrared Spectroscopy

3.6.1 Introduction

FTIR Spectroscopy is one of the most commonly used analytical techniques for materials analysis. Applications of the technique cover the whole spectrum from simple material identification to the distribution of materials to their interactions. The main reasons for its popularity are numerous: The instruments are relatively easy to use, the interpretation of results is usually simple. Sampling techniques allow for non-invasive analysis. Relatively small analysis time allows for a rapid analysis of a sample or analysis of a large number of samples.

As may be expected, the analysis of multicomponent samples and especially, quantification of chemical species is particularly challenging. Such efforts are further complicated in the analysis of long chain molecules, like polymers, that may have a variety of chain conformations, semi-crystalline regions, associations or repulsions (e.g. hydrogen bonds), time-dependent change in those quantities, or simply, some impurities. Similarly, instrumentation and sampling techniques can be of many types suited to specific results required.

3.6.2 Theory of FTIR

Infrared (IR) radiation refers broadly to that part of the electromagnetic spectrum between the visible and microwave regions [Silverstein, 1991]. The IR region can also be subdivided into three smaller region known as near-IR, mid-IR and far-IR. Of greatest practical use is the limited portion between 4000 and 400 cm^{-1} (mid-IR)[Silverstein, 1991]. There has been some interest in the near-IR (14,000-4000 cm^{-1}) and the far-IR regions, 700-200 cm^{-1} . Infrared radiation of frequencies less than about 100 cm^{-1} is absorbed and converted by an organic molecule into energy of molecular rotation. This absorption is quantized; thus a molecular rotation

spectrum consists of discrete lines [Silverstein, 1991]. Infrared radiation in the range from about 10,000-100 cm^{-1} is absorbed and converted by an organic molecule into energy of molecular vibration. This absorption is also quantized, but vibrational spectra appear as band rather than as lines because a single vibrational energy change is accompanied by a number of rotational energy changes. It is with these vibrational-rotational bands, particularly those occurring between 4000 and 400 cm^{-1} [Silverstein, 1991]. The frequency or wavelength of the absorption depends on the relative mass of the atoms, the force constants of the bonds, and the geometry of the atom.

Band positions in IR spectra are presented here as wavenumbers (ν) whose unit is the reciprocal centimeter (cm^{-1}); this unit is proportional to the energy of vibration and modern instruments are linear in reciprocal centimeters [Silverstein, 1991]. Wavenumbers are reciprocally related to wavelength as shown in equation 3.6.0 as below;

$$\text{cm}^{-1} = 10^4/\mu\text{m} \quad (3.6.0)$$

Band intensities can be expressed either as transmission (T) or absorption (A). Transmission is the ratio of the radiant power transmitted by sample to the radiant power incident on the sample as shown in figure 3.8. and relationship between transmittance and ratio of the radiant power transmitted by sample (I) to the radiant power incident on the sample (I_0) as shown in equation 3.6.1.

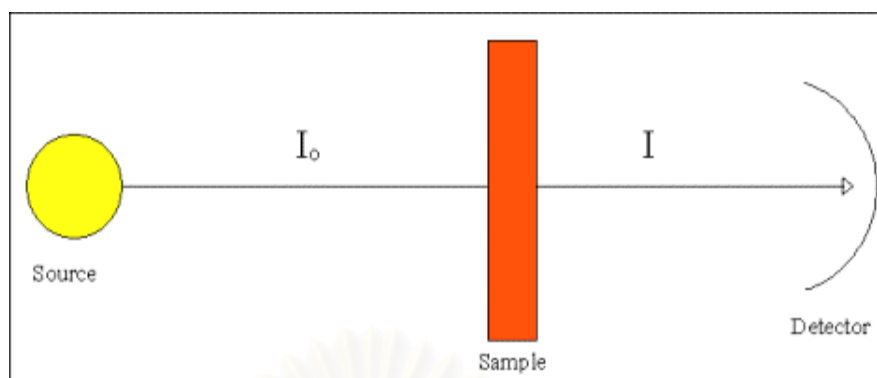


Figure 3.8 Procedure of Transmission

$$T = \frac{I}{I_0} \quad (3.6.1)$$

where: T = Transmittance

I / I_0 = the ratio of the radiant power transmitted by sample to the radiant power incident on the sample

Absorbance is the logarithm, to the base 10, of the reciprocal of the transmission as shown in equation 3.6.2

$$A = + \log (1/T) = -\log (T) \quad (3.6.2)$$

When infrared light is passed through a sample of an organic compound, some of the frequencies are absorbed, while other frequencies are transmitted through the sample without being absorbed. After that the molecules absorb the infrared radiation of the same frequencies as the bond's vibration in the molecules, the amplitude of vibration increases. It means that the molecules stay at excited state, but those in excited state is not stable. So the molecules that stay at excited state come down to the ground state (more stable) by emission energy. There is one important restriction, the molecule will only absorb radiation if the vibration is accompanied by a change in the dipole moment of the molecule. A dipole occurs when there is a difference of

charge across a bond. If the two oppositely charged molecules get closer or further apart as the bond bends or stretches, the moment will change. This phenomenon is called infrared active. To calculate the frequency of light absorbed, requires Hook's law:

$$\nu_{\text{osc}} = \frac{1}{2\pi} \sqrt{k \frac{m_1 + m_2}{m_1 m_2}}$$

where:

- k = force constant indicating the strength of the bond
- m_1 and m_2 are the masses of the two atoms

When the molecules vibrate, there are two types of molecules vibrations: stretching and bending. A stretching vibration is the rhythmical movement along the bond axis such that the interatomic distance is increasing or decreasing as shown in figure 3.9.

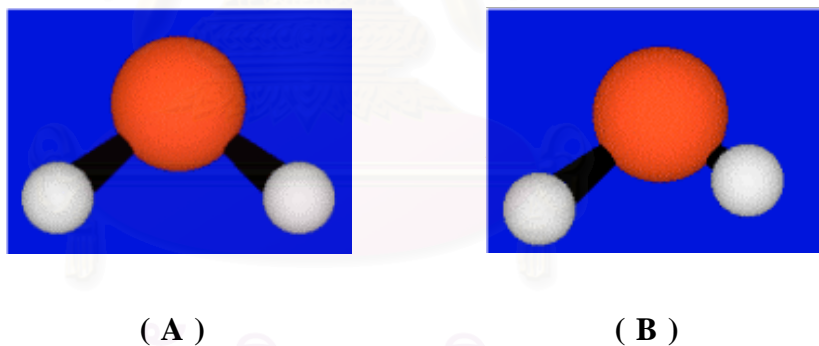


Figure 3.9 The stretching vibration of molecule: (A) Symmetric Stretching , (B) Asymmetric stretching

A bending or deformation vibration may consist of change in the bond angle between bonds with a common atom or the movement of the group of atoms with respect to the one another. The example of the bending vibration was shown in figure 3.10. and a stretching absorption of bond appear at higher frequencies in the infrared spectrum than the bending absorption of the same bond [William, 1994].

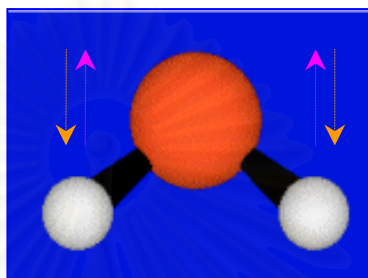


Figure 3.10 The bending vibration of molecule

3.6.3 Instrumentation

There are two main types of instruments that are used for qualitative analysis are dispersive-grating spectrophotometers and multiplex instruments that employ Fourier transform. Wavelength selection in dispersive-grating instruments is accomplished using filters, prisms, or reflection gratings. Traditional instruments have consisted of a filter-grating or prism-grating system that covers the range between $4000\text{-}650\text{ cm}^{-1}$. The most common is a double-beam instrument that uses reflection grating for dispersing radiation. Fourier transform has been applied to infrared spectroscopy and is now a very common technique. Fourier transform infrared (FTIR) spectroscopy offers enhanced sensitivity compared to dispersive IR spectroscopy. Signal-to-noise ratios are often improved by an order of magnitude.

Most commercial FTIR instruments are based on the Michelson interferometer and require a computer interface to perform the Fourier transform and process data. Using an interferometer provides an increase in resolution and results in accurate and reproducible frequency determinations. This offers an advantage when using background subtraction techniques. The principle of Michelson interferometer as shown in figure 3.11.

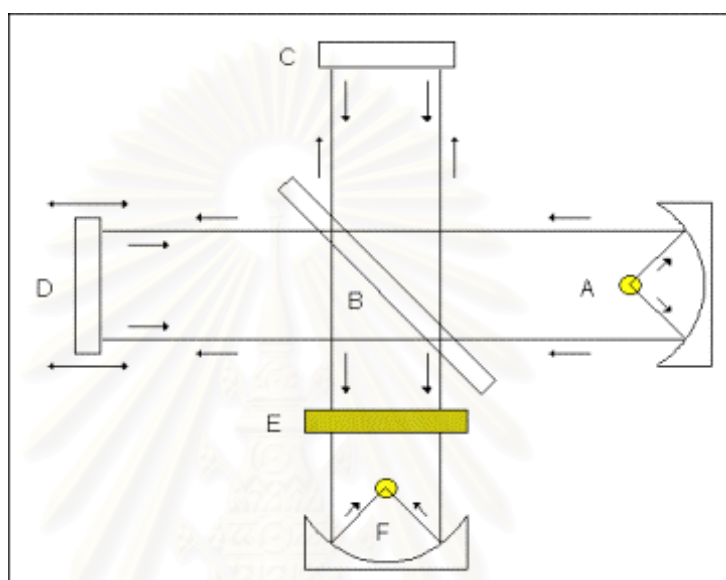


Figure 3.11 The Schematic of the Michelson interferometer

From the figure 3.11, the Michelson interferometer, a parallel polychromatic beam of radiation from a source (A) is directed to a beam splitter (B), made from an infrared transparent material, such as KBr. The beam splitter reflects approximately half of the light to a mirror, known as the fixed mirror (C), which in turn reflects the light back to the beam splitter. The rest of the light passes through to a mirror, moving continuously, at a known velocity, back and forth along the direction of the incoming light and this is known as the moving mirror (D). Upon reflection from the moving mirror, radiation is then directed back to the beam splitter. At the beam splitter some of the light that has been reflected from the fixed mirror combines with light reflected from the moving mirror and is directed towards the sample. After passing through the sample (E) the radiation is focused onto the detector (F). The detectors are sufficiently fast to cope with time domain signal changes from the modulation in the interferometer.

The radiation source of IR spectroscopy used continuous sources in the mid-infrared region and includes the incandescent wire source, the Nernst glower, and the Globar. The Nernst glower is hotter and brighter than the incandescent wire. The Globar is a rod of silicon carbide that is electrically heated and that typically requires a water cooling system. The Globar provides greater output than the Nernst glower in the region below 5 millimetre. Otherwise, their spectral energies are similar.

The detector of FTIR can be subdivided into three general types: thermal, pyroelectric and photoconducting detectors. Thermal detectors measure very minute temperature changes as a method of detection. They operate over a wide range of wavelengths and can be operated at room temperature. The main disadvantages of thermal detectors are slow response and less sensitivity when compared to other detectors. Pyroelectric detectors are specialized thermal detectors that provide faster response and more sensitivity. Photoconducting detectors rely on interactions between incident photons and a semiconductor material. These detectors also provide an increased sensitivity and faster response.

3.6.4 Sample Techniques

A wide range of techniques is available for mounting the sample in the beam of the infrared spectrometer. These sample techniques depend on whether the sample is a gas, a liquid or a solid.

3.6.4.1 Gas Sample

The density of sample in the vapor phase is much less than that of the same sample in its condensed phase. So, in order to get a spectrum of suitable intensity, it's necessary to resort to cells with much longer pathlengths (distance that radiation pass) than are used for liquids and solutions. A typical short path gas cell has a pathlength of 5 or 10 cm and is usually fitted with 1 or 2 stopcocks for introducing and removing the gaseous sample. Glass-bodied cells are most common and should not be used at pressures greater than 1 atmosphere absolute.

3.6.4.2 Liquid Sample

For the liquid sample using cells prepared from alkali halides such as sodium chloride are widely used due to their transparent properties in the infrared region. A common problem with sodium chloride cells is that they absorb moisture and become fogged. Polishing is required to restore the cells to a more transparent state. Liquids may be analyzed in their neat form by placing a small amount of sample on a sodium chloride plate and then placing a second plate on top to form a sample film. The plates are then placed in an appropriate holder in the sample compartment of the instrument. This technique provides adequate spectra for qualitative use.

3.6.4.3 Solid Sample

There are three methods to prepare the solid sample. The first method commonly used for analysis of neat solid samples is the mull technique. The technique consists of grinding the material into a fine powder and then dispersing it into a liquid or solid matrix to form a mull. Liquid mulls have been formed by combining the powdered analyte with Nujol (a heavy hydrocarbon oil). The liquid mull is analyzed between salt

plates as described above. The disadvantage of Nujol is that hydrocarbon bands may interfere with analyte absorbances.

A second method involves grinding the powdered analyte with dry potassium bromide and forming a disk. The ratio of analyte to potassium bromide is usually about 1:100. The materials are ground together using a mortar and pestle or a small ball mill. The mixture is then pressed in a die at 10,000-15,000 psi to form a small transparent disk and analyzed. Carefulness must be taken when preparing the disk to protect it from moisture. It is very common to see absorbances for moisture when using potassium bromide disks.

A last method involves preparing a cast film. This is a procedure that is widely used for obtaining spectra of polymers. The sample is first dissolved in a moderate to highly volatile solvent. The concentration is not critical. A few drops of the solution are then placed on the central position of an infrared window, and the solution is allowed to spread out over the surface of the window. The solvent evaporates, leaving behind a very thin film of sample adhering to the window. The single window is now placed in a demountable cell mount and a spectrum taken.

3.6.5 Interpreting the spectrum

The figure 3.12 shows percentage transmission against wave number. If no radiation is absorbed at a particular frequency, then the line on the graph will be at 100% at the corresponding wave number. Different types of bonds have characteristic regions of the spectrum where they absorb:

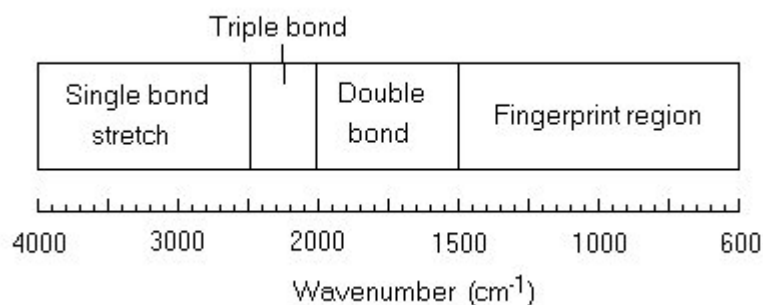


Figure 3.12 The absorption of bonds

Most functional groups absorb above 1500 cm⁻¹. The region below 1500 cm⁻¹ is known as the "fingerprint region". Every molecule produces a unique pattern here, so if an unknown sample produces a spectrum which matches that of a known compound, the sample can be confirmed to be that compound.

3.6.6 FTIR for Quantitative Analysis

Polymer chains are made up of sequences of chemical repeating units. Because the stretching and bending vibration in a polymer closely resemble to those in monomer, so that infrared spectroscopy is practically applicable to polymer structure deformation. It can be used to investigate many parameters such as polymer end group, chain branching, configuration, and conformation. It has also been used to identify and determine the concentration of impurities, antioxidants, emulsifiers, additives, and residual monomers in polymer materials. In addition, FTIR spectroscopy is now widely employed to detect interaction bond of polymer blend such as hydrogen bond or shifting of interesting bond or occurring the new bond. By the theory, the principle of polymer blend is consisted of mixing between two or more pure polymer together, so ratio of pure polymers in polymer blend is importance for quantitative analysis. The quantities of pure polymers in polymer blend are calculated directly from the transmission data or absorption

intensity (A) of characteristic vibration bands presented on FTIR spectra. From the Beer-Lambert law,

$$A = -\log(I/I_0) = \epsilon cl \quad (3.6.6)$$

where: I is the radiant power transmitted by sample (sample spectrum)
 I_0 is the radiant power incident on the sample (background spectrum)
 ϵ is the extinction coefficient (absorptivity)
 c is the concentration of samples
 l is the pathlength of sample through which the infrared beam passes.

From the equation 3.6.6, the absorbance (A) is measured in terms of whether peak height or peak area from the FTIR spectrum. The absorptivity is an absolute measurement of infrared absorption intensity for a certain molecule at a specific wave number. It is a functional physical property of the molecule. Absorbance is a unitless quantity, so the unit of absorptivity is defined in $(concentration \times pathlength)^{-1}$ to cancel the units of the other two variables in Beer-Lambert's law. As a consequence, the absorbance is linearly proportional to the concentration of sample observed by IR technique.

In principle, transmittance (T) is defined as shown in equation 3.6.1.

Substituting equation 3.6.1 into equation 3.6.6 and by raising both sides of the equation to the power of 10 as shown in equation 3.6.7,

$$10^{\epsilon cl} = 1/T \quad (3.6.7)$$

And by rearranging the above equation we get,

$$T = 10^{-\epsilon cl}$$

Thus, the transmittance is not linearly proportional to the concentration. An infrared spectrum can be a plot of either absorbance or transmittance versus wavelength or wavenumber. Traditionally, infrared spectra have been plotted in the absorbance unit because it is linearly proportional to concentration (as shown in Beer-Lambert's law).

3.6.7 Consideration for Solid Polymer Sample

For the quantitative analysis of solid polymer samples, there are three methods for getting the spectrum: a mull technique, KBr disc technique and film technique.

3.6.7.1 Mull Technique and KBr Technique

In mull and KBr disc techniques, they are involved with sample grinding. There are two effects from sample grinding, that is sample alterations and uniformity.

3.6.7.1.1 Sample Alterations:

When the morphology of a sample requires that it acquire the form of fine powder for examination, usually grinding in a ball mill or in a mortar with a pestle are the two methods most commonly practiced. However, the pressure and heat generated from the process can induce numerous changes in the sample, including polymerization, degradation, oxidation, loss of symmetry, and alteration of crystallinity. Both the induction of, and destruction of, polymorphism (ability of a chemical compound to crystallize in several forms, which are structurally distinct) are

sources of error providing potential pitfalls for the unwary analyst. Structural damage caused by the grinding process may be minimized or eliminated by performing a moist grind or using ultrasonic radiation.

Performing the grinding in the presence of a halide salt is not advised for several reasons; thus, the ground powder is typically added to the sample after grinding. The reason is that differences in hardness between the sample and the salt will cause nonuniformity of particle size between the two materials, with the softer material being ground finer or simply deformed.

3.6.7.1.2 Uniformity

A major problem, which arises when a finely powdered sample is needed for the acquisition of a spectrum, is making the particle size, uniform, and reproducible. Light scattering takes over from absorption with increasing particle size and may become the predominant effect reflected in an infrared spectrum. Therefore, size should be small, less than the wavelength of radiation used for its examination. The likelihood of reproducibility in particle size is increased by always grinding the same amount of sample for the same length of time. An aid to assuring sample uniformity is using wire mesh sieves for isolation of particle size fractions and using only one of the fractions for analysis.

3.6.7.2 Film Technique

In film techniques by hydraulic press, there are two effects, that is uniformity and pressure and temperature effects.

3.6.7.2.1 Uniformity of Film Technique

A sample in physical form of a film can simply be examined by standard transmission techniques, and is typically easy to make and store. However, one of the most difficult problems in such transmission measurements is that of uniformity, both sample thickness and homogeneity. Free-standing films may have their thicknesses measured directly through use of micrometer. It's best to obtain an average thicknesses based upon several measurements taken across the film. Samples are expected to exhibit some variation in thickness due to preparation practices, but those possessing significant nonuniformity, or nonconformity to the reference standards or other samples being prepared as references, should be discarded. Typically, a retaining ring or a spacer in mold can be used to achieve reproducible uniform films.

3.6.7.2.2 Pressure and Temperature Effects

Pressed film, usually prepared between the platens of a hydraulic press, can exhibit spectral features due to the conditions used during their preparation. When samples require elevated temperatures to allow the deformation necessary for making a film, it must be carefully controlled so as not to introduce irreproducible crystallinity effects or chemical change. The pressure used to press the material thin enough for examination by transmission must be reproducible to insure that the same physical and chemical state of the sample is achieved. Spacers may be used to ensure that all films are produced with the same thickness. Most importantly, the length of time that sample is exposed to heat and pressure must be carefully regulated.

CHAPTER IV

EXPERIMENTS

4.1 Materials

4.1.1 Styrene-Acrylonitrile Copolymer (SAN)

In this study the random copolymer of styrene acrylonitrile (SAN) containing 23% by weight of acrylonitrile was kindly provided by Bayer Polymers Co., Ltd. It appears in light yellow transparent pellet. The repeating units of styrene and acrylonitrile are shown in figure 4.1. The glass transition temperature (T_g) of this SAN is around 105 °C.

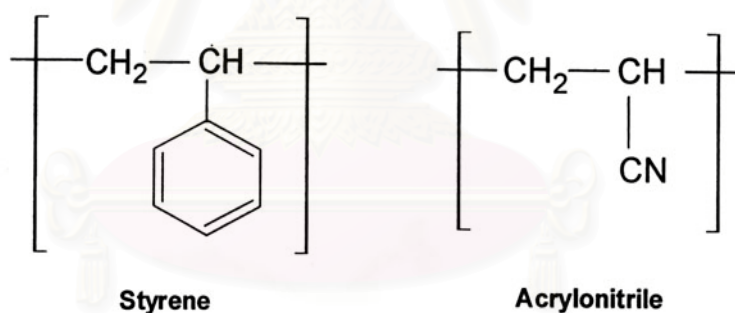


Figure 4.1 The repeating units of styrene and acrylonitrile.

4.1.2 Poly(methyl methacrylate) (PMMA)

The Commercial grade of poly (methyl methacrylate) (PMMA) was kindly provided by TPI Polyacrylate Co., LTD. The PMMA was usually having the miscible blend with styrene-acrylonitrile copolymer (SAN) and usually supplied in a transparent pellet form. The repeating unit of poly (methyl methacrylate) is shown in figure 4.2. The glass transition temperature (T_g) is around 106 °C.

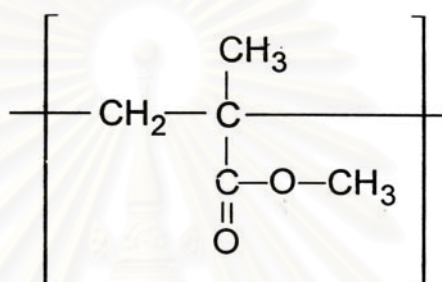


Figure 4.2 The repeating units of poly (methyl methacrylate)

4.2 Equipment

4.2.1 Digital Hot Plate Stirrer

The Cole-Palmer which is a programmable digital laboratory hot plate was used for preparing the phase diagram of the blends and samples by melted mixing between styrene-acrylonitrile copolymer (SAN) and poly (methyl methacrylate). All functions can be set from digital panel and display their status on LCD. The plate temperature, stir speed and time are controllable.

4.2.2 Automatic Hydraulic Hot press

The LAB TECH hydraulic hotpress LP-50 series model no. M/C 9701 was used for preparing the thin film from polymer blend between styrene-acrylonitrile copolymer (SAN) and poly (methyl methacrylate) (PMMA). It has both the automatic mode and manual mode. In automatic mode, it has four steps (preheat, vent, full press and cooling step), that can be controlled in one touch which times adjustment of each of step separately. The hotpress can be compressed up to maximum 50 ton (160 kg/cm²). The picture of hydraulic hotpress are showed in figure 4.3

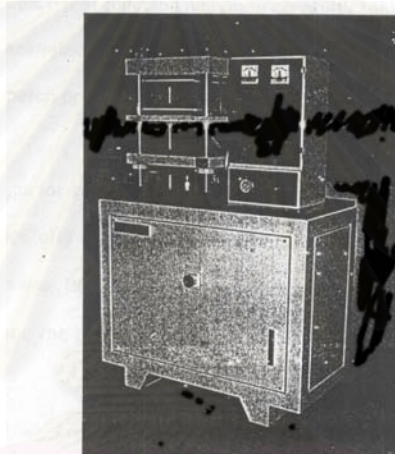


Figure 4.3 Automatic Hydraulic Hotpress LP-50.

4.2.3 Surface Temperature Probe and Digital Thermometer

The Cole-Palmer surface probe model E-08516-60 with 0.5 inch tip diameter, which has a temperature range from -250 to 649 °C, was used for measuring the temperature during the mixing of sample and measuring the temperature of hot plate during the phase separation of miscible samples.

4.2.4 Fourier Transform Infrared Spectrometer (FTIR)

The FTIR spectrometer is apparently used as a tool to observe all of the functional groups. Infrared radiation is generated by electrically heating source, which is fabricated from oxides of zirconium, thorium and cerium. The radiation splits into two beams, one beam is of fixed length and the others of variable length (movable mirror), as shown in figure 4.4. The combined beam then passes through a sample cell and once molecules absorb infrared radiation, each absorbed peak of molecule can represent different kinds of molecular rotation and vibration reflecting its functional groups. An analog signal is detected and transformed into a digital signal, which is then analyzed by a computer. Details of this machine can be found elsewhere [Silverstein *ed. al*, 1991]. A FTIR-Bruker spectrometer at the Spectroscopy Research Group, Department of Chemistry, Faculty of Science, Chulalongkorn University was used in this study as shown in Figure 4.5. Measurements were taken at 4.0cm^{-1} resolution and 1000 cycle per one scan.

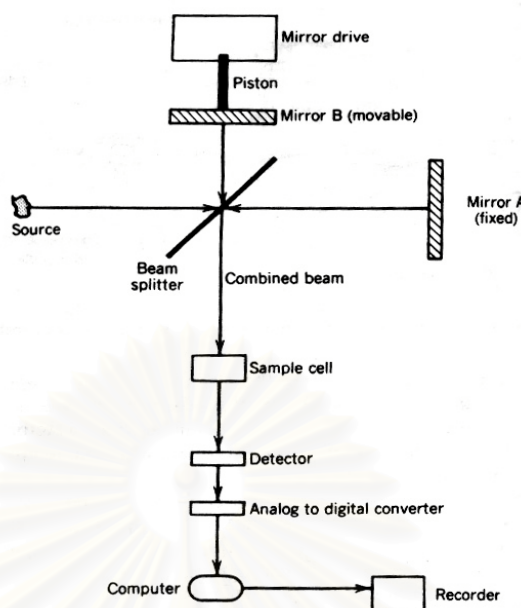


Figure 4.4 A schematic diagram of an FTIR spectrometer [Silverstein *et al*, 1991]



Figure 4.5 A FTIR-Bruker spectrometer at the Spectroscopy Research Group, Department of Chemistry, Faculty of Science, Chulalongkorn University

4.3 FTIR Studies

4.3.1 Sample Blending Preparation

The corrected amount of styrene-acrylonitrile polymer (SAN) and poly(methyl methacrylate) (PMMA) at desired weight ratio (30/70, 40/60, 50/50, 60/40, 70/30, 80/20, 90/10) were heated at 130 °C in a vacuum oven for 4 hours in order to remove any water. Pellets of the weight composition were melt and mixed in a PRISM twin screw extruder, which was operated at a torque of 60%, the screw speed of 30 rpm and the processing temperature range was 190-210 °C. The extrudate was cut into small beads using a PRISM pelletiser.

4.3.2 Sample Preparation Methods for FTIR Quantitative Analysis

Three methods: KBr disc, KBr cubics and film preparation, were used for preparing samples of FTIR quantitative analysis of SAN/PMMA blends

4.3.2.1 KBr Disc

One gram of blend samples of SAN/PMMA at following weight ratio: 30/70, 40/60, 50/50, 60/40, 70/30, 80/20, 90/10 were taken. Pellets at the determined weight composition were heated in oven for 1 hour in order to remove any water before melting hotplate at 180 °C for about 1 hour. The result sheets were abraded by the end of cutter in order to get powder samples as shown in figure 4.6. Then powder samples were blended with Potassium Bromide (KBr) that was heated in oven for 1 hour in order to remove any water. And then KBr powder was mixed with powder sample in ratio sample: KBr (1:100) in a mortar. After that the mixing samples were compressed at 5000 pounds in order to form the thin and clear disc. The

equipments for preparing KBr disc were shown in Figure 4.7. After that KBr Disc was put in sample holder for examining the IR-spectra.

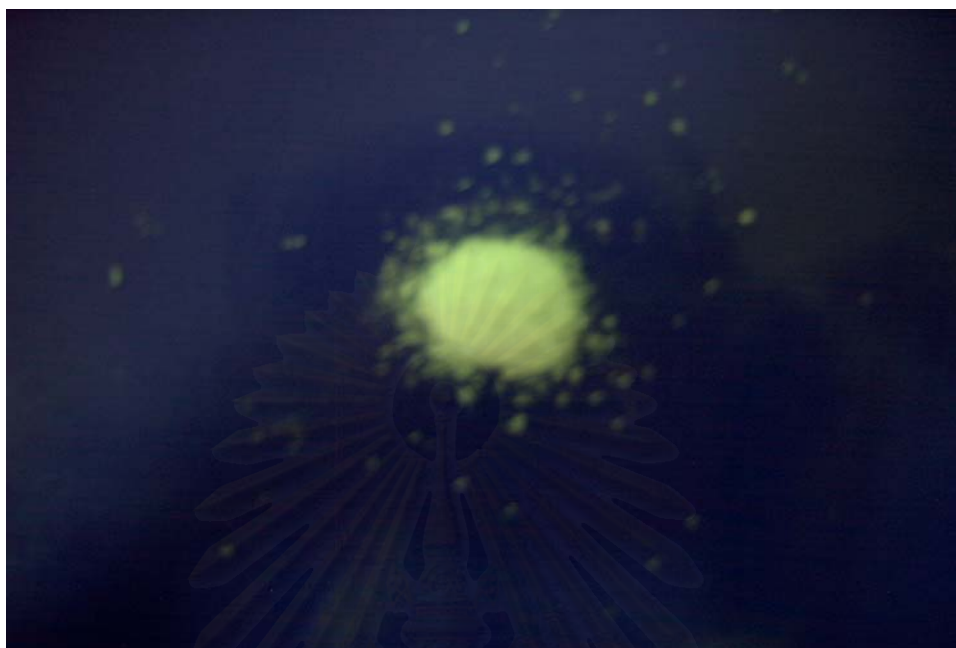


Figure 4.6 The powder sample of SAN/PMMA at blending Ratio 5:5



Figure 4.7 The equipment for preparing KBr disc.

4.3.2.2 KBr Cubics

One gram of blend samples of SAN/PMMA at following weight ratio: 30/70, 40/60, 50/50, 60/40, 70/30, 80/20, 90/10 were taken. Pellets at the determined weight composition were heated in oven for 1 hour in order to remove any water before melting on hotplate at 180 °C for 1 hour. The result sheets were cut in order to get the small samples by the cutter that was clean with water and acetone. Then small samples were melt on KBr cubic that were polished by sandpaper number 2000 and cleaned with water for smoothness surface and clearance. The suitable KBr cubics were shown in Figure 4.8. After that KBr cubics were put in sample holder for getting the IR-spectra.

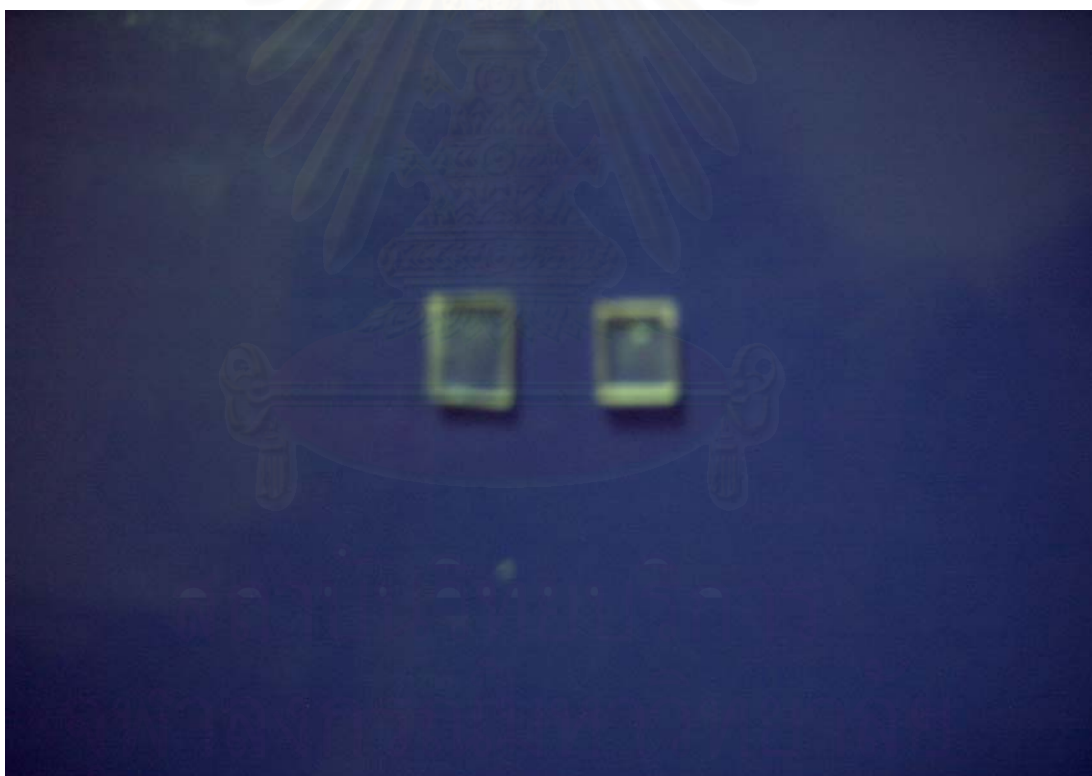


Figure 4.8 The Suitable Cubic KBr.

4.3.2.3 Film Preparation

One gram of blend sample of the desired weight 30/70, 40/60, 50/50, 60/40, 70/30, 80/20, 90/10 between styrene-acrylonitrile copolymer (SAN) and poly(methyl methacrylate) (PMMA) were taken. Pellets of the weight composition were heated in oven for 1 hour in order to remove any water before being compressed at 180 °C (miscible samples) between two keptons and two steel molds as shown in figure 4.9 under pressure of 50 ton by hotpress. The two keptons and two steel molds were cleaned by water and acetone two times before using. There are four modes in one compressing time that is preheating step, venting step, full compressing step and cooling step. In each of step, the times used were 10, 5, 30 and 5 min respectively. The resulted films, after first compressing, were approximately 0.03 mm in thickness. After that the thin film were cut in 0.5 * 0.5 mm for being compressed between two keptons and two steel molds by hotpress for four times at 180 °C under pressure of 50 ton. Finally the thickness of the resulted film was approximately 0.01 mm.

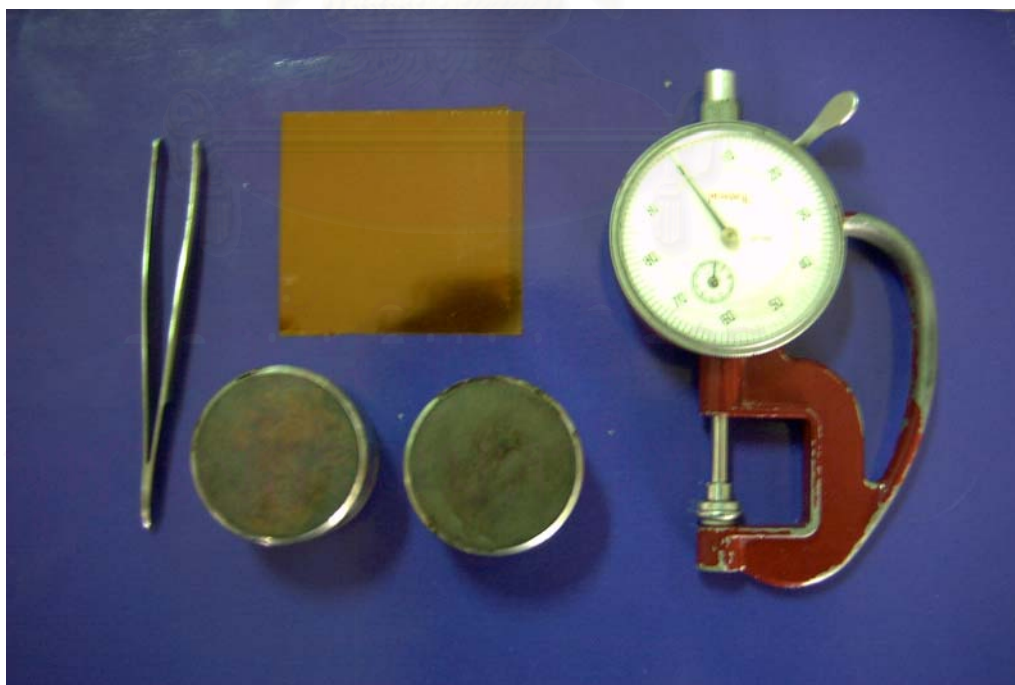


Figure 4.9 The set of apparatus for compressing films

4.3.3 Determination of Homogeneity in Three Preparation Methods by FTIR

4.3.2.1 For KBr Disc Method

The three KBr discs are prepared from blending KBr powder and samples of (50:50) SAN/PMMA at different positions of blend sample in each mortar. Each KBr disc was mounted on a holder for subsequent measurement of the spectra by FTIR spectrometer for comparing homogeneity and other effects.

4.3.1.2 KBr Cubics

The three KBr cubics are prepared by melting samples of (50:50) SAN/PMMA that were examine at different positions in sample sheet. After each sandwiched cubic was mounted on a holder for subsequent measurement of the spectra by FTIR spectrometer for comparing homogeneity and other effect.

4.3.1.3 Film Preparation

The 0.01 mm thick films of SAN/PMMA sample at blending ratio 5:5(SAN/PMMA) were prepared for three samples. The films were cut to a size of 5*5 mm to be examined at various different positions of the film. Each of the film was mounted on a holder for subsequent measurement of the spectra by FTIR for comparing homogeneity and other effects.

4.3.4 The Studies of Phase Separated Effect

The phase separation study of this polymer blend prepared by this method were continued to determined as follows:

4.3.4.1 Sample Preparation

The film with 0.01 mm thickness was cut to a size 5*5 mm for three pieces with different position of the film and was heated at 220 °C until the cloudiness was occurred in the film about 30 min and then the film was quenched. After that each of film was mounted on a holder for subsequent measurement of the spectra by FTIR spectrometer for comparing effects of phase separation in this polymer blend.

4.3.4.2 Second Derivative Method

Since an infrared spectrum is a mathematic function, its derivative can be calculated. The derivative of a spectrum can be taken a number of times, producing derivatives of different order. For instance, the first derivative of a spectrum is called a first order derivative, the derivative of the first derivative is called a second derivative [Brian, 1996]. The example a second derivative is shown in Figure 4.10. The second derivative contains three features corresponding to each absorbance peak in the original spectrum, two pointing upward and one pointing down. The bottom of a downward pointing feature in a second derivative corresponds exactly to wavenumber of maximum absorbance of a band in the original spectrum. For this reason the second derivative are used in library searching and peak picking. If there is a region of a spectrum where several bands have overlapped to form on broad band, the number of down pointing peaks in the second derivative gives a estimate of the number of overlapped bands in the region [Brian, 1996]. As a result, the second derivative of s spectrum should be examined prior to curve fitting.

For this blend, the FTIR spectra of phase separation samples were similar to miscible blend samples except the carbonyl peak. The peaks were compared with miscible samples by taking second derivative to both of spectra at carbonyl peak by using OMNIC program. At top of the second derivative peak in spectra was shown the position of wave number under carbonyl peak that occur, disappear or hidden in under carbonyl peak. The numbers of top of second derivative peaks between miscible sample and phase separation samples under carbonyl peak were compared.

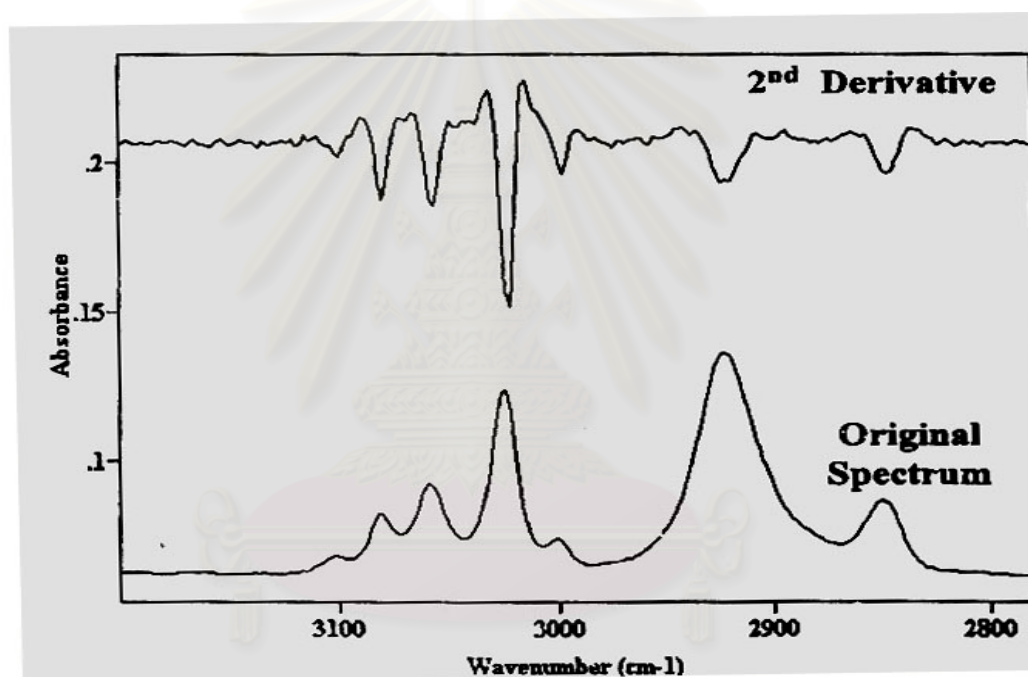


Figure 4.10 The example of second derivative technique. Bottom : The spectrum of polystyrene around 3000 cm^{-1} . Top: The second derivative of this spectrum [Brian, 1996].

4.3.4.3 Curve Fitting Technique and Detecting Area under Interesting Peak

The broad, overlapped feature of interest is examined by second derivative method for searching the number and position of interesting peaks. And then the curve fitting is used to simulate the position, width, height, location and shape of a several peaks that overlap to give a broad spectral feature. An example of an initial guess for a curve fitting is seen in Figure 4.11. The top spectrum is of a polystyrene/polycarbonate mixture. The middle spectrum in the figure shows the four peaks to be used in the initial estimate, and the bottom shows the residual. The residual is the difference between the actual spectrum and the spectrum calculated using the current set of curve fitting parameters.

For this blend, after the wavenumber of all peaks under carbonyl peak were noted from secondary derivative method, the curve fitting method was demanded in order to simulate the ratio of peaks that are hidden in the carbonyl peak of miscible sample and phase separation sample at the wavenumber that were noted. The curve fitting method OPUS program, which can demonstrate the ratios of hidden peaks under carbonyl peak. After that the hidden peaks were determined the area under each peak by using OMNIC program. The results of each area under hidden peaks of miscible samples were compared with each area of phase separation samples.

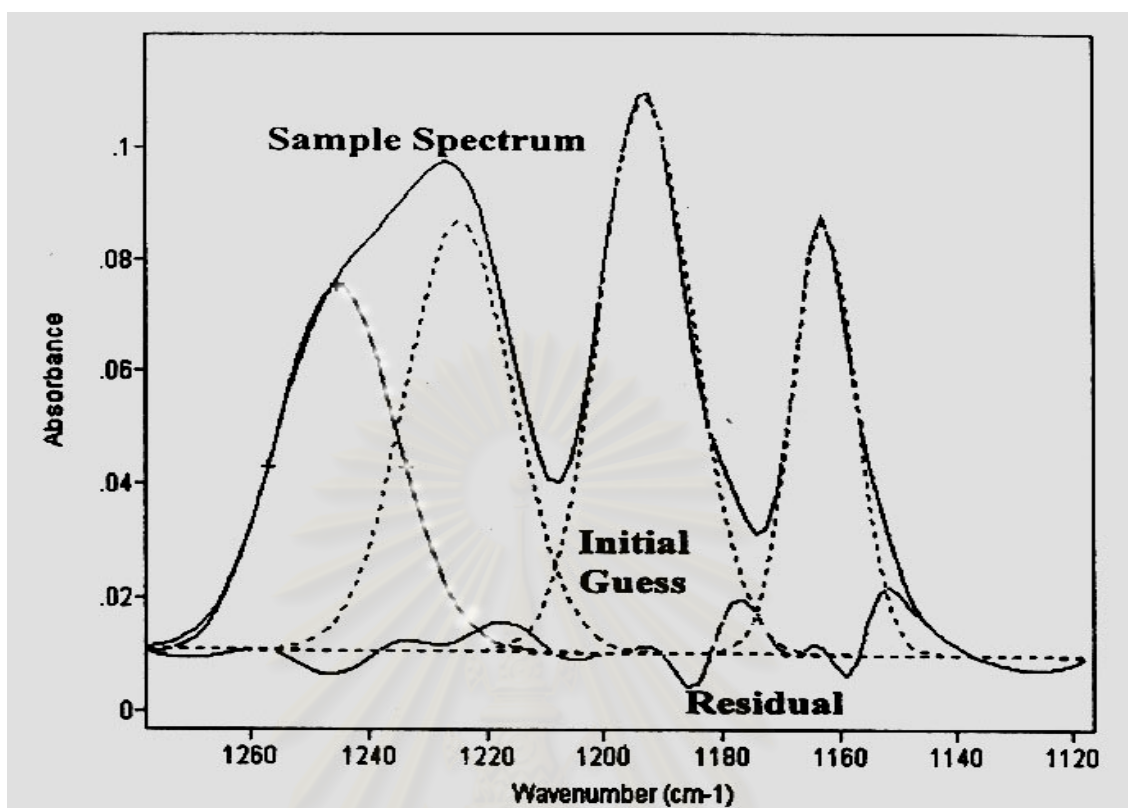


Figure 4.11 An example of an initial a guess at a set of bands to be used in a curvefit. The top spectrum is of the sample, the middle displays the bands to be used as the initial guess, and the bottom shows the residual.

สถาบันวิทยบริการ
จุฬาลงกรณ์มหาวิทยาลัย

CHAPTER V

RESULT & DISCUSSIONS

Polymer blends of styrene-acrylonitrile copolymer (SAN) and poly (methyl methacrylate) (PMMA) were examined here. The objectives of this thesis are to find the suitable sample preparation method for FTIR quantitative analysis, study of miscible spectra and phase separation spectra at any ratio of blending and predict the ratio of unknown sample of this polymer blend by using Fourier Transform Infrared Spectroscopy (FTIR).

The explorations performed in these works are divided into three parts as follows.

Part I The finding of the suitable sample preparation method for FTIR quantitative Analysis.

In this part, the blending preparation via melt mixing was performed. Polymer blends of SAN/PMMA were mixed by twin screw extruder. Then the blending samples of SAN/PMMA were prepared in several methods for quantitative FTIR such as KBr disc method, KBr cubic method and film preparation method. The preparation methodologies of mixing sample and the sample preparation methodologies for FTIR quantitative analysis were described in Chapter 4 section 4.3. The spectra of these polymer blends at the same ratio were compared in order to study the effects of preparation method for examination by FTIR and find the suitable sample preparation method that gave the accurate spectra for quantitative FTIR analysis. The FTIR spectra of this polymer blend can be constructed by plotting absorbance (A) against wavenumber (cm^{-1}).

Part II The studies of the spectra of miscible samples and phase separation samples at any blending ratio by FTIR.

In this part, the accurate FTIR spectra of miscible and phase separated blend that have the suitable preparation method were observed. The differences of spectra of miscible samples and phase separation samples were investigated by taking second derivative of the spectra of this polymer blend at those conditions by using OMNIC program. The second derivative spectra were shown the position of the small peak that hidden or overlapped in the main spectra of this polymer blend. After that by using the curve fitting of OPUS program, the area under the small peaks of miscible spectra were compared with the area under the small peaks of phase separation spectra to study effects of phase separation on this polymer blend. The comparing area under small peak between miscible spectra and phase separation spectra can be constructed by plotting area under interesting peak against blending ratio.

Part III The prediction of unknown blend sample between SAN/PMMA

In this part, the accurate FTIR spectra of miscible and phase separated blend from the suitable preparation method were investigated by using OMNIC program. The ratio of area under carbonyl peak of PMMA at wave number 1732 cm^{-1} and area of mono-substitution of aromatic in SAN at wave number 700 cm^{-1} were investigated at various compositions in order to predict the composition of unknown samples of this polymer blend.

จุฬาลงกรณ์มหาวิทยาลัย

5.1 The Finding of The Suitable Sample Preparation Method for FTIR Quantitative Analysis.

The polymer blend of styrene-acrylonitrile copolymer (SAN) and poly (methyl methacrylate) (PMMA) was investigated in this study due to the fact that it is miscible at all compositions at room temperature and can exhibit lower critical solution temperature (LCST) behavior, i.e. the blend can transform from clear (miscible) to cloudy state (phase separation) when heated and there are many studied information of this polymer blend such as the total reduction energy in system when blended because of the reduction of the dissipation energy in the SAN molecule. The preparation blending method via melt mixing was performed, because there is no effect from other impurity especially the common solvent. The sample preparation methods for FTIR quantitative analysis had three methods as aforementioned in Chapter 4 section 4.3.

The sample preparation methods for FTIR quantitative analysis were investigated at 50% weight composition of SAN and PMMA such as KBr disc, KBr Cubic and film preparation.

From the obtained absorbance (A) and wavenumber (cm^{-1}), the FTIR spectra of SAN/PMMA at 50% weight SAN/PMMA can be constructed by plotting the absorbance (A) against wavenumber (cm^{-1}).

5.1.1 Discussions

The IR spectra of the 50% weight SAN/PMMA by varying three preparation methods: KBr Disc, KBr Cubic and film preparation are shown in Figure 5.1 to 5.5. For the first method, KBr Disc, it has three effects that are considered: the absorption of moisture in air of KBr powder, the size of grounded samples and non-linearity effect.

Figure 5.1 showed the effects that occurred from absorption moisture in air of KBr powder at wavenumber 3440 cm^{-1} . Due to the moisture in air that can be absorbed by dry KBr powder, the IR spectra at the mark (*) represent the moisture peak of the moisture that can be overlapped to the C-H stretching peak of blending samples at wave number $3200\text{-}2900\text{ cm}^{-1}$. With these effects, the result spectra were hard to investigate and not suitable for preparing IR spectra for quantitative analysis by FTIR of this system.

Figure 5.2 illustrated the secondary effect of Kbr disc that is concerned with the size of grounded samples. This effect is very important because the size of grounded samples affects the spreading of the sample in KBr disc. If the sizes of grounded sample are large, there are two phenomena that can occur which are the non-homogeneity of sample in KBr Disc and the reflection of IR light. The results in figure 5.2 showed the effects of non-homogeneity of sample in KBr disc supported by the unsimilarity of the three spectra of the same material. With these effects, the result spectra were hard to investigate and can not be applied for quantitative analysis by FTIR.

Figure 5.3 showed the non-linearity effect which is also importance for examining the good IR spectra. This effect is occurred from the excess amount of sample in KBr powder. From the equation 3.7.6, Beer-Lambert law, the absorbance will be linearly proportional to concentration when the absorbance is not over one (completely absorb) when absorbance (A) of samples are higher than 1, the appeared absorbances are not linearly proportional to concentration. Because of this effect, the ratio of the sample peak that are marked to the C-H stretching are not vary linearly with the concentration, so the result spectra were hardly investigated and can not be applied for quantitative analysis by FTIR.

Figure 5.4-5.5 showed the IR spectra from the KBr cubic method. There were also two concerned effects with this method: the qualities of cubic and non-linearity effect.

Figure 5.4 showed the first effect, the quality of KBr cubic. This effects were importance to examine the good IR spectra by KBr cubic method because the IR spectra obtained is depended on IR light. If the IR light intensity was low or disturbed by clearance or air gap between two cubics, the IR spectra were unaccurated as shown in figure 5.4.

Figure 5.5, the secondary effect, non-linearity effect, is investigated. This effect was concerned with the excess amount of sample on KBr cubic. The result of this effect is similarly to the effect that occurred in KBr disc. Because the absorbance (A) is over 1, the ratio of each peak that exceed one in the spectra are unaccurated due to the absorbance is not followed the Beer & Lambert law, so the IR spectra were unaccurated as shown in figure 5.5.

Figure 5.6 showed that the suitable IR spectra for FTIR quantitative analysis was obtained by the film preparation method. However, non-linearity effect should be considered. This effect depends on the thickness of film that were prepared. In this work, the thicknesses of the films were controlled at 0.01 millimeter to fall in the range of the Beer & Lambert law (absorbance not over 1).

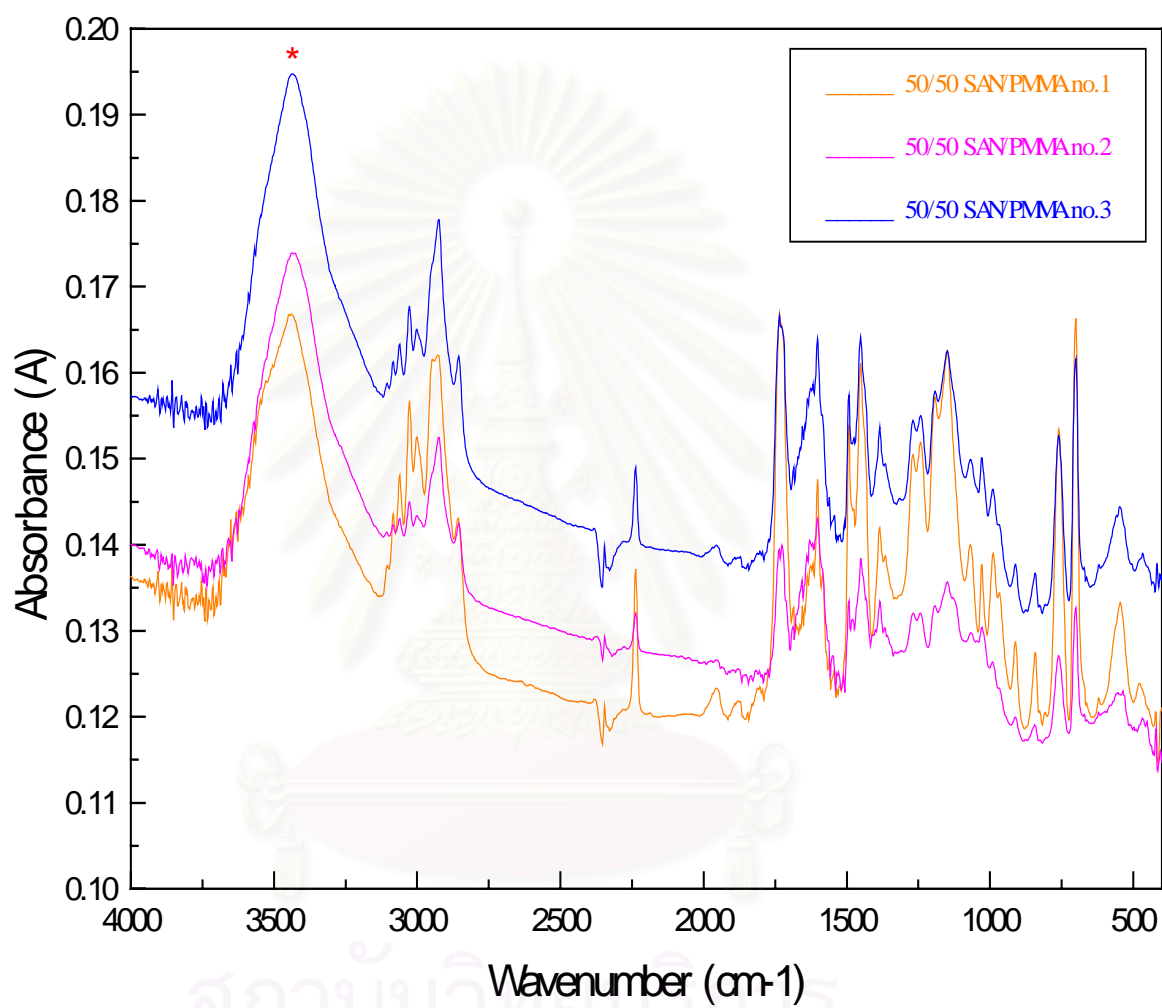


Figure 5.1 The water absorption effect in KBr Disc method.

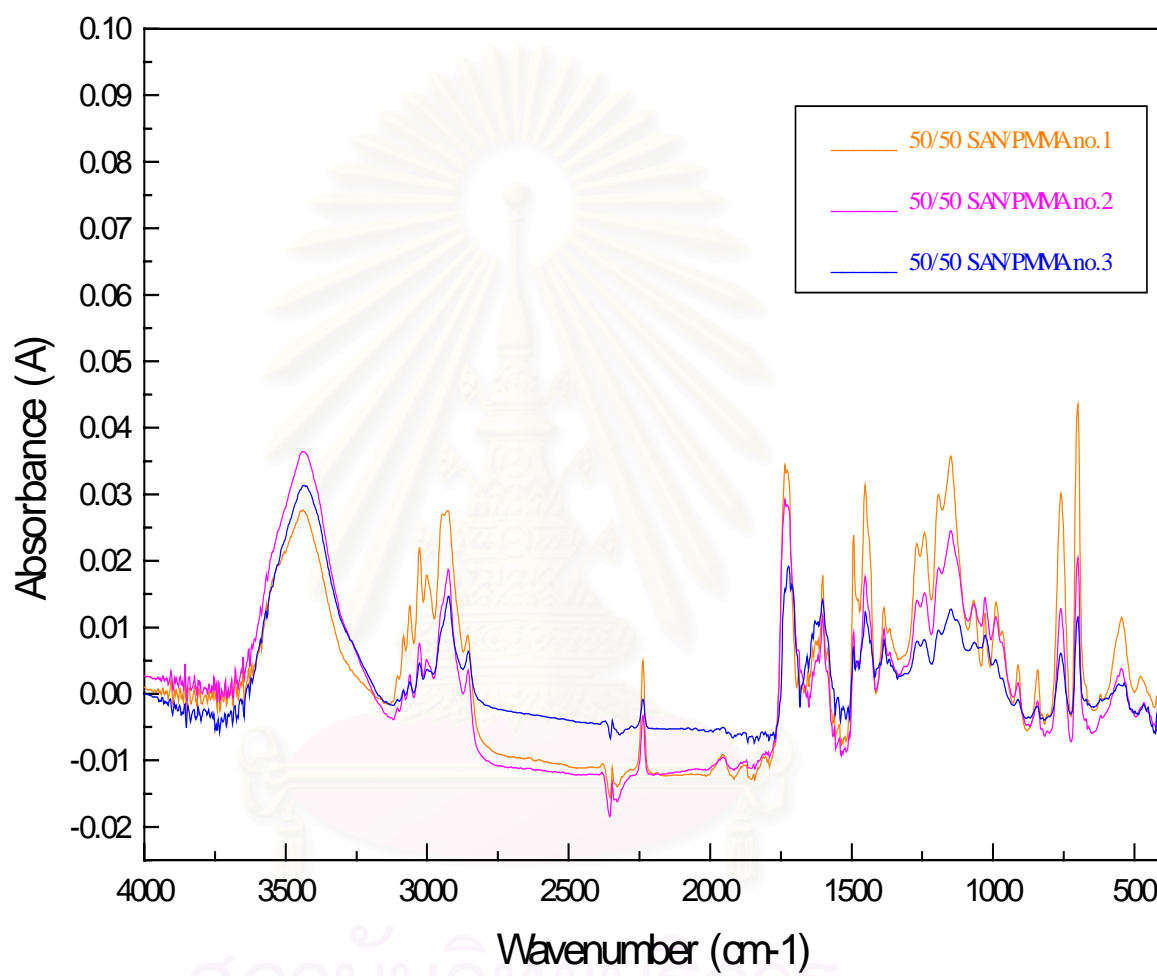


Figure 5.2 The effect from size of ground sample in KBr Disc method.

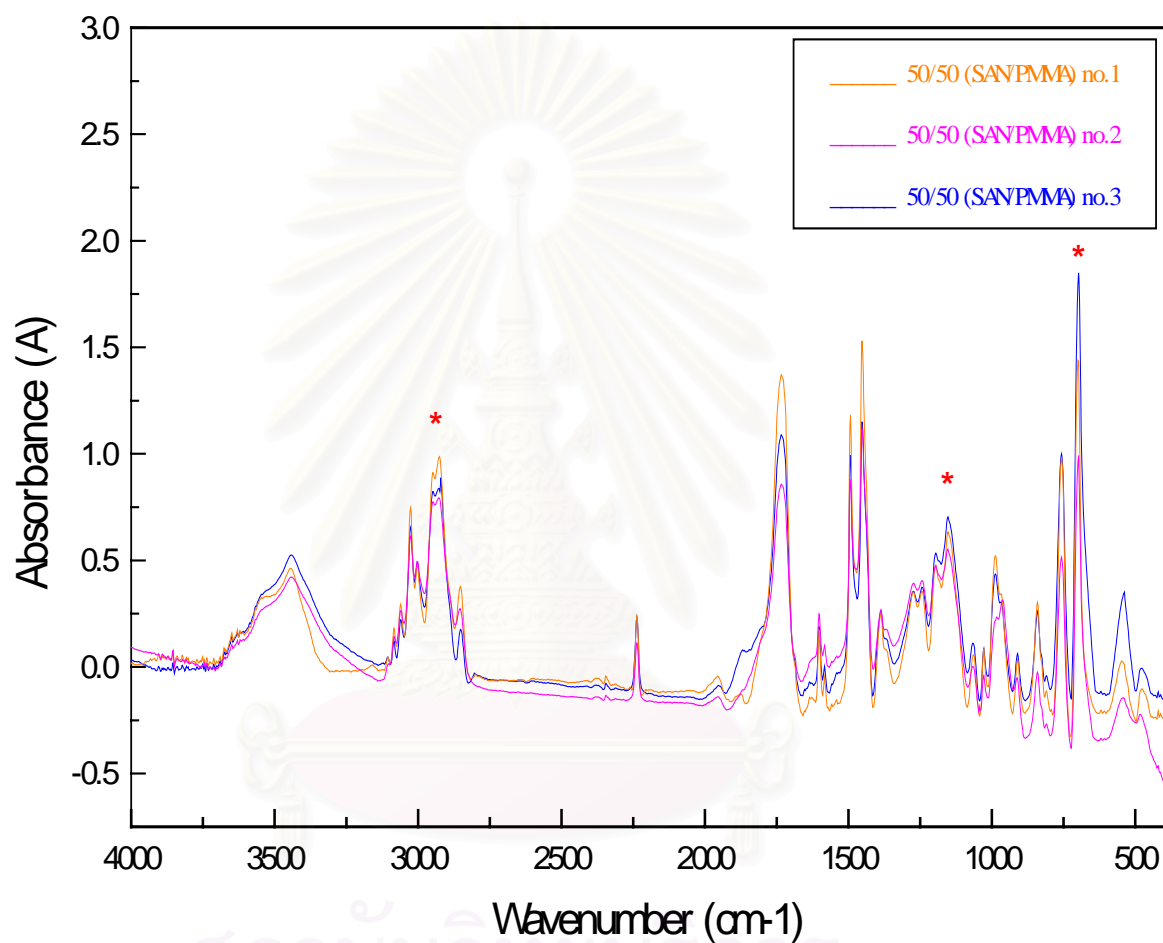


Figure 5.3 The non-linearity effect in KBr Disc method.

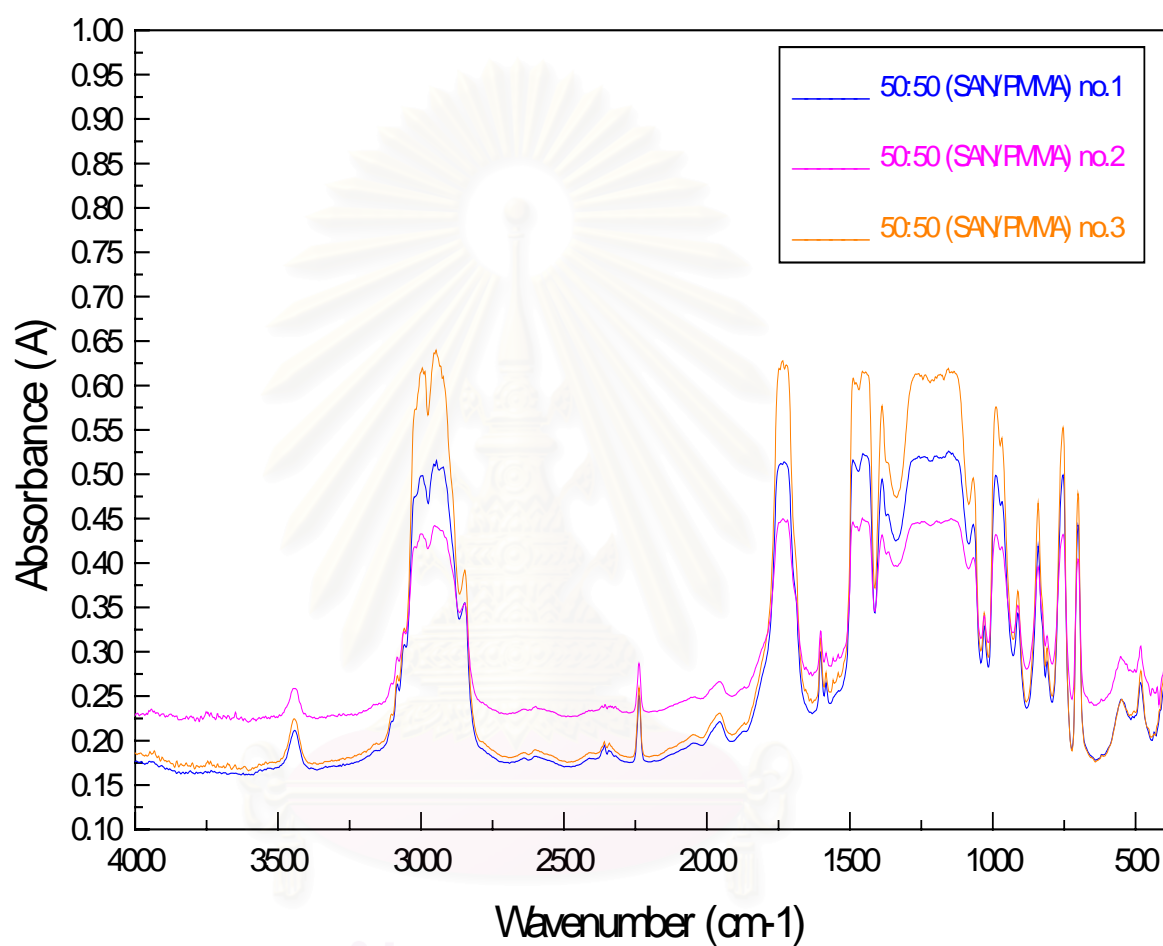


Figure 5.4 The smoothness and clearness effect in KBr Cubic method.

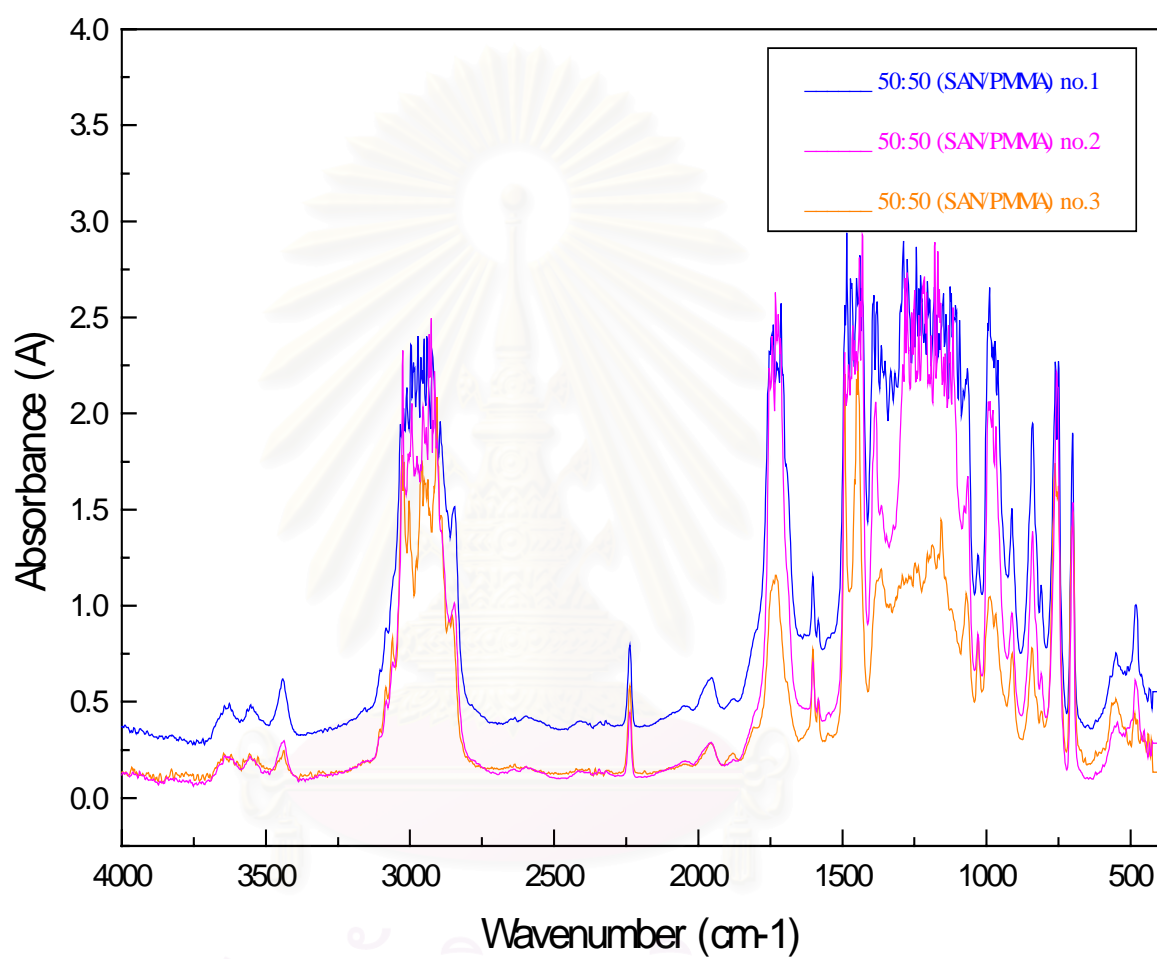


Figure 5.5 The nonlinearity effect in KBr Cubic method.

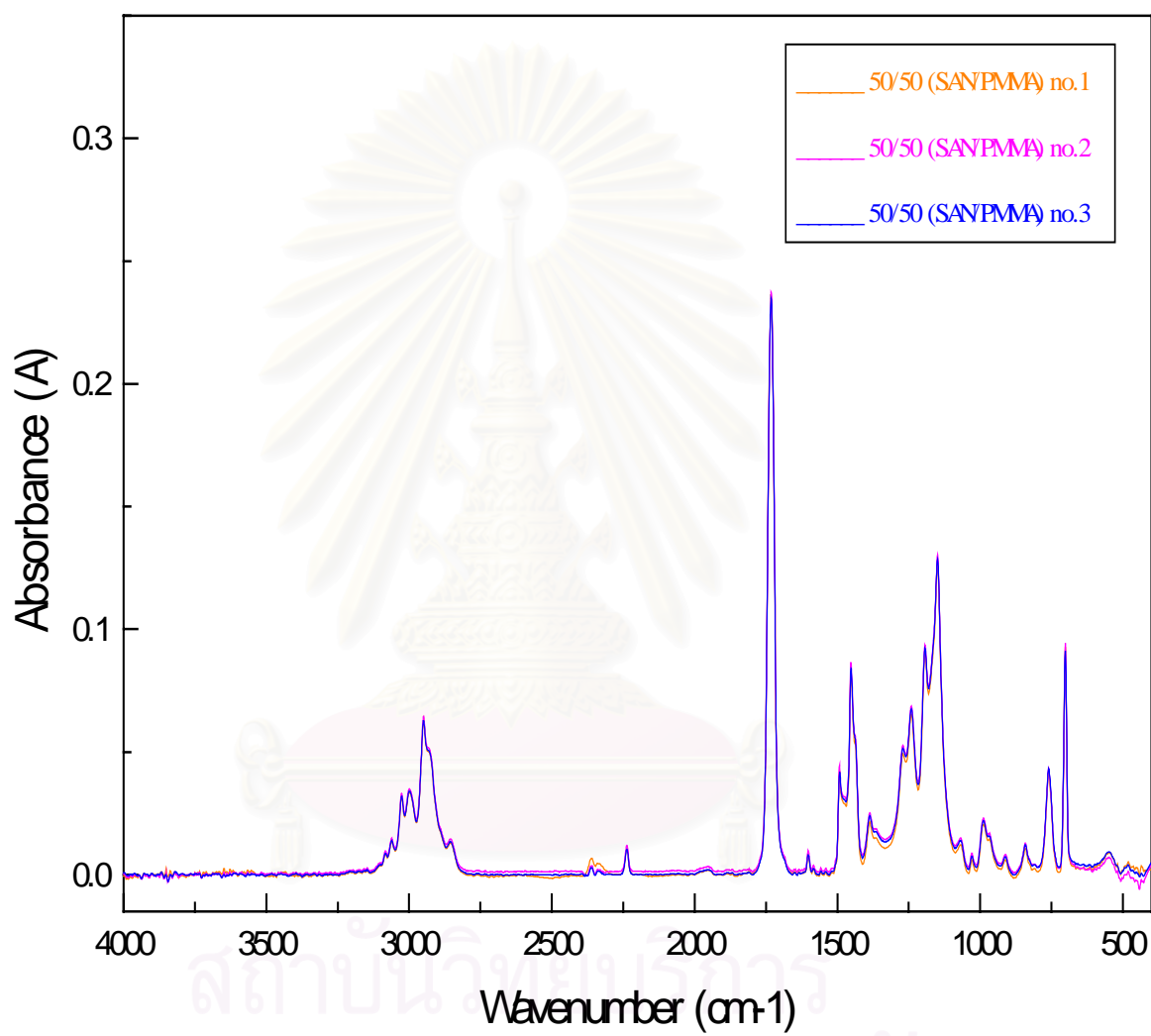


Figure 5.6 The suitable spectra for quantitative analysis by film preparation method.

5.2 The difference in spectra of the miscible samples and phase separated samples at various concentrations by FTIR

The prepared IR spectra of SAN/PMMA blends for quantitative analysis by film preparation method were performed as described in Chapter 4 section 4.3.2.3. In this section, the differences of spectra from miscible samples and phase separated samples at various compositions were shown in figure 5.7 and 5.8 respectively. The films of each composition were prepared in two times (1, 2) and each films were cut in three pieces (A, B, C) for examining the spectra. The spectra obtained were checked for the homogeneity of mixing in both of the samples by using OMNIC program at various concentrations as shown in Figure 5.9 to 5.22. When the homogeneity were accepted, the comparing of second derivative and finding the number of peaks under carbonyl peaks between miscible samples and phase separated samples were continued as shown in Figure 5.23 to 5.29. Then the curve fitting method were applied to simulate the ratio of the peaks under carbonyl peaks of SAN/PMMA at various compositions as shown in Figure 5.30 to 5.45. After the ratio of all peaks under carbonyl peaks of miscible samples and phase separated samples were obtained, the areas of each peak under carbonyl peak between miscible samples and phase separated samples were compared and investigated as shown in Figure 5.46 to 5.50. In Figure 5.7 to 5.45, the FTIR spectra can be constructed by plotting the absorbance (A) against wavenumber (cm^{-1}). In Figure 5.7 to 5.22, the homogeneities of various compositions can be showed. In Figure 5.46 to 5.50, the area of each peak under carbonyl peaks can be constructed and compared by plotting the ratio of area under interesting peak to area under cyanide peak against weight percent of SAN in the samples.

5.2.1 Discussion

In order to study the effect of phase separation to IR spectra of the SAN/PMMA blends at various compositions by using FTIR. Firstly the IR spectra of miscible samples and phase separated samples at weight percent of SAN (30, 40, 50, 60, 70, 80, 90% wt) were prepared by film preparation

method. At all compositions of samples, the films were prepared two times (1, 2) and were cut to three parts (A, B and C), each part of film was measured by FTIR in order to check homogeneity of sample mixtures as shown in figure 5.9-5.22.

After getting the suitable IR spectra at various compositions, the differences of spectra of miscible samples and phase separated samples were investigated by taking second derivative to the spectra of these samples by using OMNIC program. The second derivative spectra of miscible samples were compared with the second derivative spectra of phase separated samples. After taking second derivative of the spectra, the results showed that under the carbonyl peak of all miscible spectra, there were five hidden peaks. But at carbonyl peak of all phase separated spectra, there was four peak under them. The differences of peak at wave number 1726 cm^{-1} of all composition of blending were investigated as shown in figure 5.23-5.29.

The peak positions of wavenumber that examined from taking second derivative of all compositions of mixture samples between miscible samples and phase separated samples were noted, which are at wave number $1720, 1726, 1732, 1738$ and 1747 cm^{-1} . But, due to the resolution that used in this measurements for FTIR spectrometer can not set to be narrower than 4 cm^{-1} , FTIR will scan the sample with increasing wavelength every four cm^{-1} . So at this resolution FTIR might not be sensitive enough for finding small peaks of phase separated samples. For this reason, the root mean square error (RMS error) of simulated spectra that occurred from five hidden peaks in case of miscible blends and that occurred from four hidden peaks in case of phase separated blends were begun at 50 %wt composition (SAN/PMMA) as shown in figure 5.30 and 5.31. Figure 5.30 and 5.31 showed that the carbonyl of phase separated samples should be better represented from five hidden peaks more than from four peaks because the RMS error of simulated peak from five hidden peak is lower than that from four hidden peaks. The result from second derivative and curve fitting technique showed the number of hidden peaks that hid under carbonyl peak. The numbers of hidden peaks demonstrated the environments of carbonyl bond in the blend. For example, in case of miscible

samples and phase separated samples, there are five hidden peaks under carbonyl peaks. It illustrated that there are five types of carbonyl movement that combine to real carbonyl peak. But FTIR can not distinguish the conformation of each carbonyl peaks in polymer blend. After known the actual number of simulated peaks of both miscible samples and phase separated samples, the area under five hidden peaks of both miscible spectra and phase separated spectra were compared by using OMNIC program. The curve fitting technique by OPUS program was applied in order to simulate the actual ratio of the five positions of hidden peaks that form carbonyl peak at all compositions of the mixture samples as shown in figure 5.32-5.45.

After simulating the ratio of hidden peaks, the area under the interesting peak of miscible samples and phase separated samples were measured by using OMNIC program. Figure 5.46, 5.47 and 5.49 showed the area of peak at wavenumber 1720, 1726, 1738 cm^{-1} that had the same trend. It shows that there are three types of carbonyl peaks in polymer blend. When considered each of miscible samples or phase separated samples, the area under each peak at high concentration of PMMA was larger than at low concentration of PMMA. So that the quantity of this peak was depended on quantity of PMMA composition. When comparing the carbonyl peak of the same composition of the blend, the areas under peak 1720, 1726, 1738 cm^{-1} of miscible samples are higher than the area under peaks of phase separated samples. It might be concluded that the peak at wavenumber 1720, 1726 and 1738 cm^{-1} might be the difference movement of carbonyl bond of PMMA at different conformation in this polymer blend. Because of the phase separation, the Gibb's free energy between SAN and PMMA blend in the system will be increased. For this reason, the phase separated samples should absorbed the IR energy less than miscible samples so the areas under carbonyl peak of miscible sample are higher than those of phase separated samples at the same movement of carbonyl peak(λ). Figure 5.48 and 5.50 showed that the area of the peak at wavenumber 1732, 1747 cm^{-1} did not have the correlation. So no conclusion for this was made.

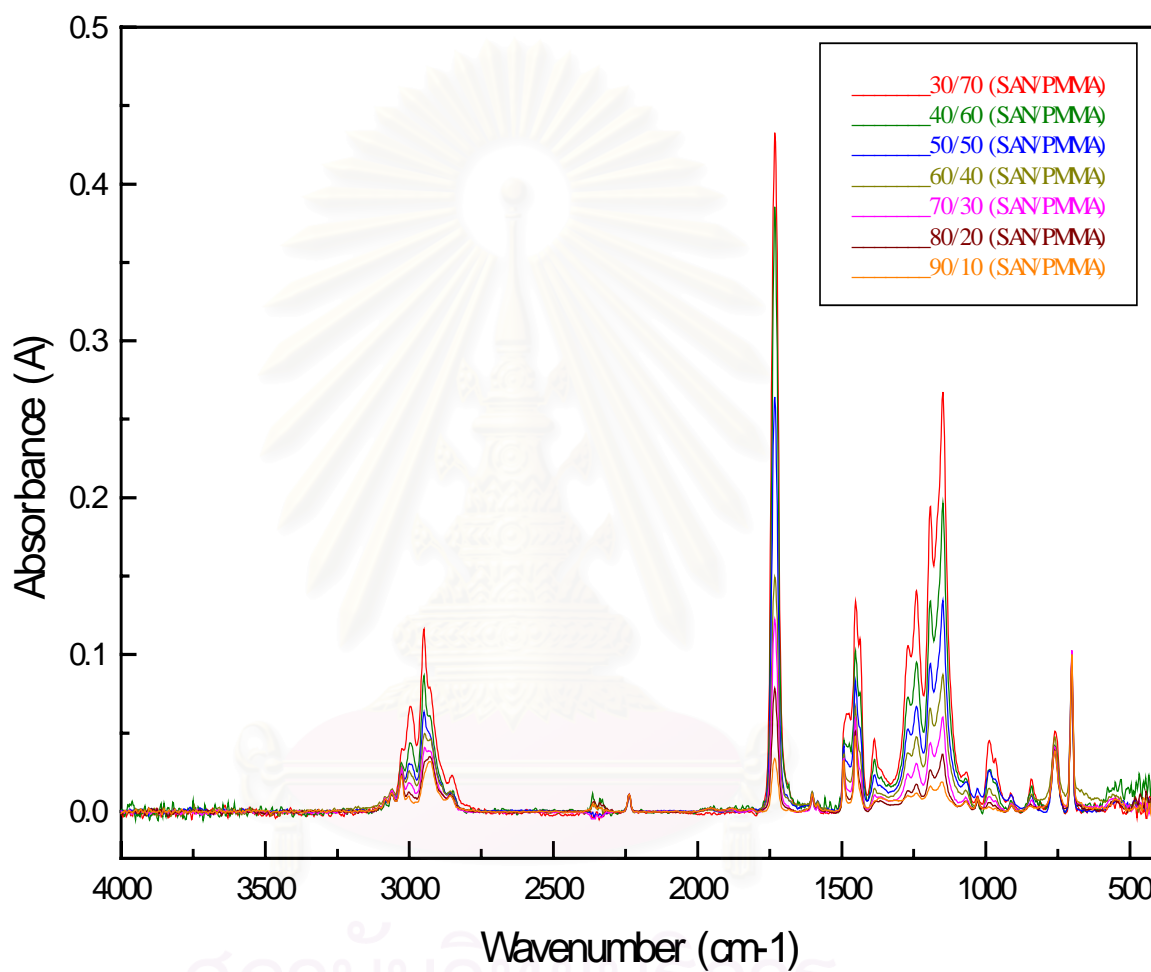


Figure 5.7 The IR spectra of miscible sample between SAN/PMMA blends prepared by film preparation method.

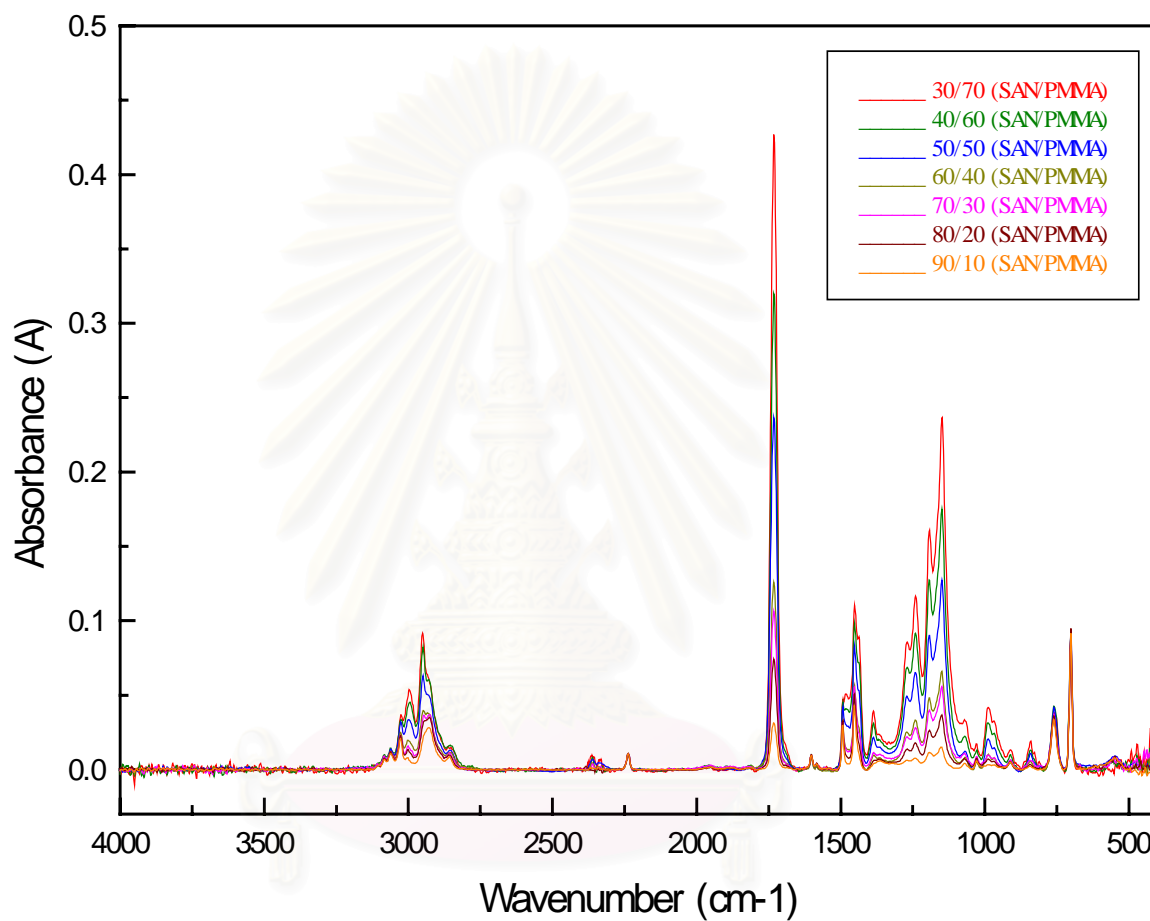


Figure 5.8 The IR spectra of phase separation sample between SAN/PMMA blends prepared by film preparation method.

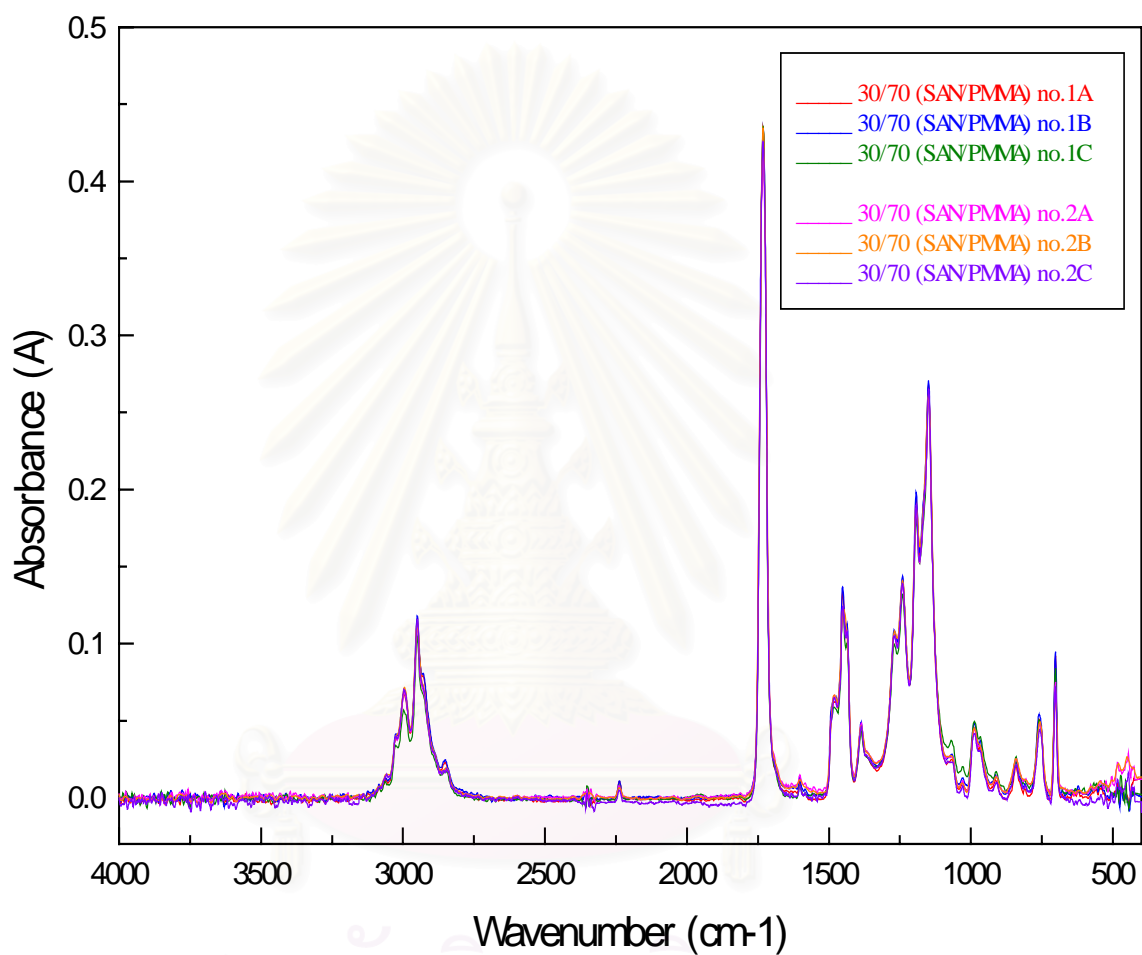


Figure 5.9 Detecting homogeneity of the IR spectra of miscible sample at composition ratio of blending 30% weight of SAN.

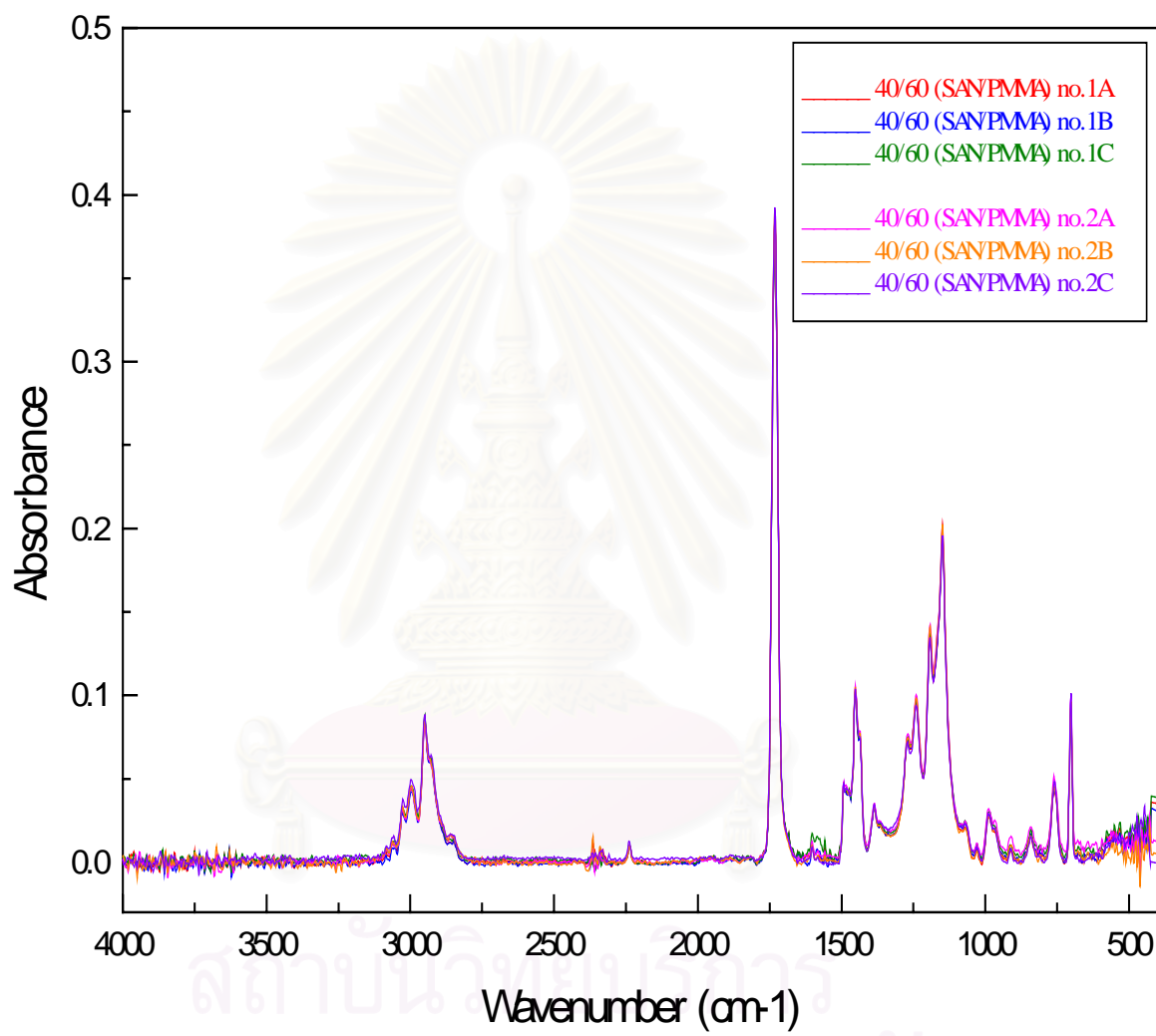


Figure 5.10 Detecting homogeneity of the IR spectra of miscible sample at composition ratio of blending 40% weight of SAN.

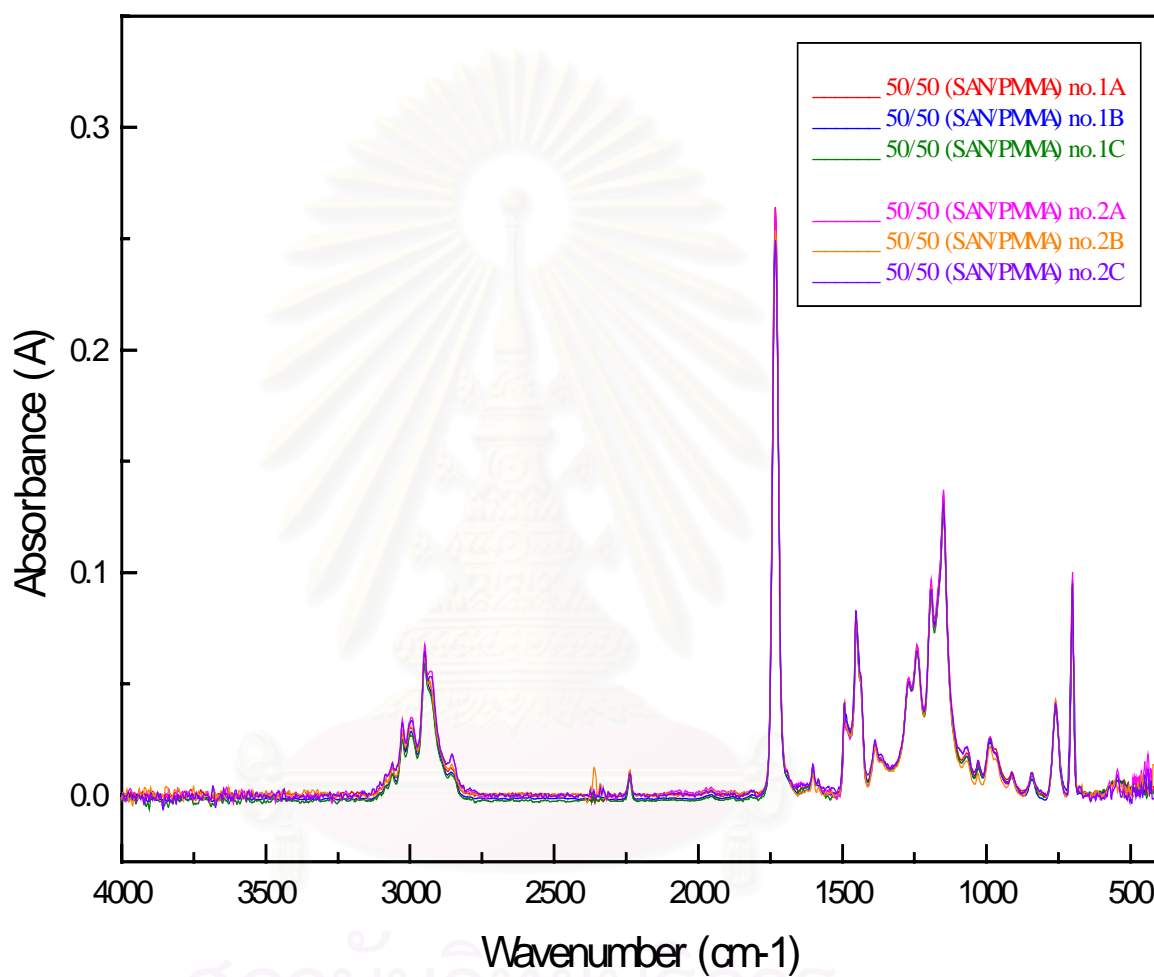


Figure 5.11 Detecting homogeneity of the IR spectra of miscible sample at composition ratio of blending 50% weight of SAN.

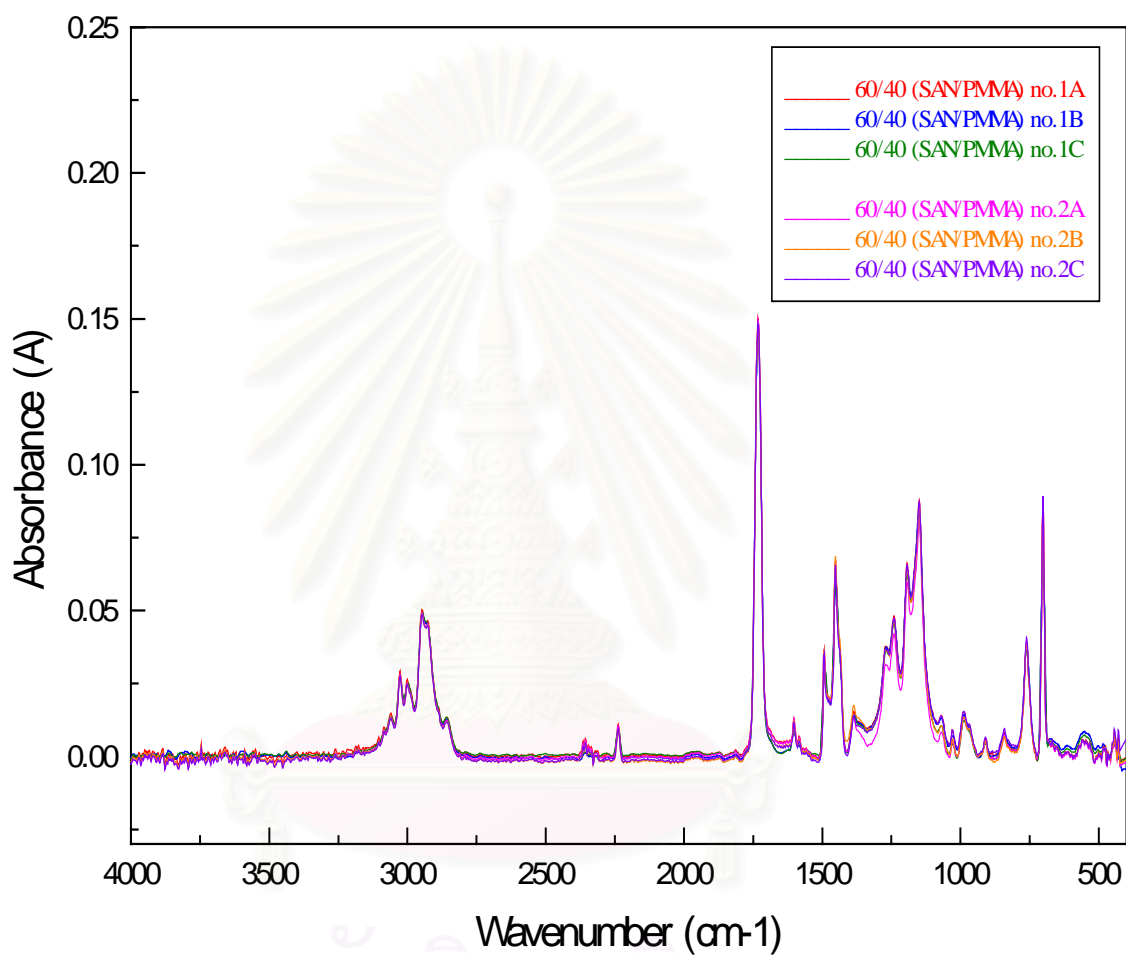


Figure 5.12 Detecting homogeneity of the IR spectra of miscible sample at composition ratio of blending 60% weight of SAN.

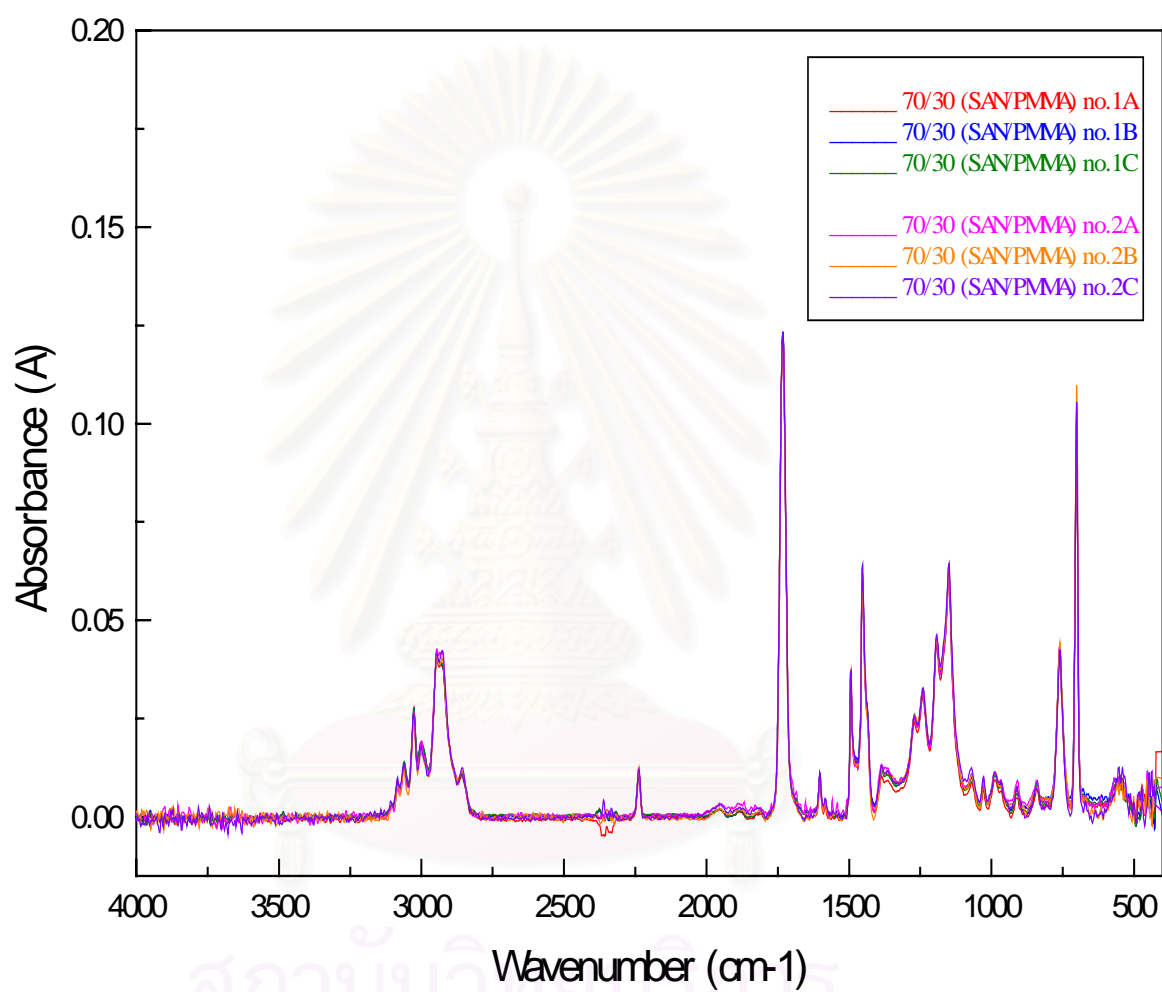


Figure 5.13 Detecting homogeneity of the IR spectra of miscible sample at composition ratio of blending 70% weight of SAN.

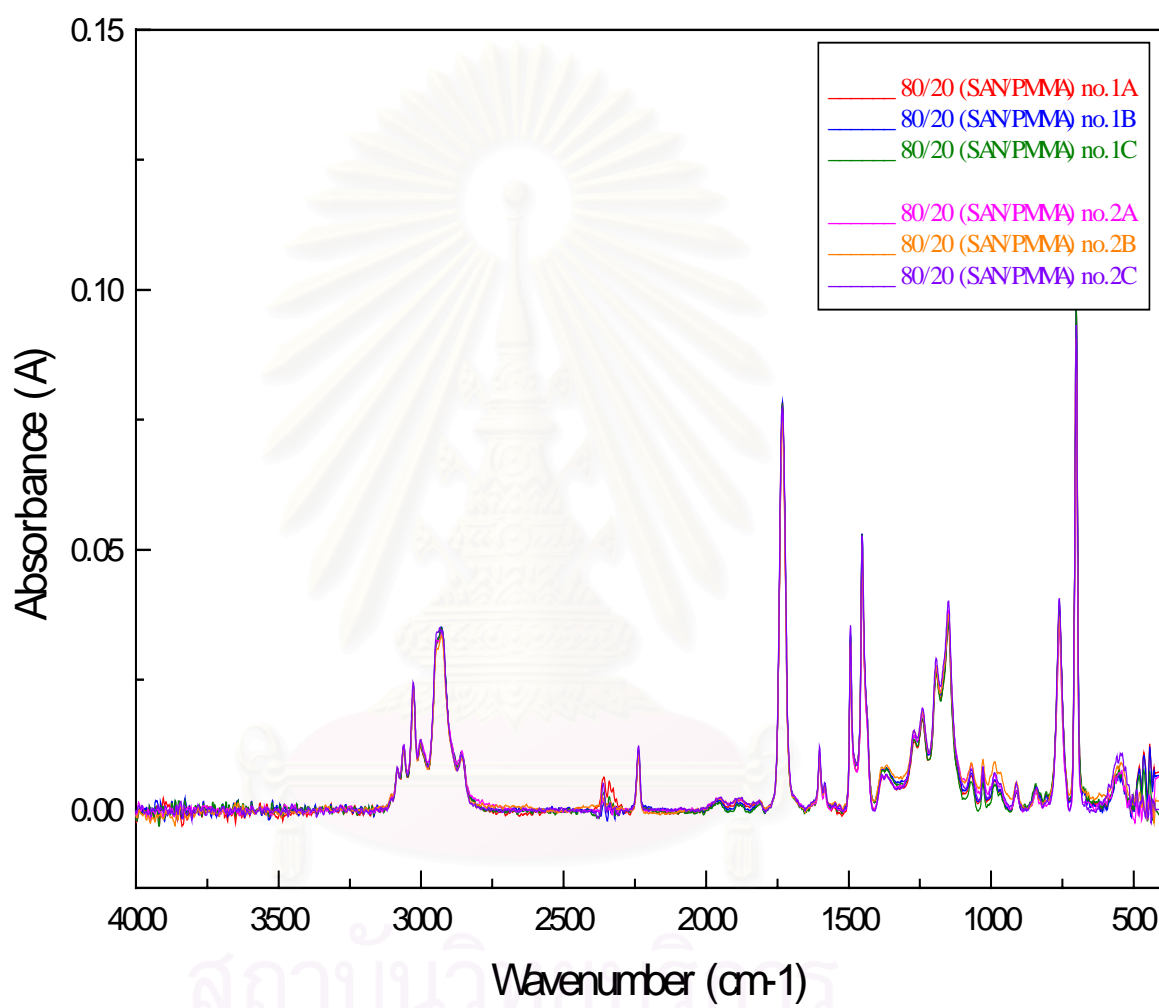


Figure 5.14 Detecting homogeneity of the IR spectra of miscible sample at composition ratio of blending 80 % weight of SAN.

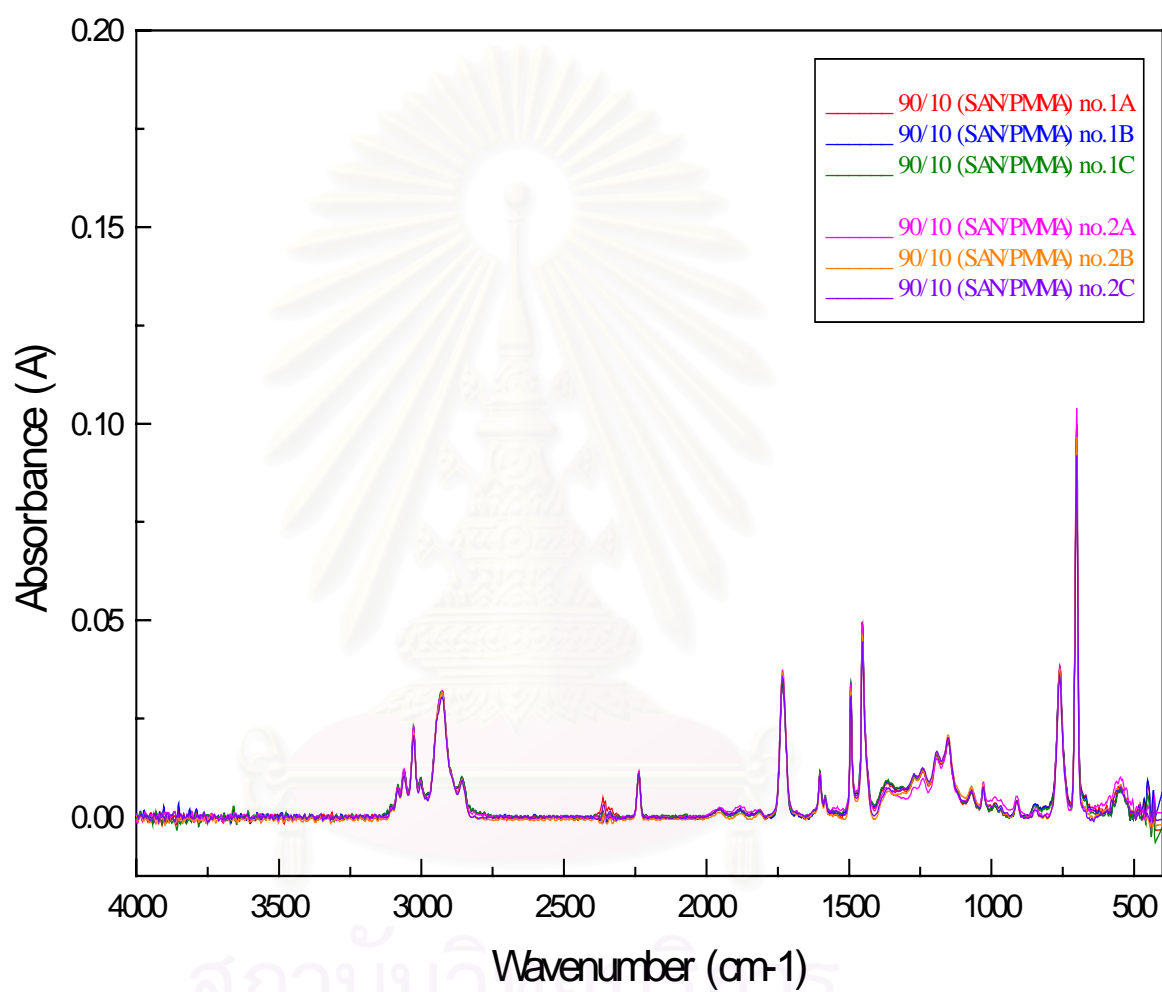


Figure 5.15 Detecting homogeneity of the IR spectra of miscible sample at composition ratio of blending 90% weight of SAN.

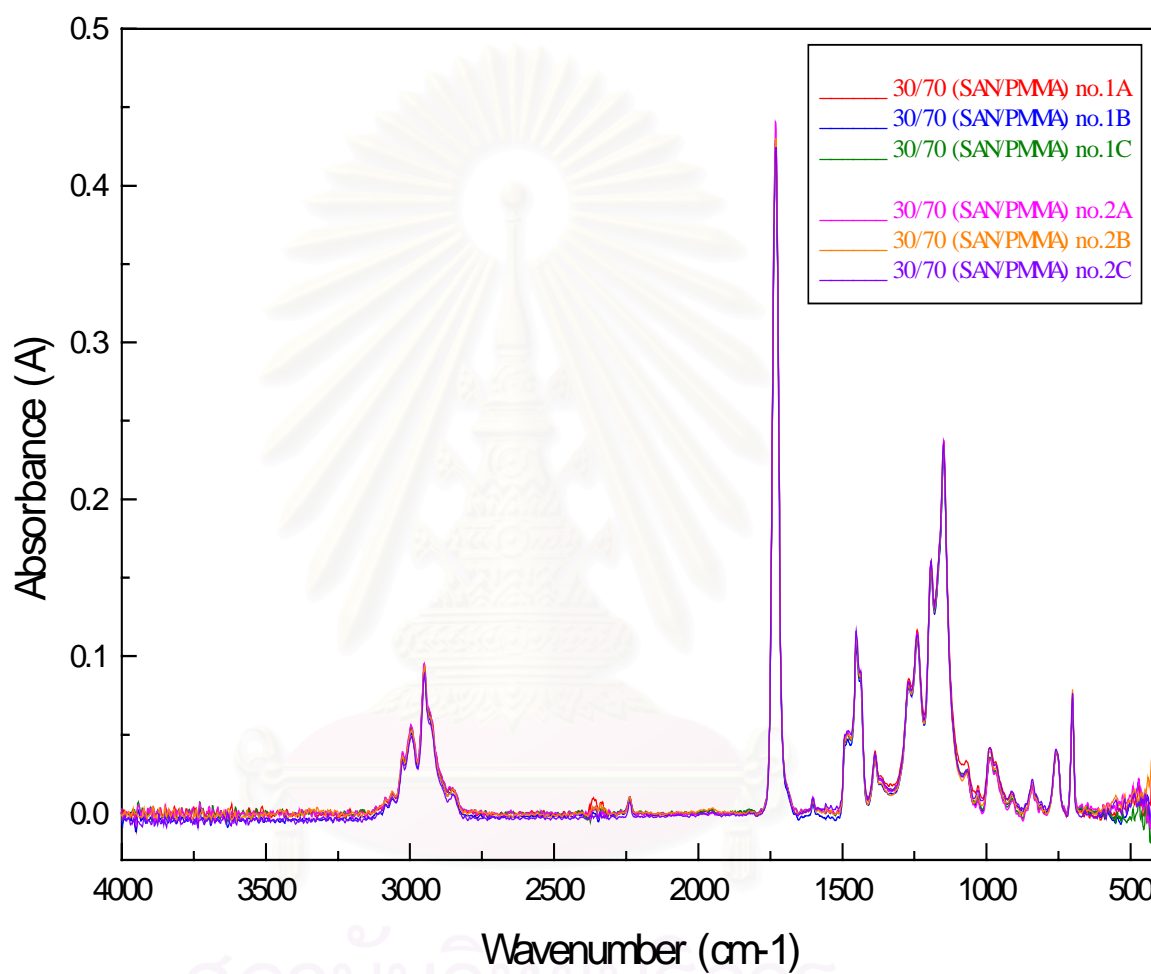


Figure 5.16 Detecting homogeneity of the IR spectra of phase separation sample at composition ratio of blending 30% weight of SAN.

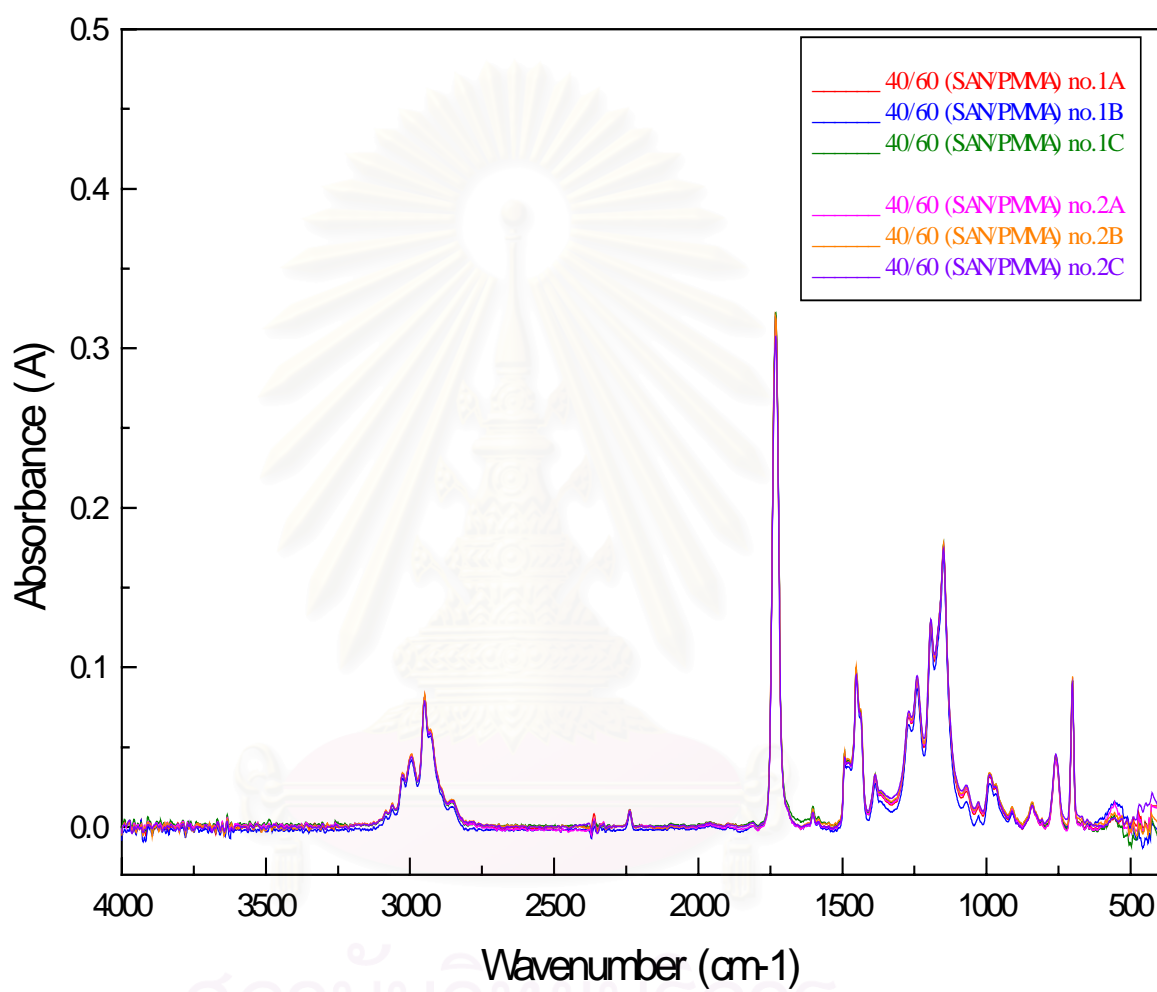


Figure 5.17 Detecting homogeneity of the IR spectra of phase separation sample at composition ratio of blending 40% weight of SAN.

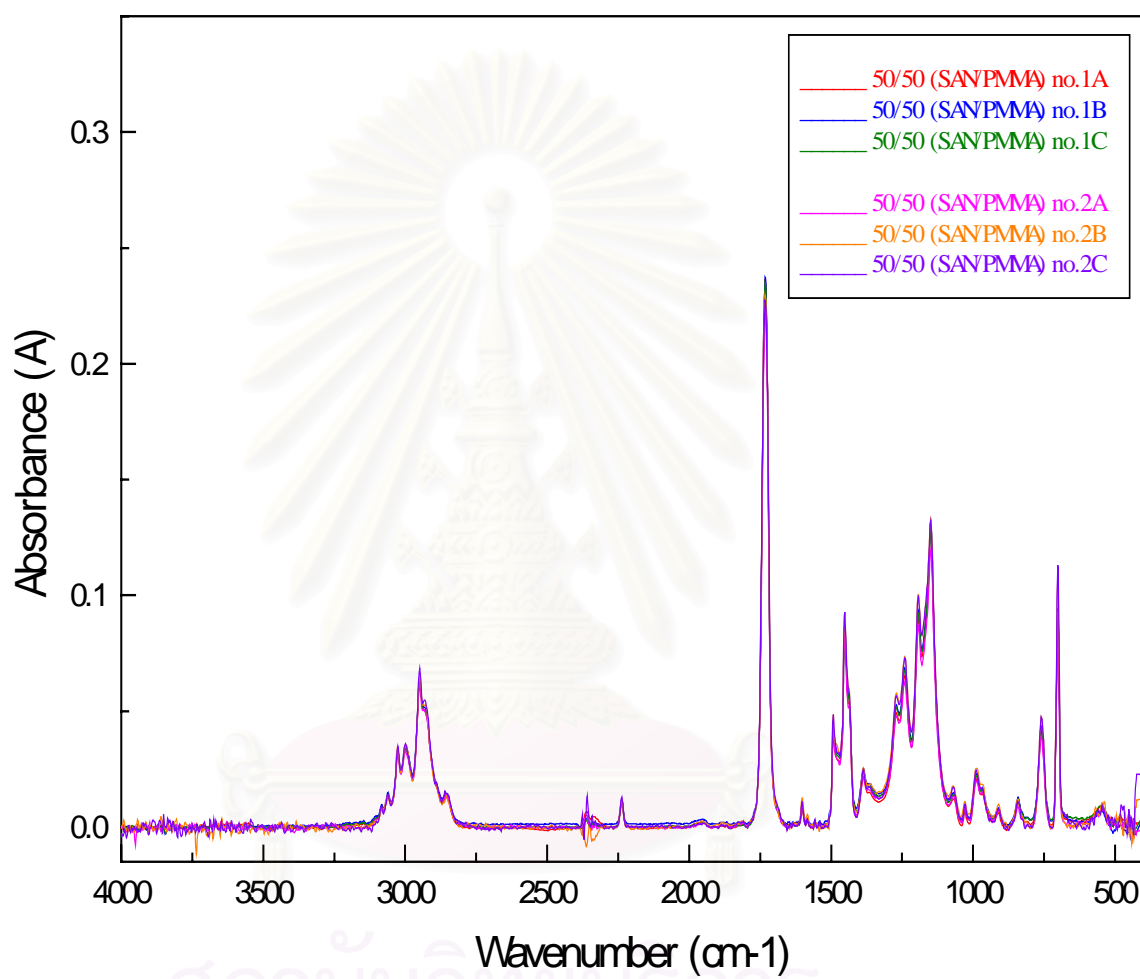


Figure 5.18 Detecting homogeneity of the IR spectra of phase separation sample at composition ratio of blending 50% weight of SAN.

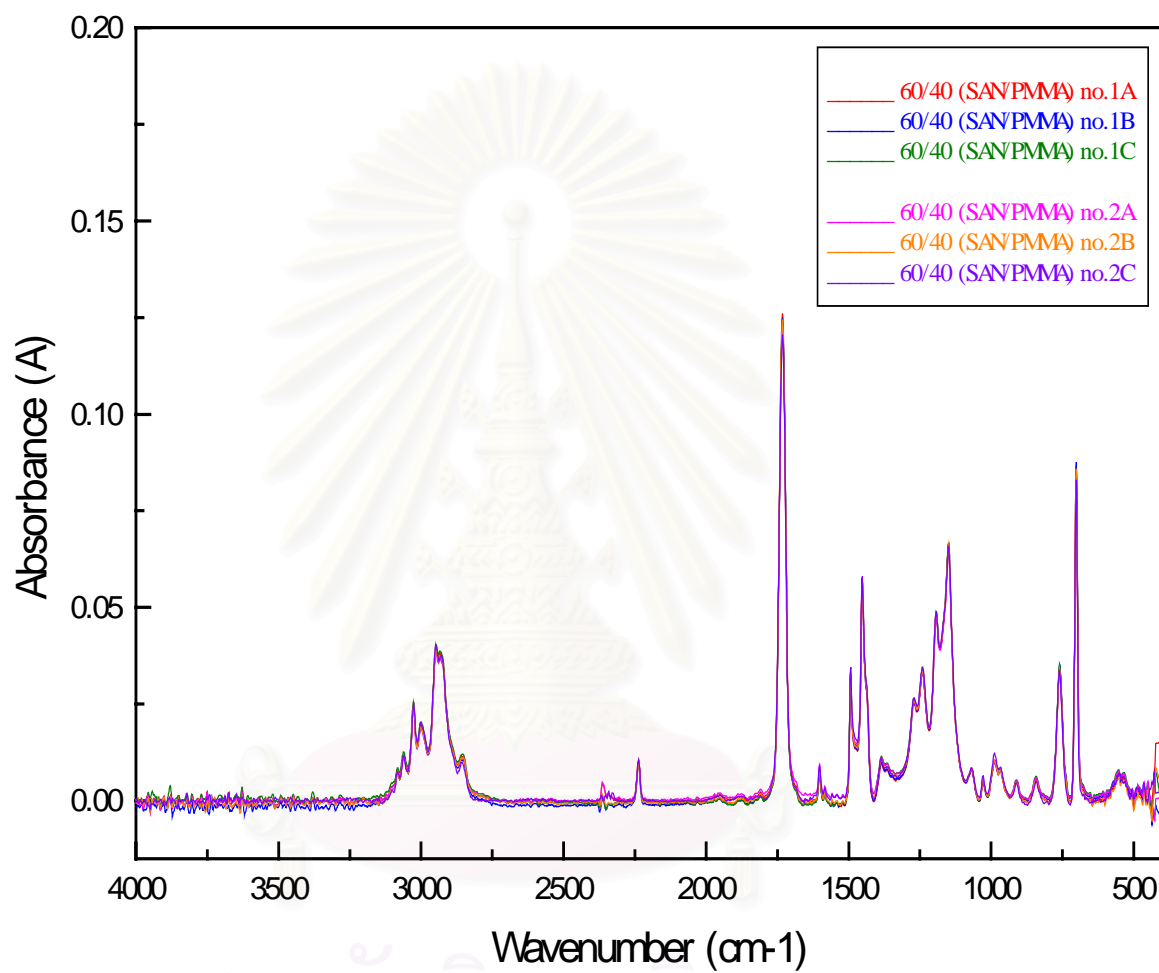


Figure 5.19 Detecting homogeneity of the IR spectra of phase separation samples at composition ratio of blending 60% weight of SAN.

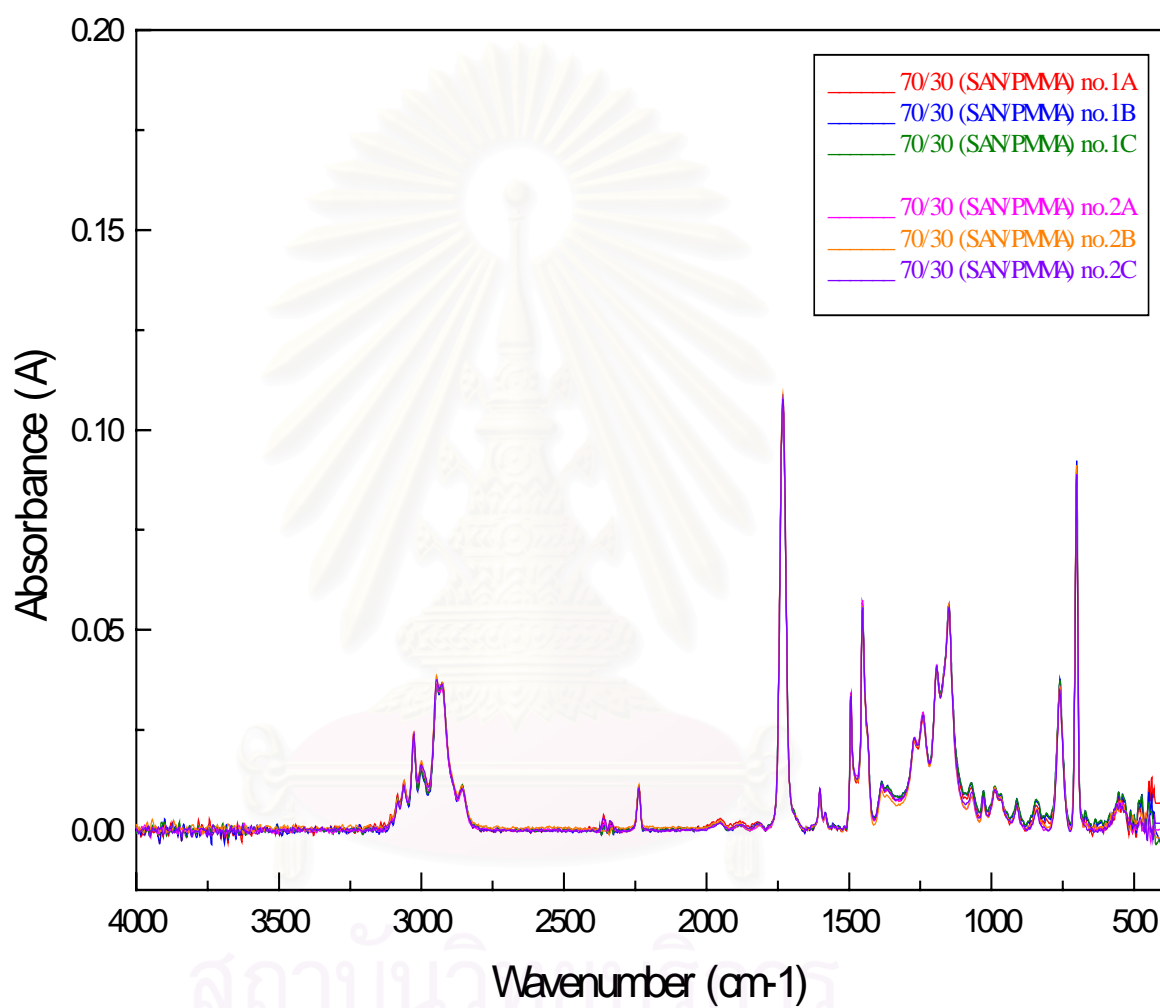


Figure 5.20 Detecting homogeneity of the IR spectra of phase separation samples at composition ratio of blending 70% weight of SAN.

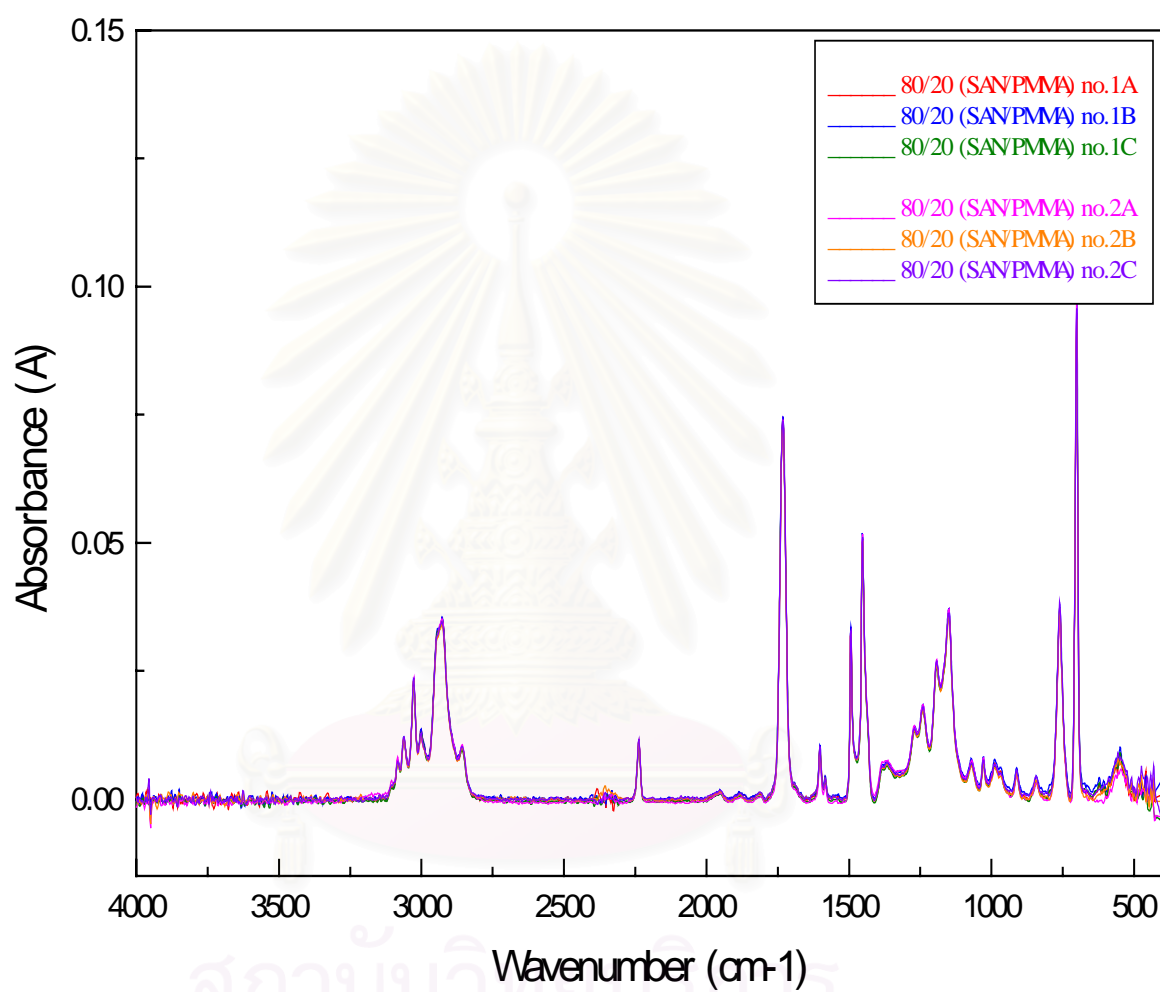


Figure 5.21 Detecting homogeneity of the IR spectra of phase separation samples at composition ratio of blending 80% weight of SAN.

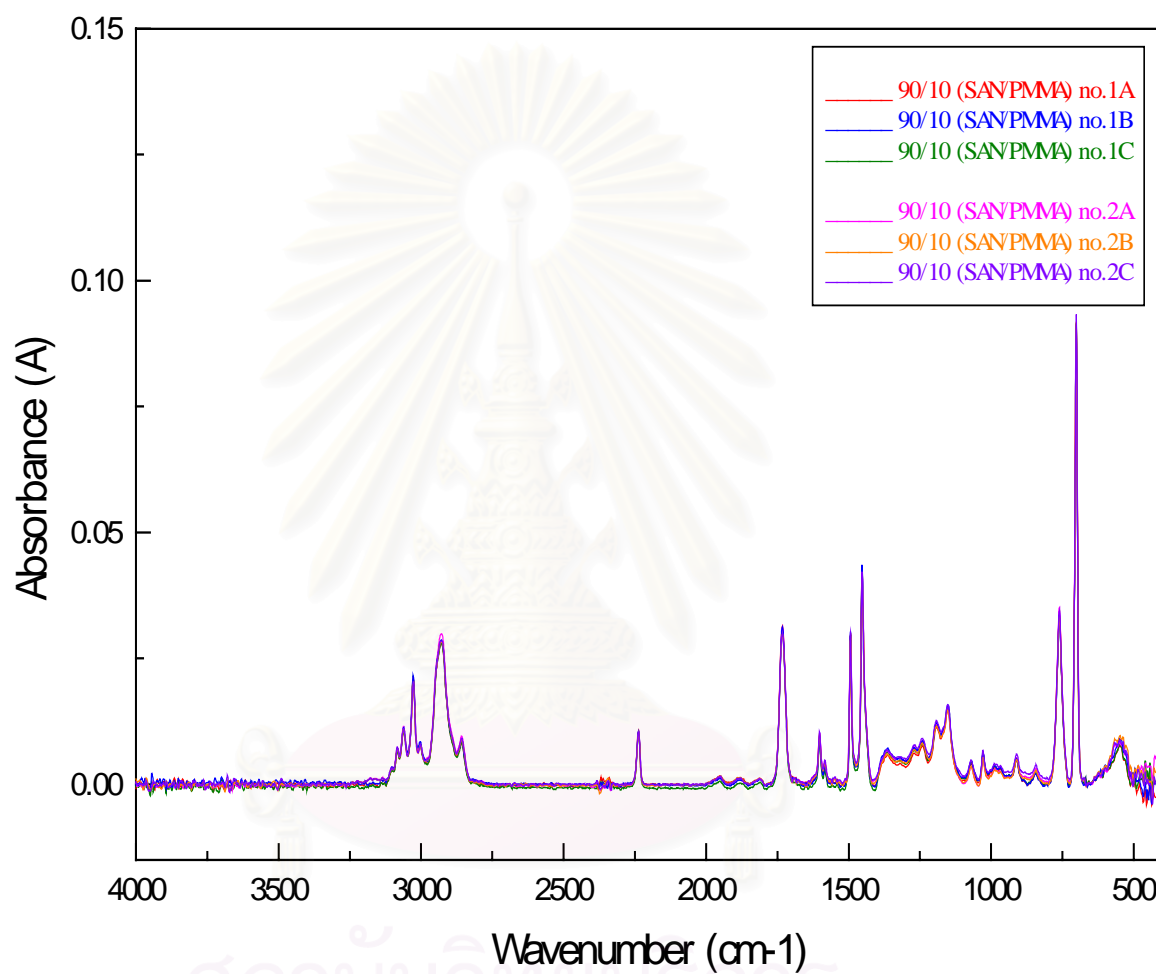


Figure 5.22 Detecting homogeneity of the IR spectra of phase separation samples at composition ratio of blending 90% weight of SAN.

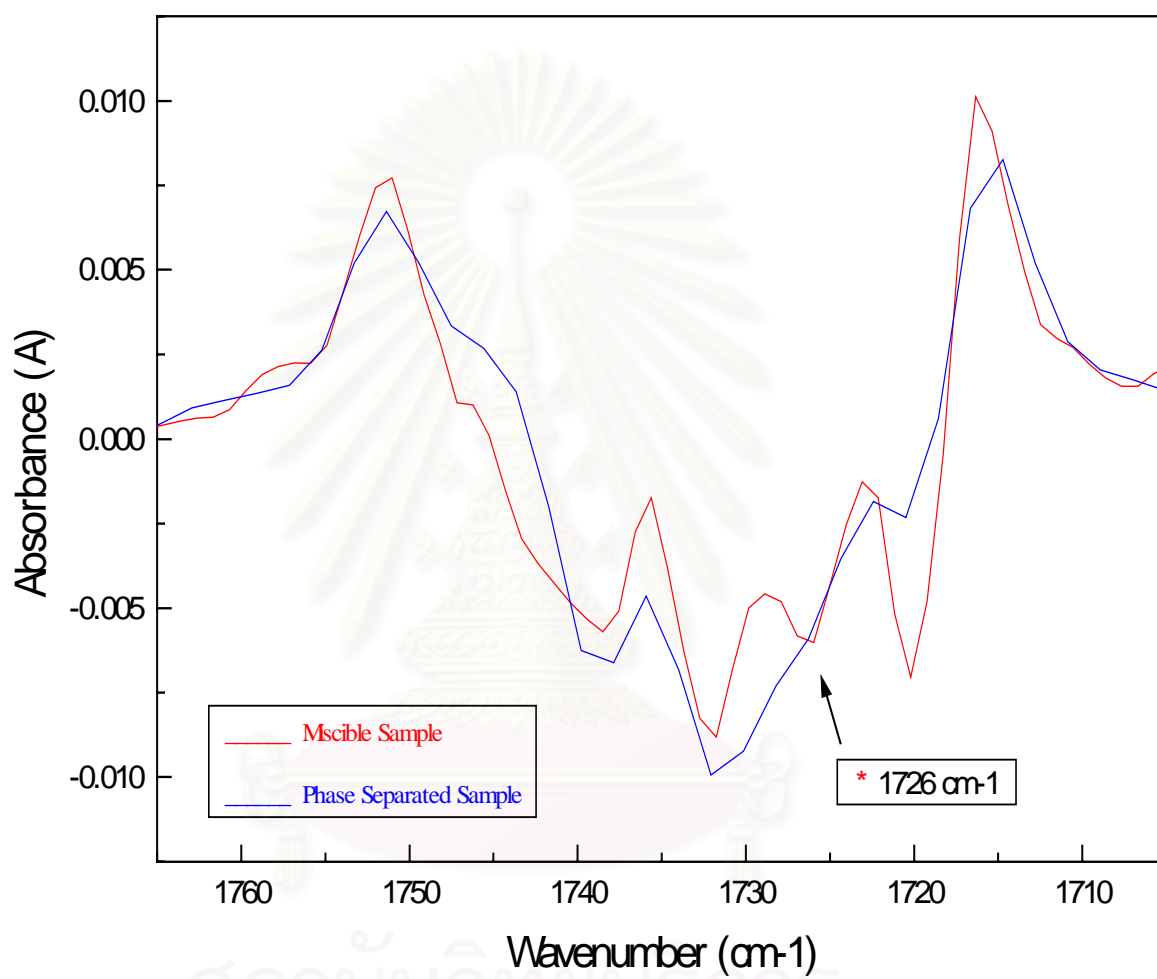


Figure 5.23 Comparing the second derivative of carbonyl peak at composition ratio of blending 30% weight of SAN.

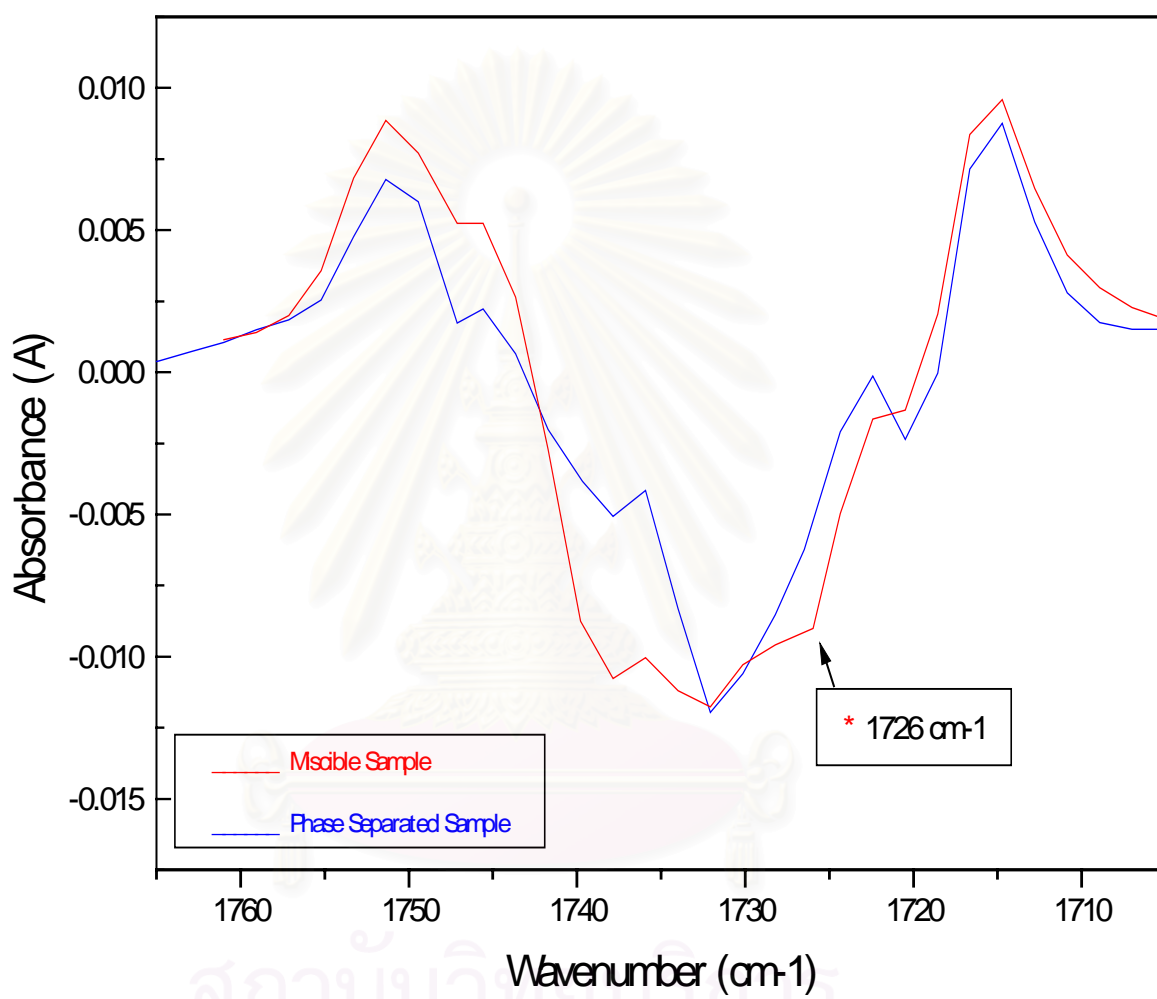


Figure 5.24 Comparing the second derivative of carbonyl peak at composition ratio of blending 40% weight of SAN.

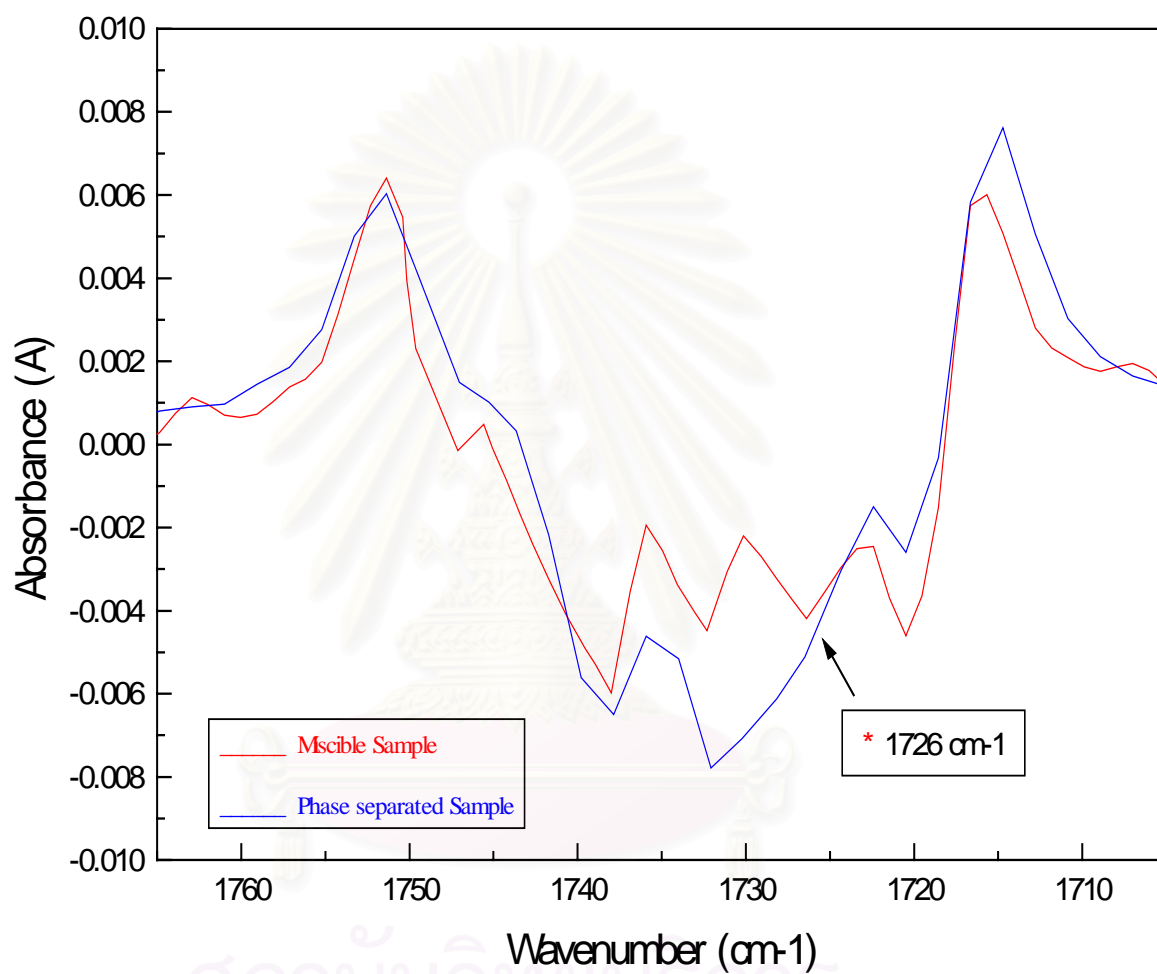


Figure 5.25 Comparing the second derivative of carbonyl peak at composition ratio of blending 50% weight of SAN.

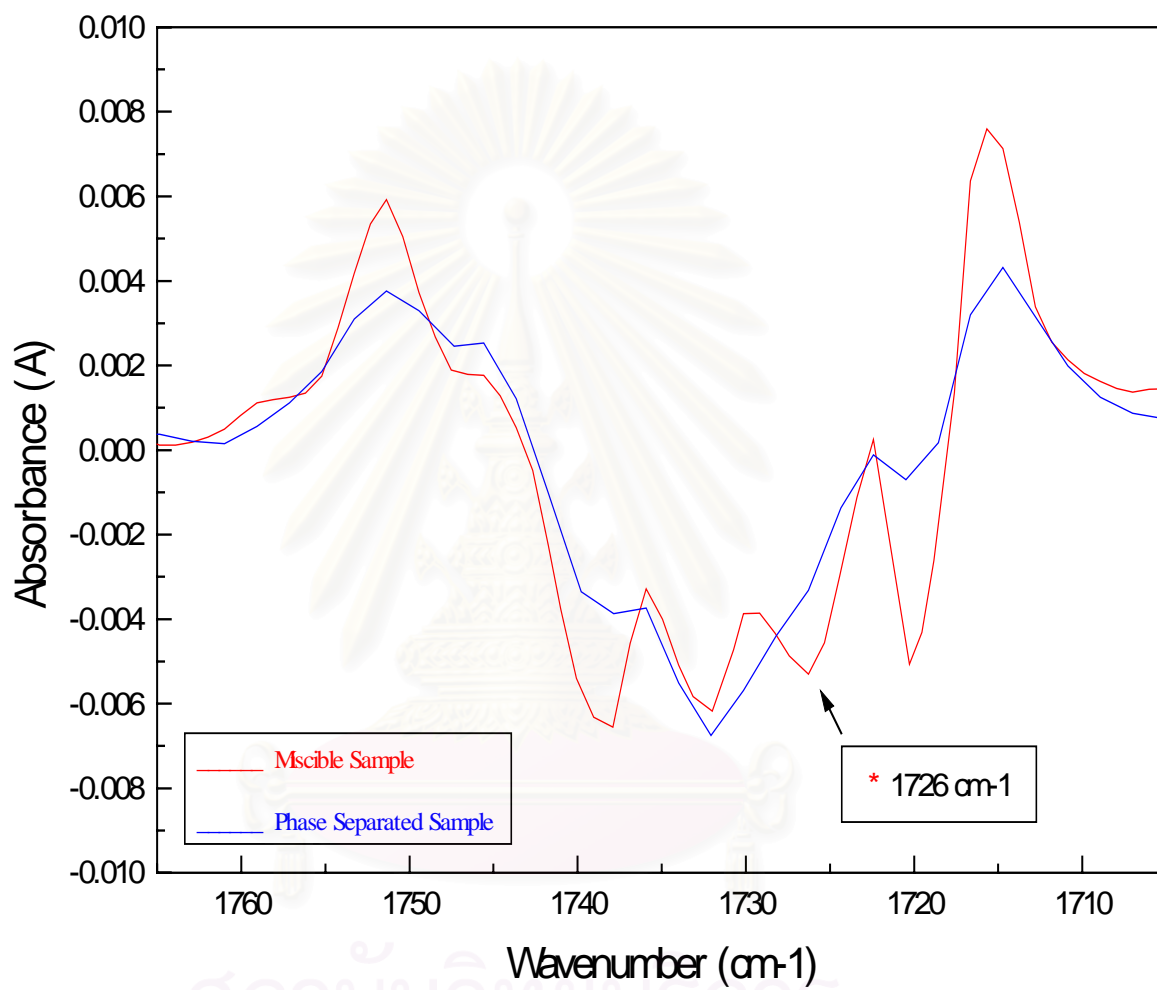


Figure 5.26 Comparing the second derivative of carbonyl peak at composition ratio of blending 60% weight of SAN.

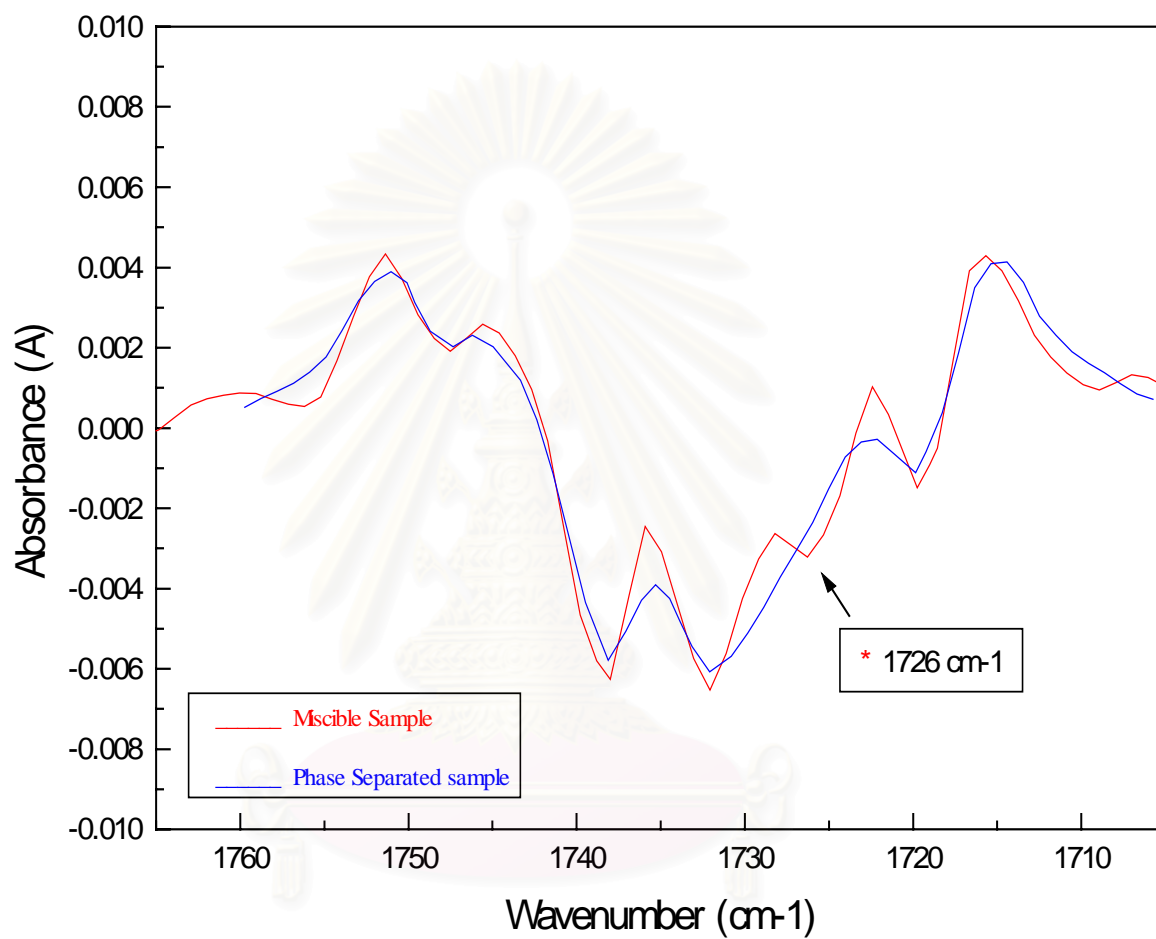


Figure 5.27 Comparing the second derivative of carbonyl peak at composition ratio of blending 70% weight of SAN.

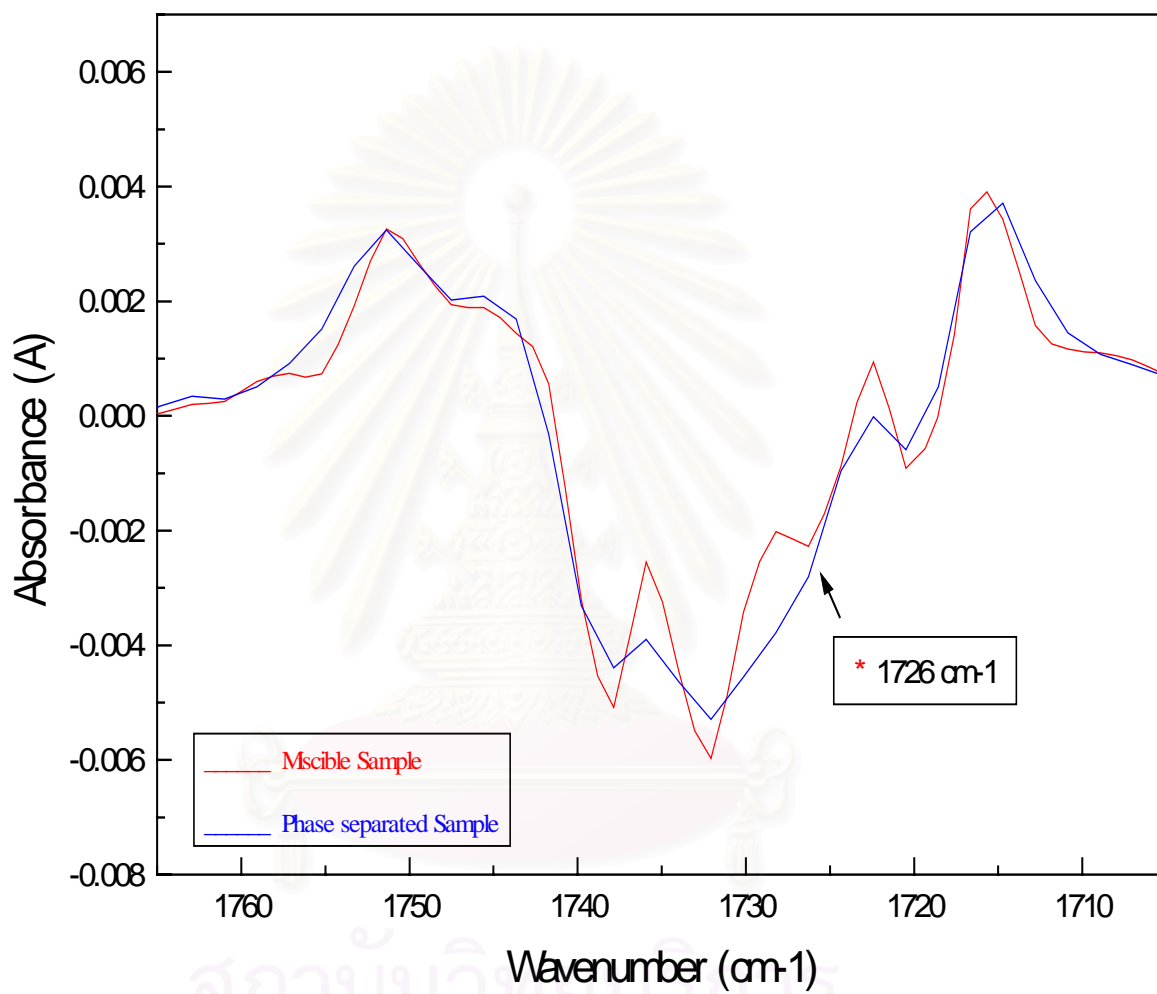


Figure 5.28 Comparing the second derivative of carbonyl peak at composition ratio of blending 80% weight of SAN.

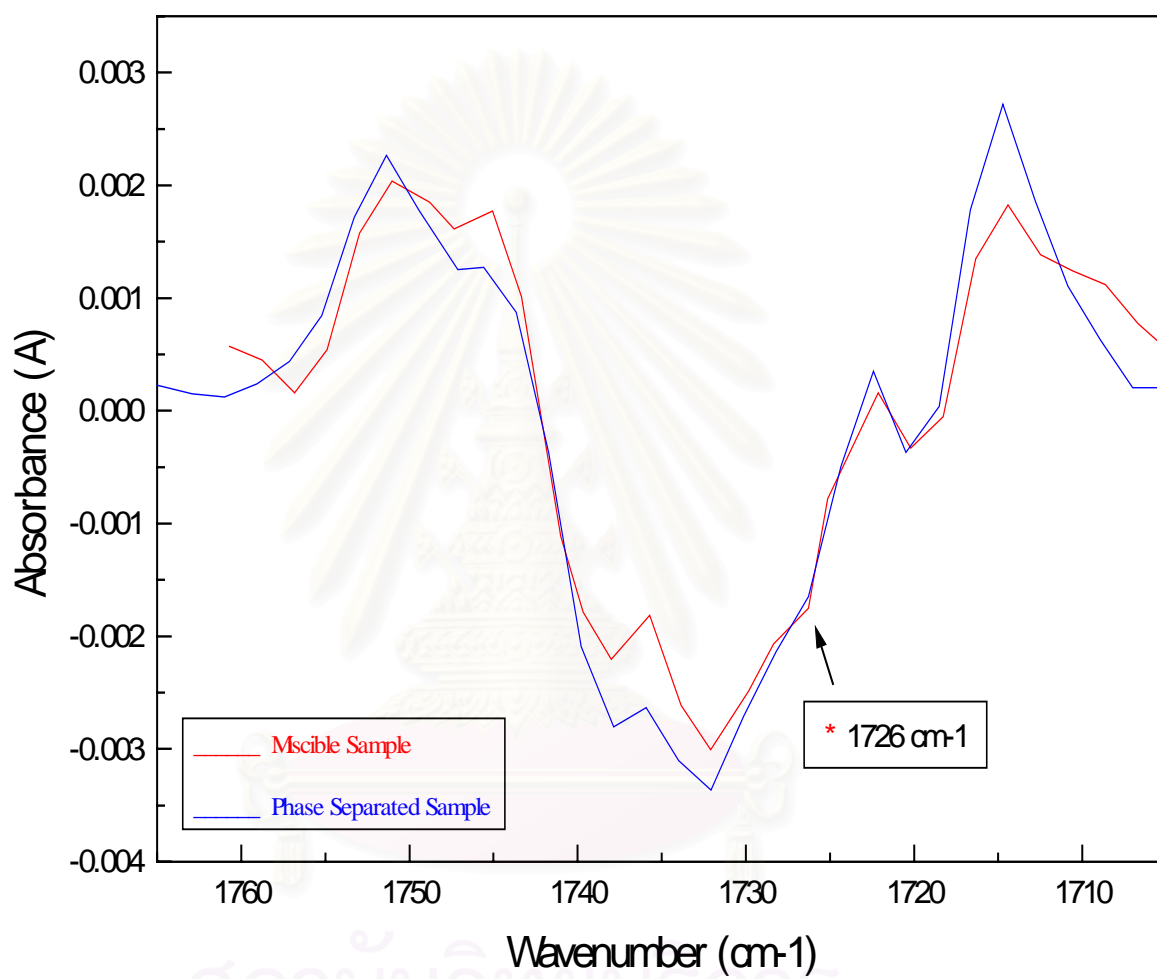


Figure 5.29 Comparing the second derivative of carbonyl peak at composition ratio of blending 90% weight of SAN.

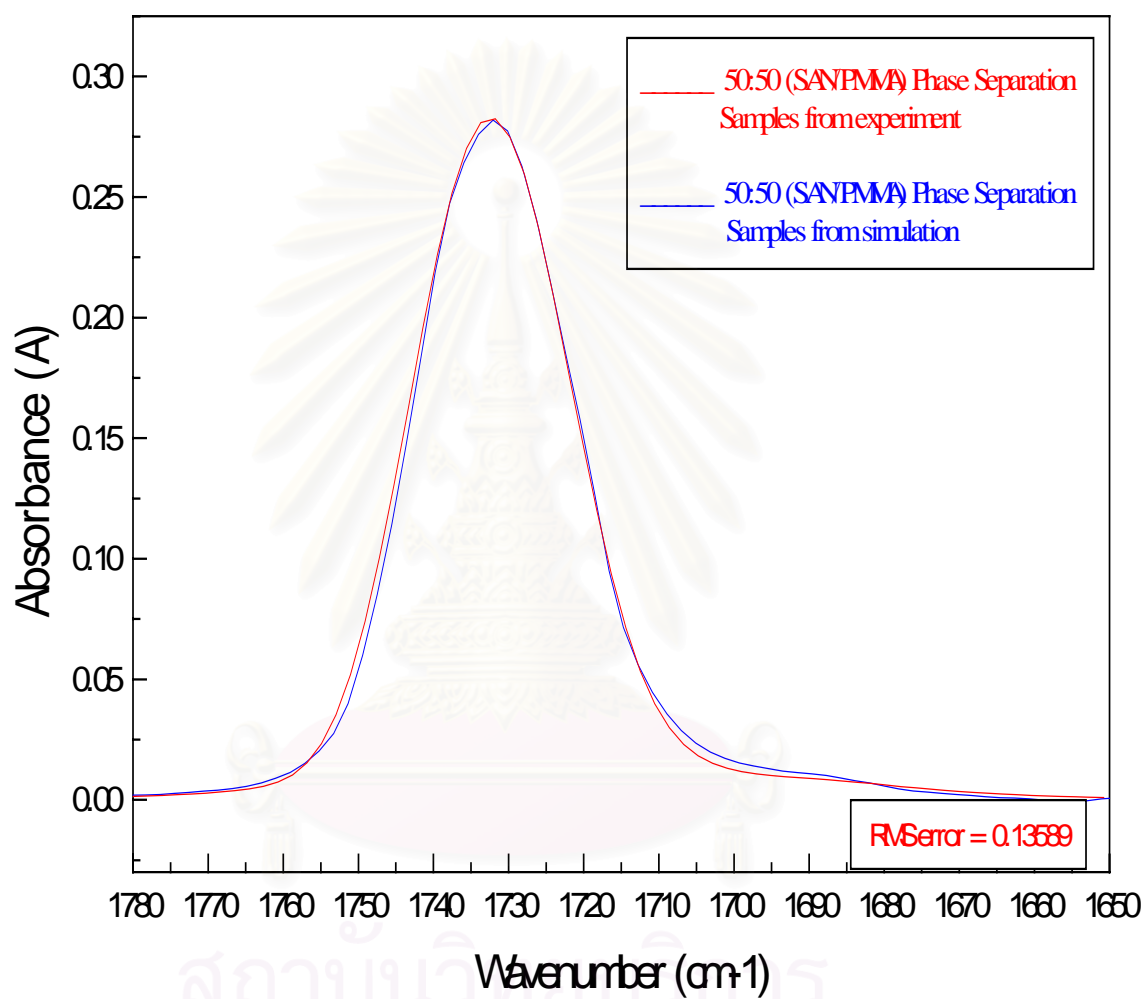


Figure 5.30 Comparing the simulated carbonyl peak from four hidden peaks with real carbonyl peak from the experiment.

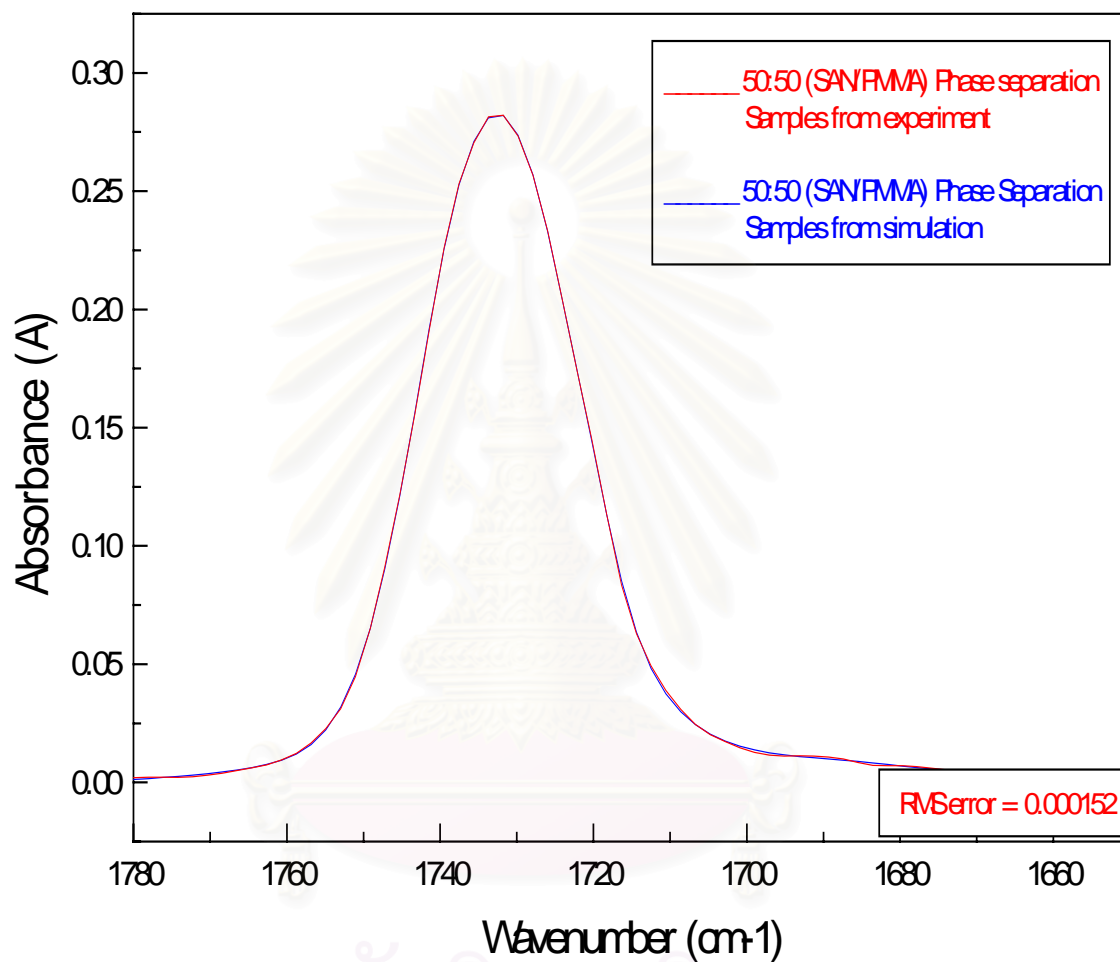


Figure 5.31 Comparing the simulated carbonyl peak from five hidden peaks with real carbonyl peak from the experiment.

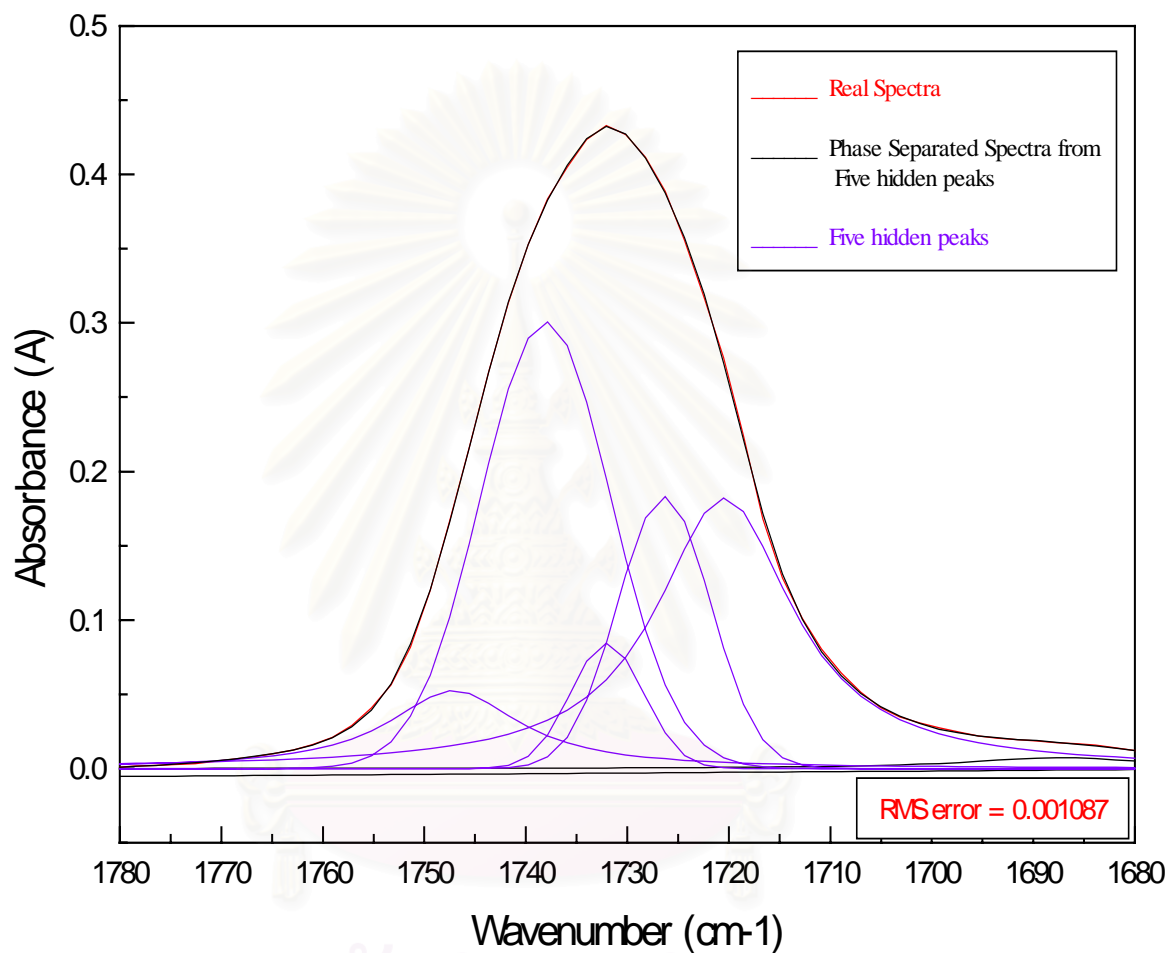


Figure 5.32 Comparing real spectra and simulated spectra from five hidden peaks of miscible sample at composition ratio of blending 30% weight of SAN.

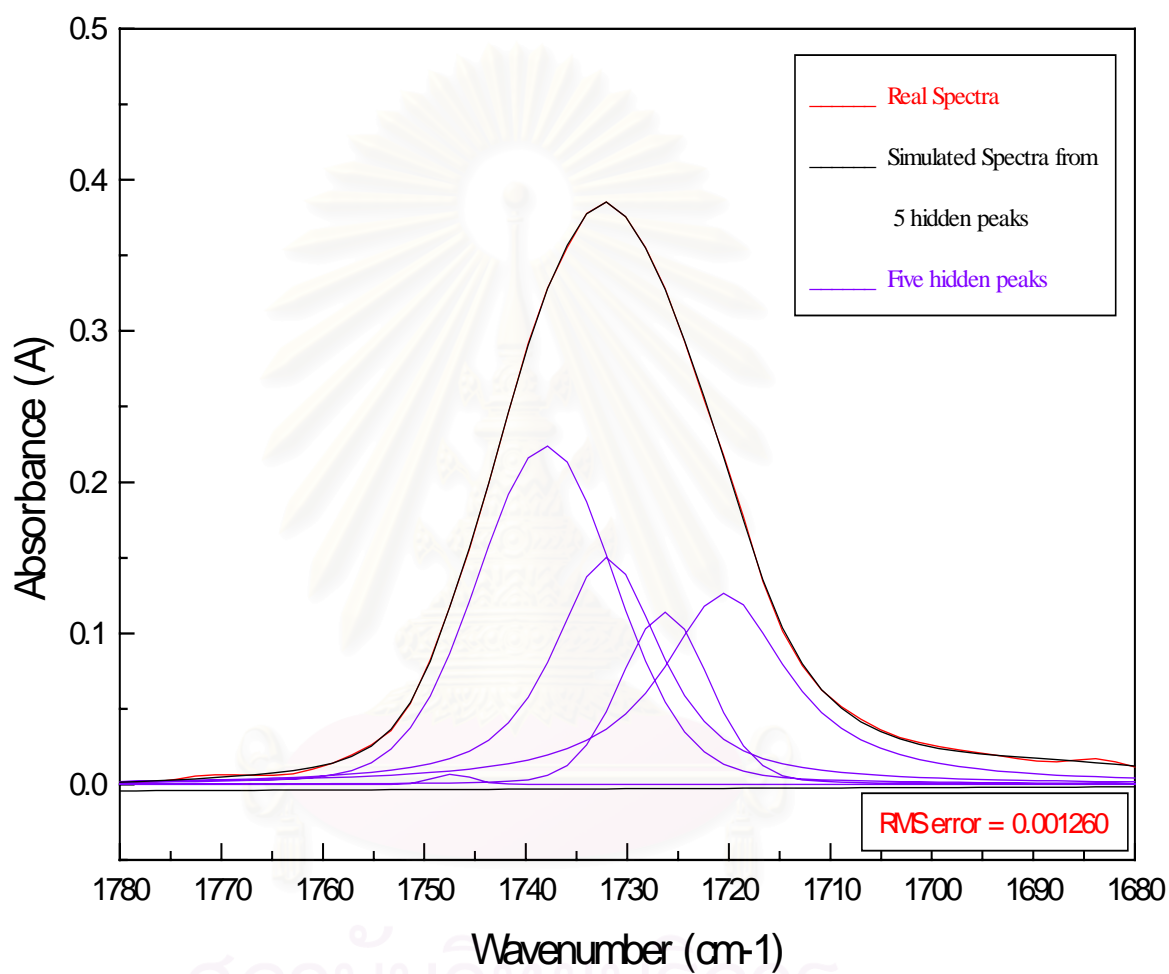


Figure 5.33 Comparing real spectra and simulated spectra from five hidden peaks of miscible sample at composition ratio of blending 40% weight of SAN.

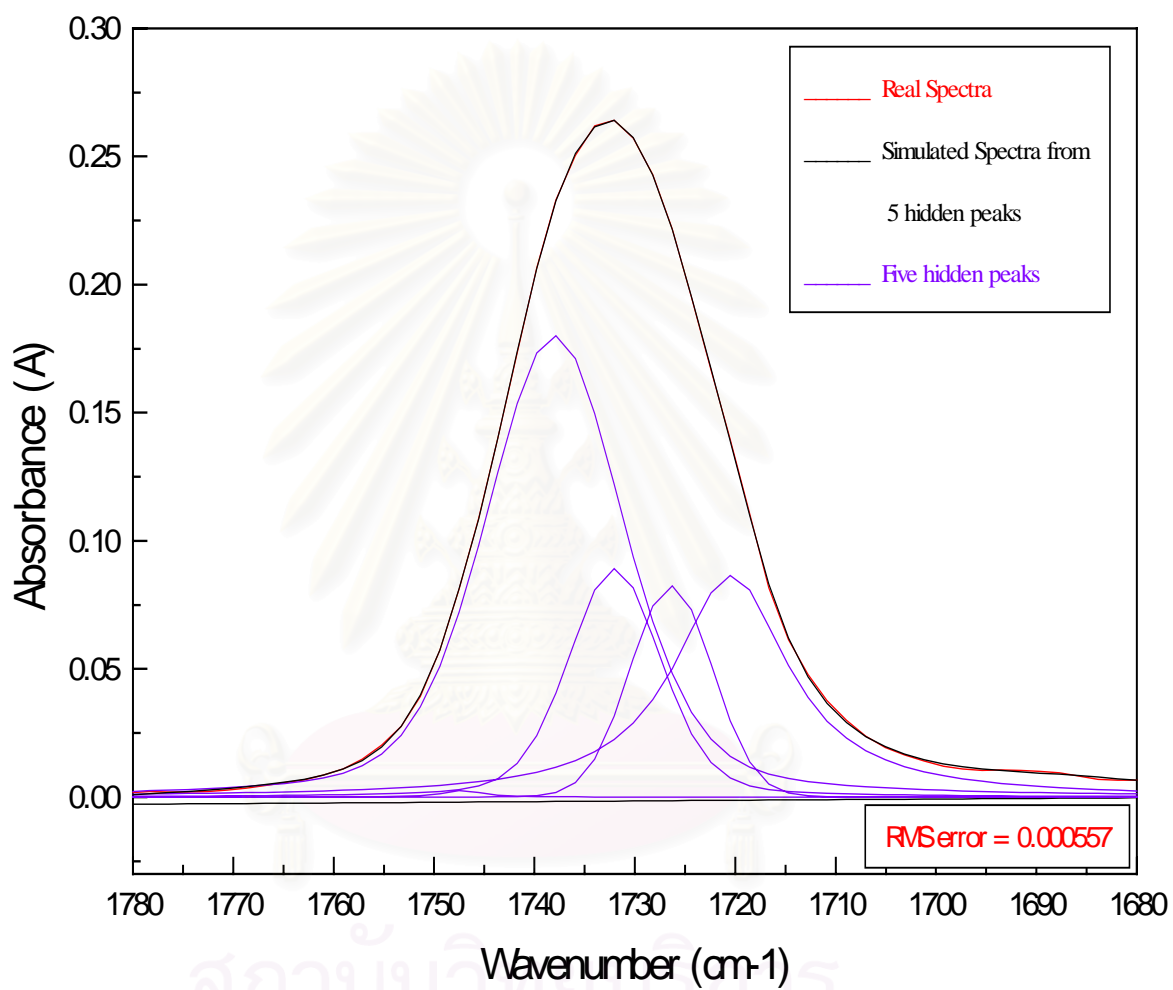


Figure 5.34 Comparing real spectra and simulated spectra from five hidden peaks of miscible sample at composition ratio of blending 50% weight of SAN.

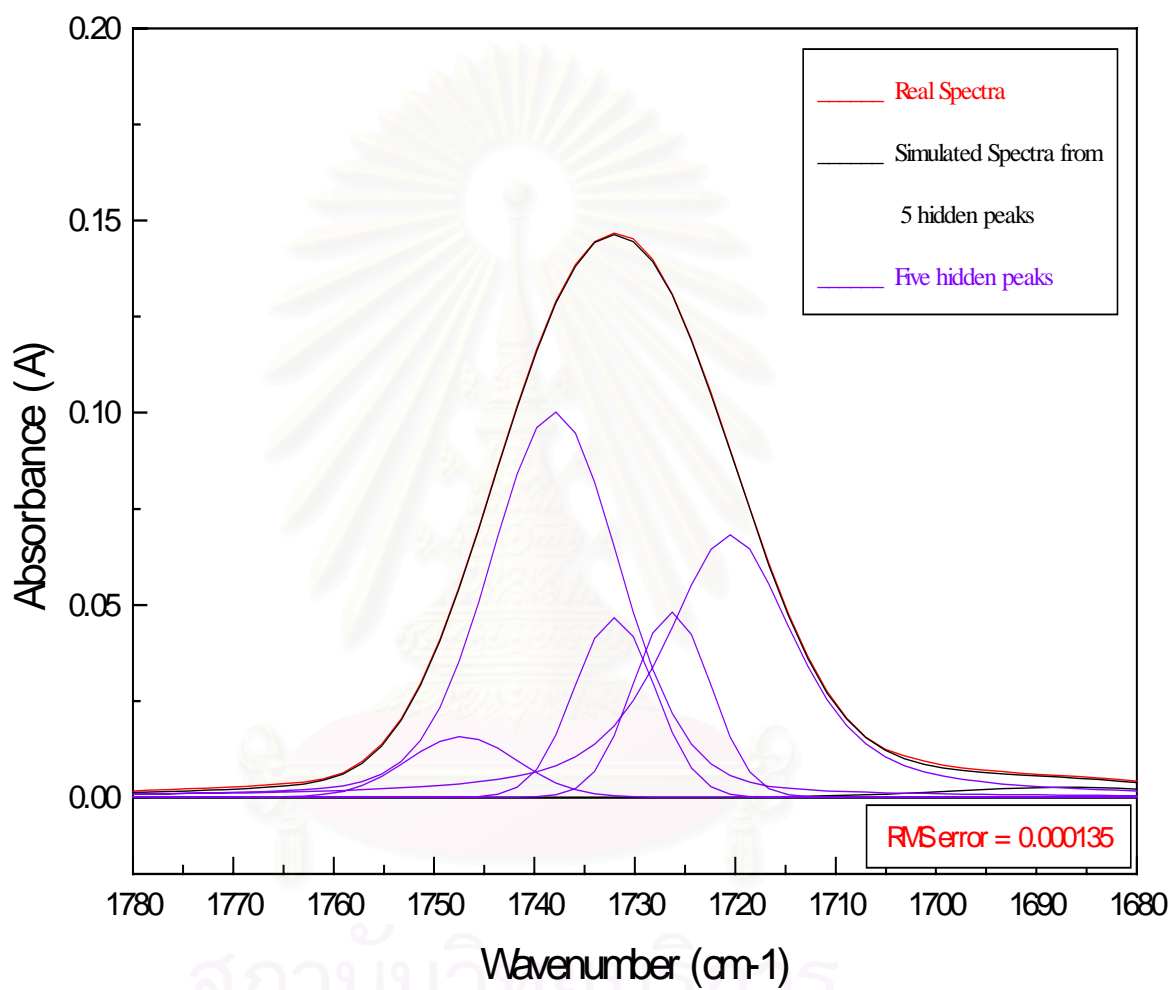


Figure 5.35 Comparing real spectra and simulated spectra from five hidden peaks of miscible sample at composition ratio of blending 60% weight of SAN.

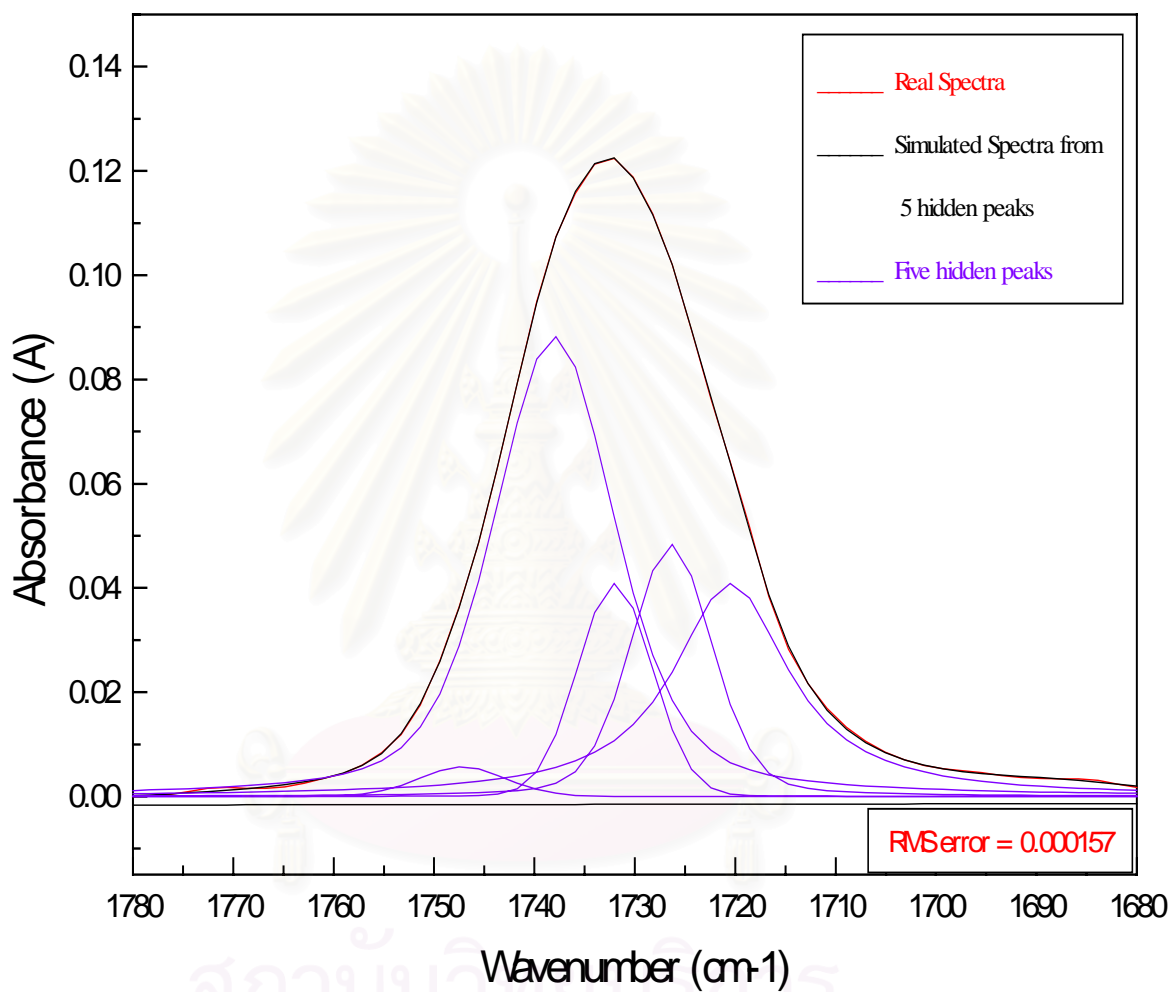


Figure 5.36 Comparing real spectra and simulated spectra from five hidden peaks of miscible sample at composition ratio of blending 70% weight of SAN.

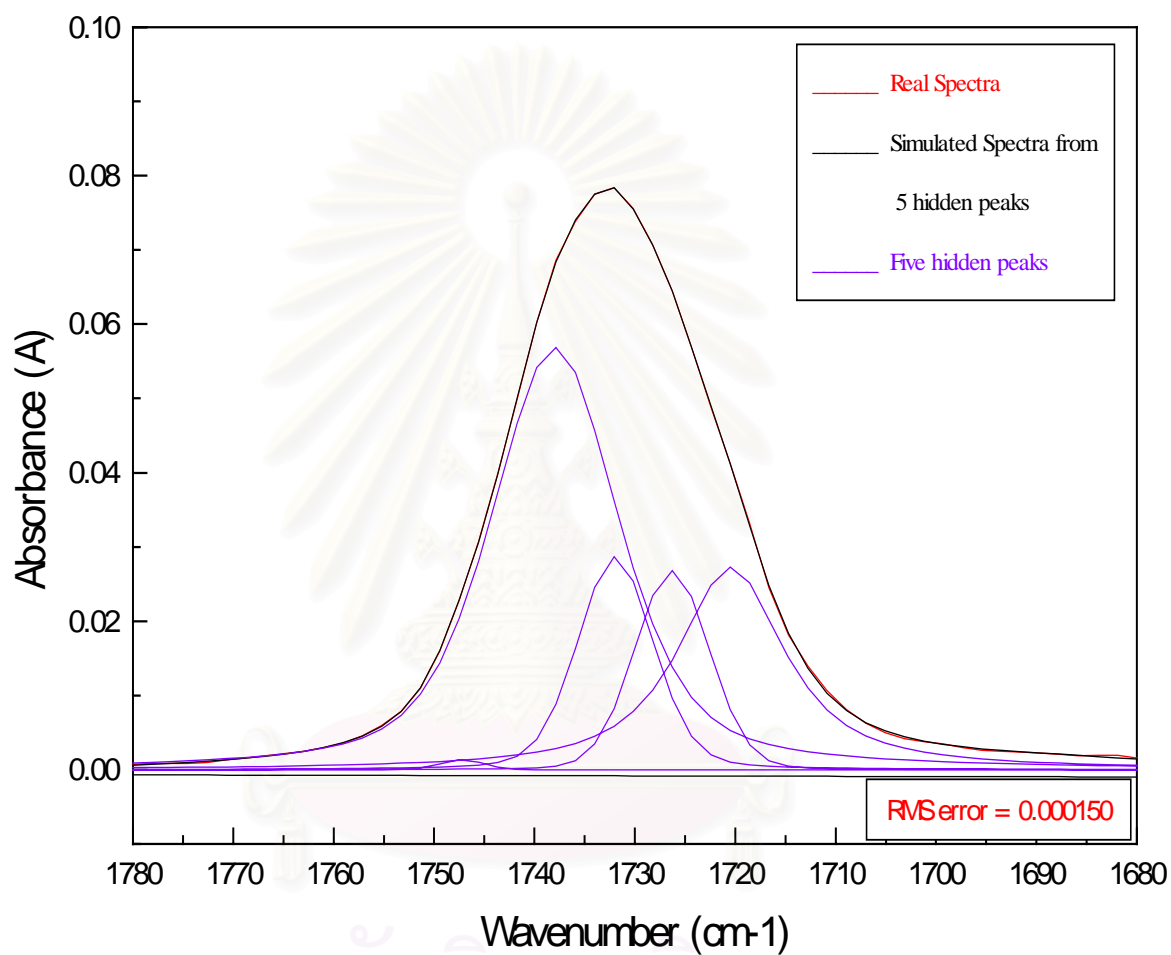


Figure 5.37 Comparing real spectra and simulated spectra from five hidden peaks of miscible sample at composition ratio of blending 80% weight of SAN.

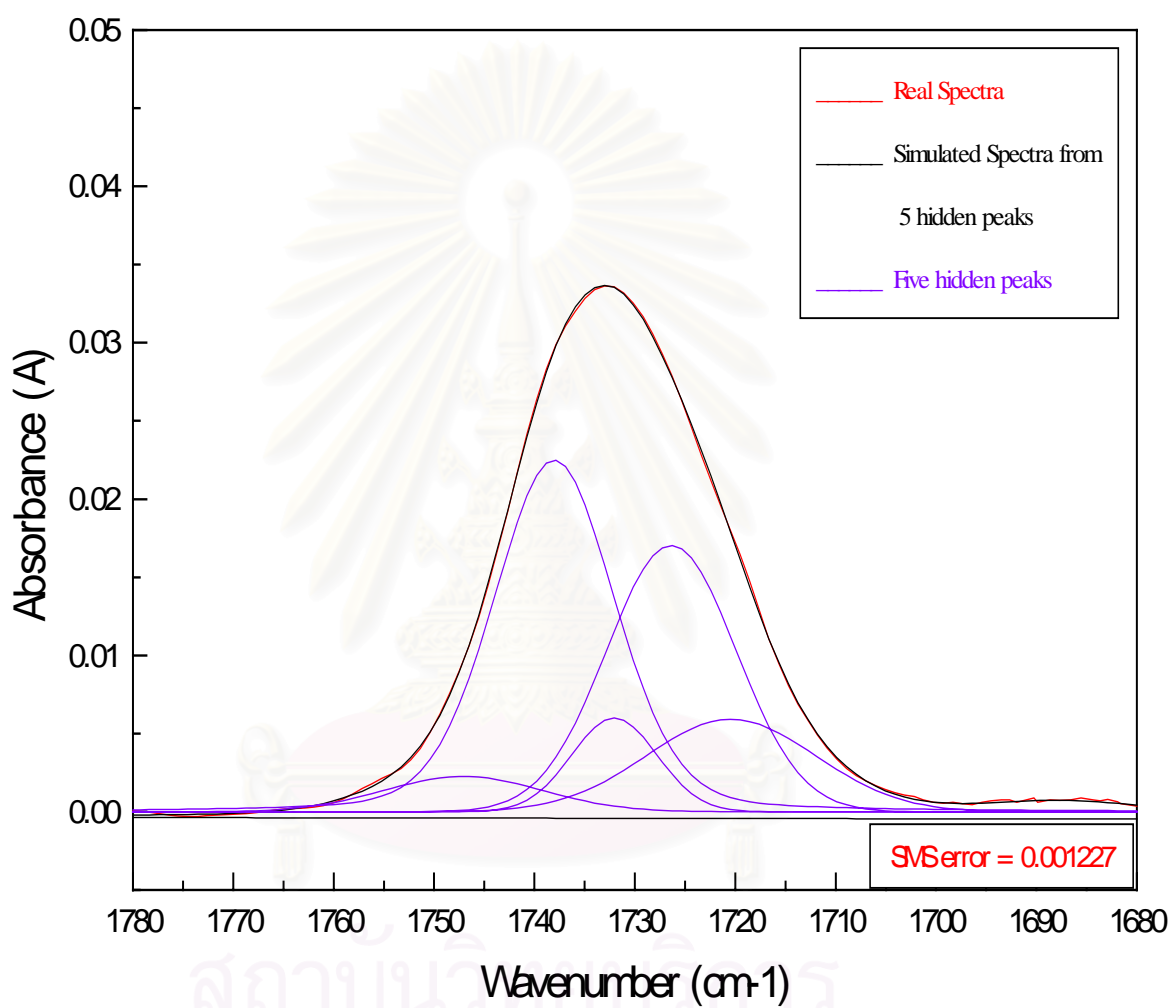


Figure 5.38 Comparing real spectra and simulated spectra from five hidden peaks of miscible sample at composition ratio of blending 90% weight of SAN.

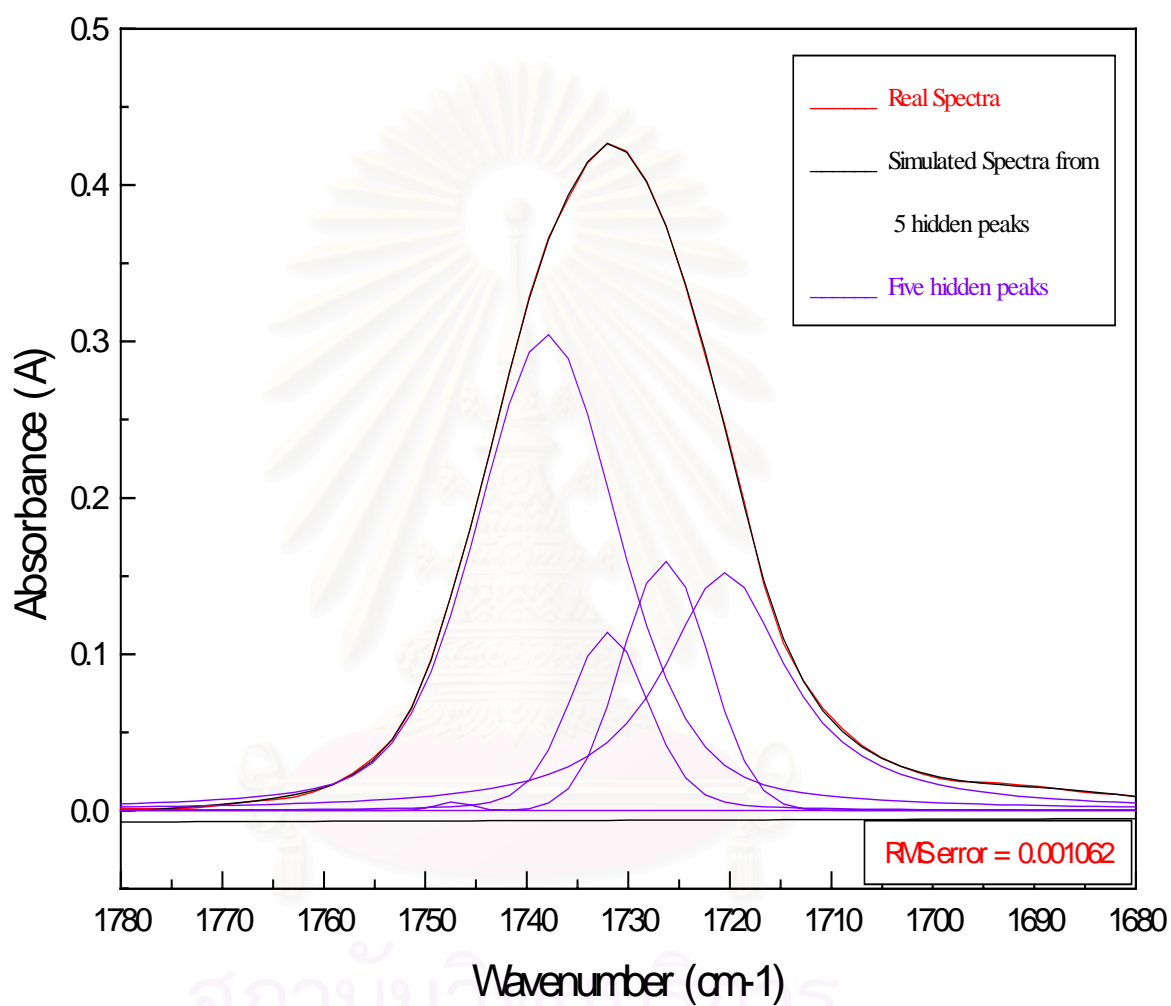


Figure 5.39 Comparing real spectra and simulated spectra from five hidden peaks of phase separation sample at composition ratio of blending 30% weight of SAN.

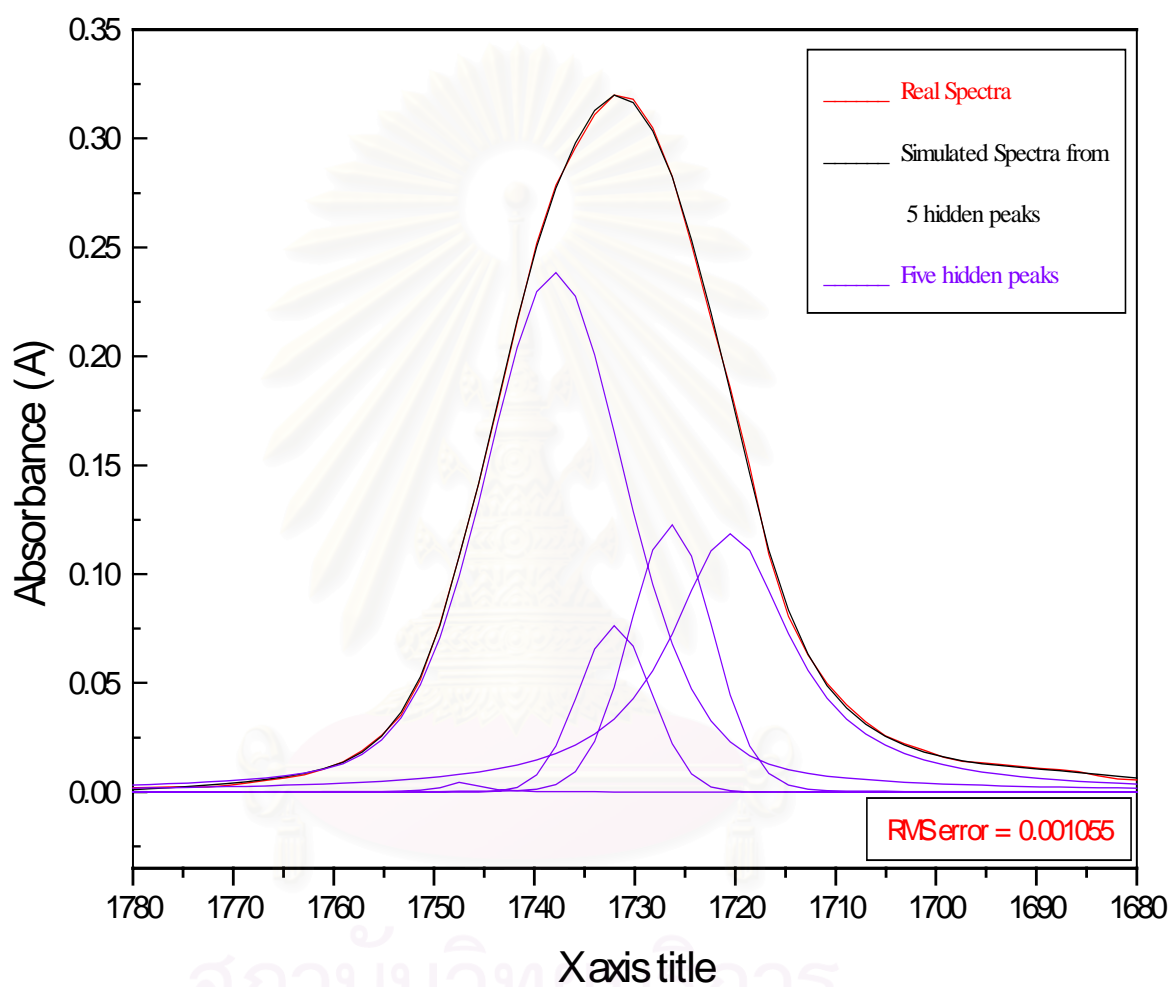


Figure 5.40 Comparing real spectra and simulated spectra from five hidden peaks of phase separation sample at composition ratio of blending 40% weight of SAN.

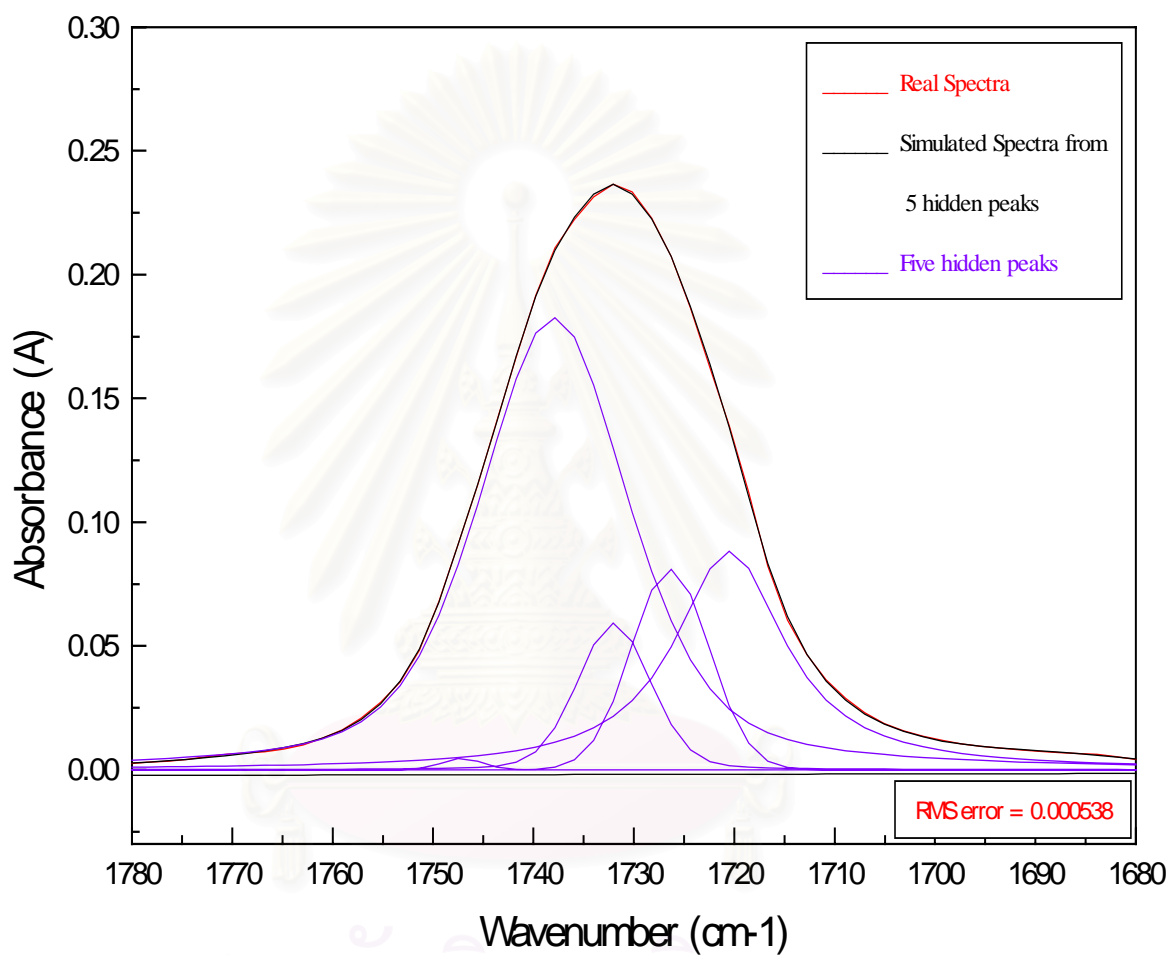


Figure 5.41 Comparing real spectra and simulated spectra from five hidden peaks of phase separation sample at composition ratio of blending 50% weight of SAN.

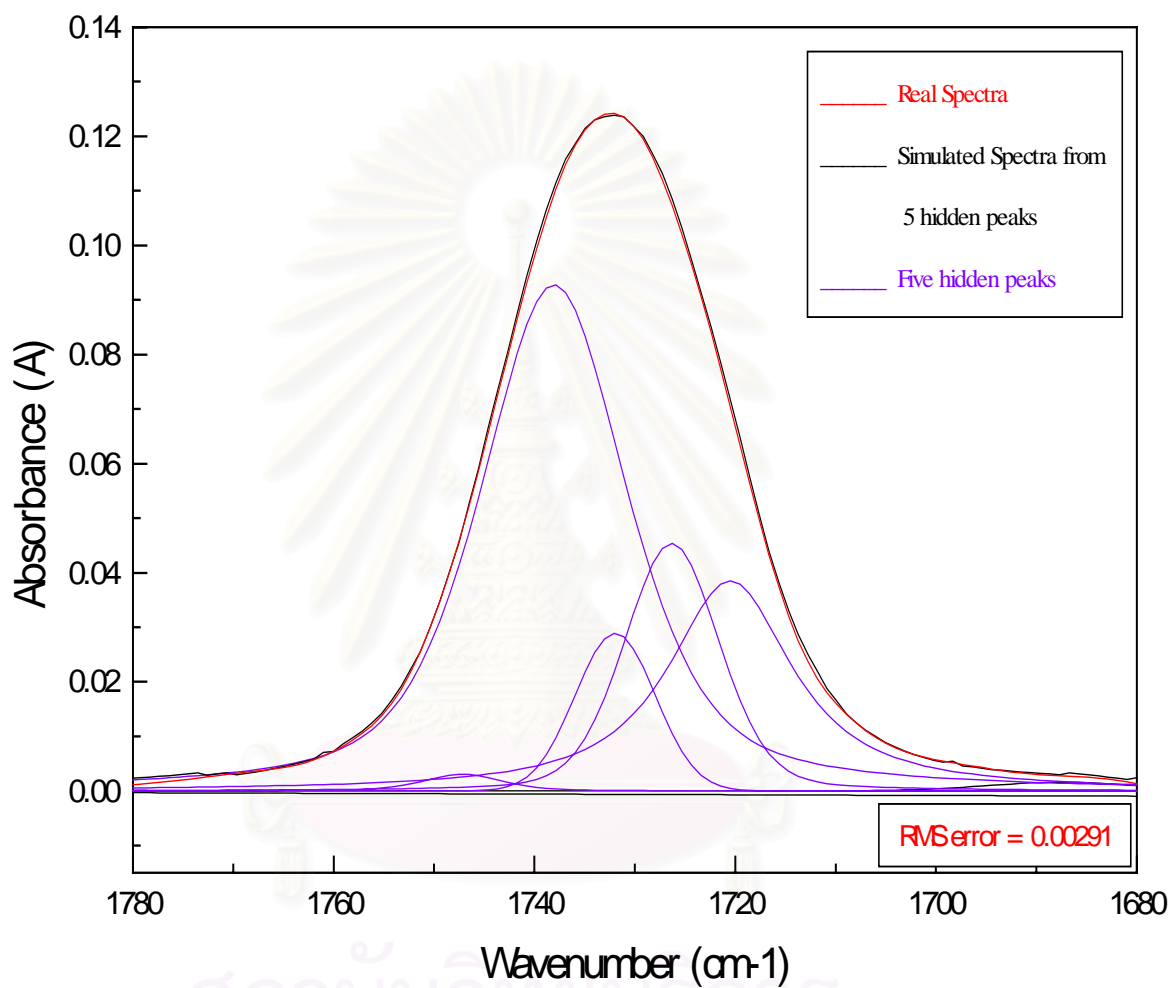


Figure 5.42 Comparing real spectra and simulated spectra from five hidden peaks of phase separation sample at composition ratio of blending 60% weight of SAN.

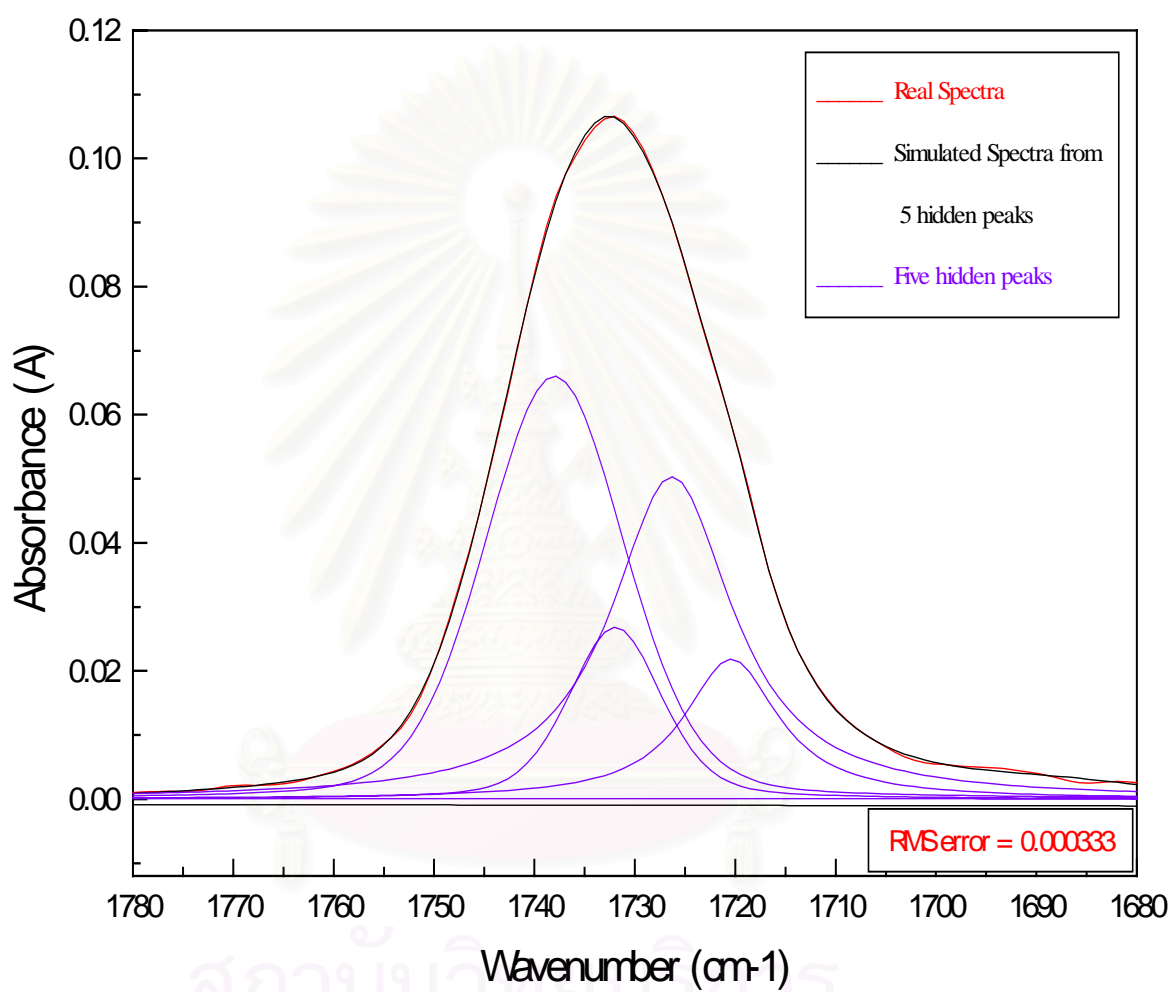


Figure 5.43 Comparing real spectra and simulated spectra from five hidden peaks of phase separation sample at composition ratio of blending 70% weight of SAN.

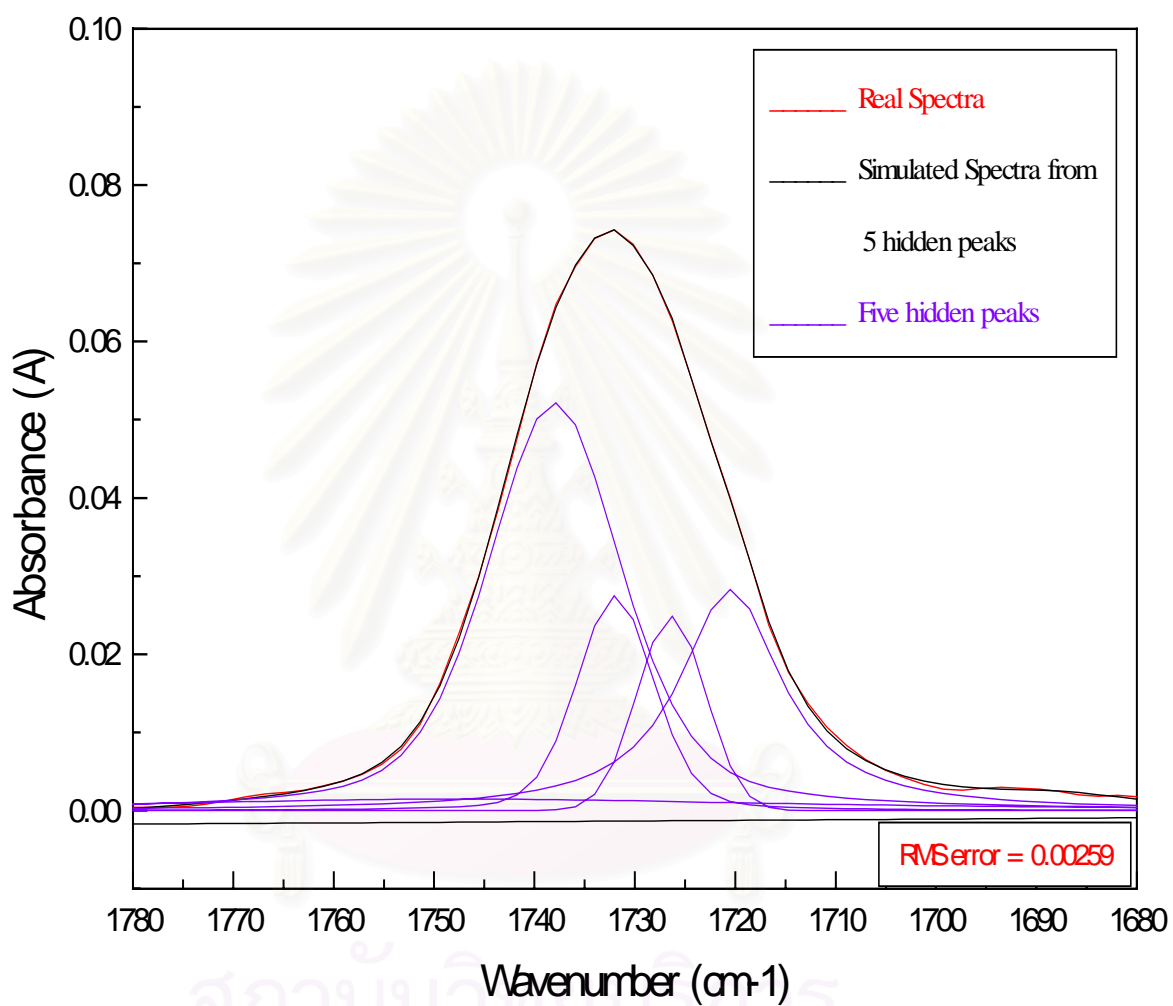


Figure 5.44 Comparing real spectra and simulated spectra from five hidden peaks of phase separation sample at composition ratio of blending 80% weight of SAN.

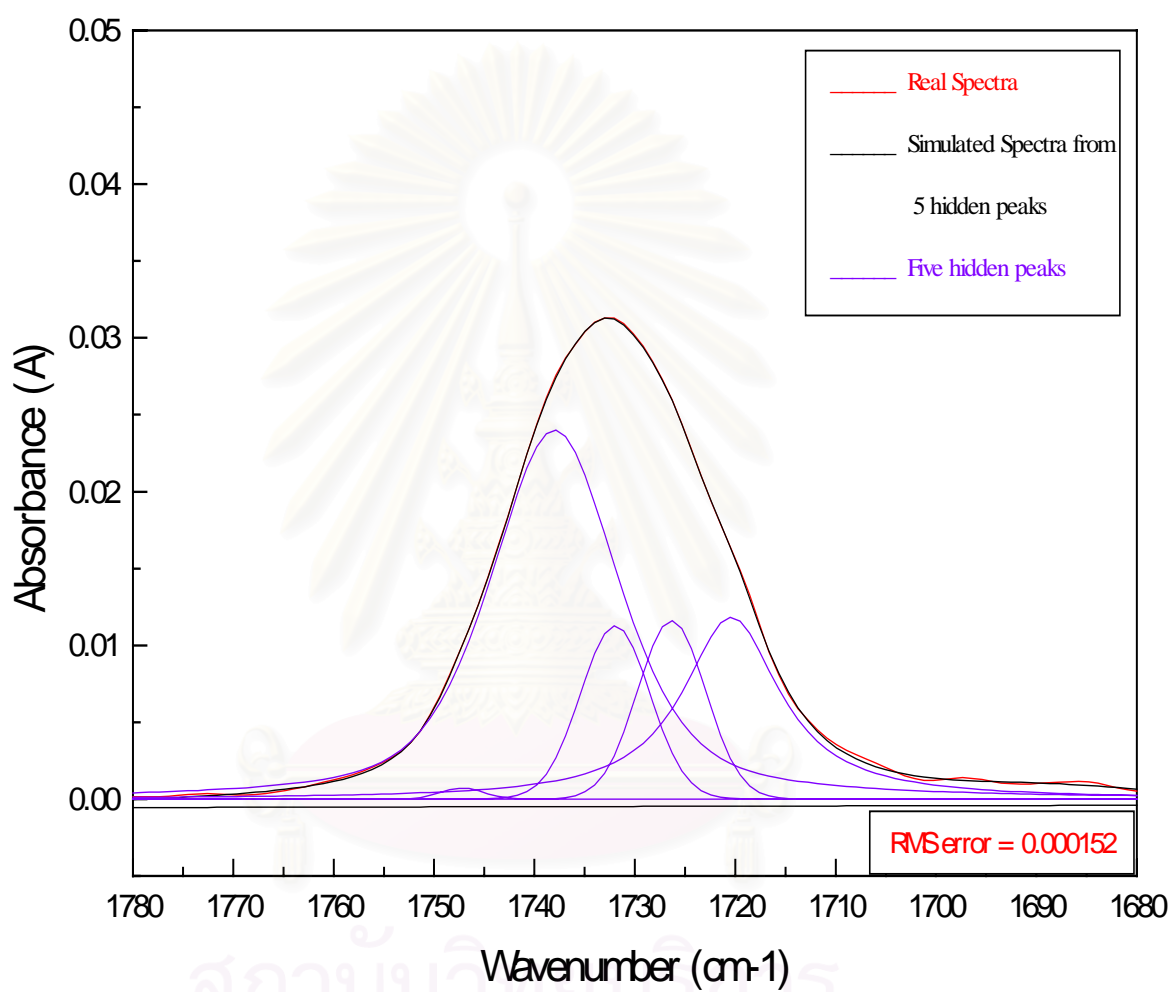


Figure 5.45 Comparing real spectra and simulated spectra from five hidden peaks of phase separation sample at composition ratio of blending 90% weight of SAN.

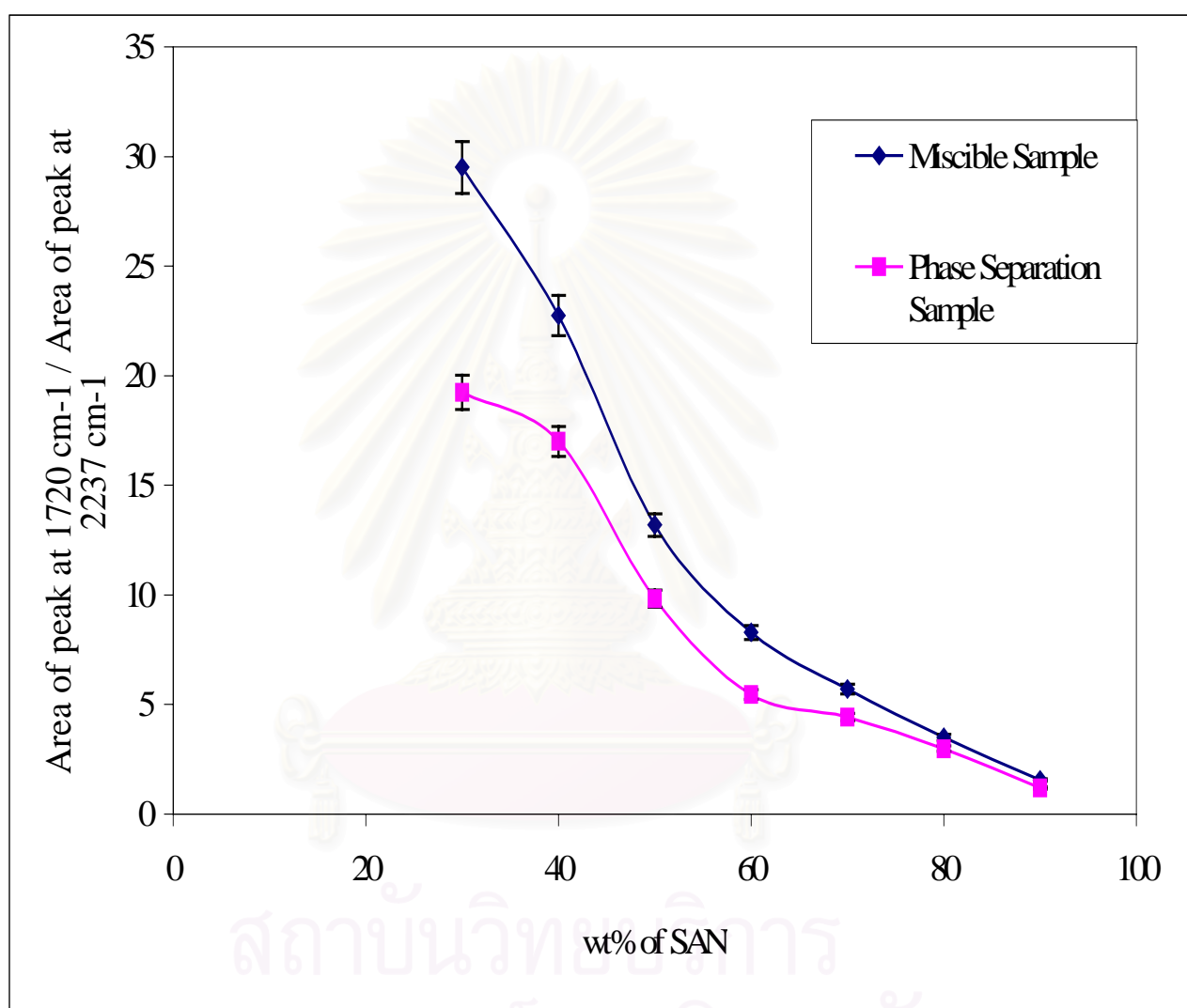


Figure 5.46 Comparing ratio of area under peak 1720 cm⁻¹ and area under peak 2237 cm⁻¹ with %weight of SAN

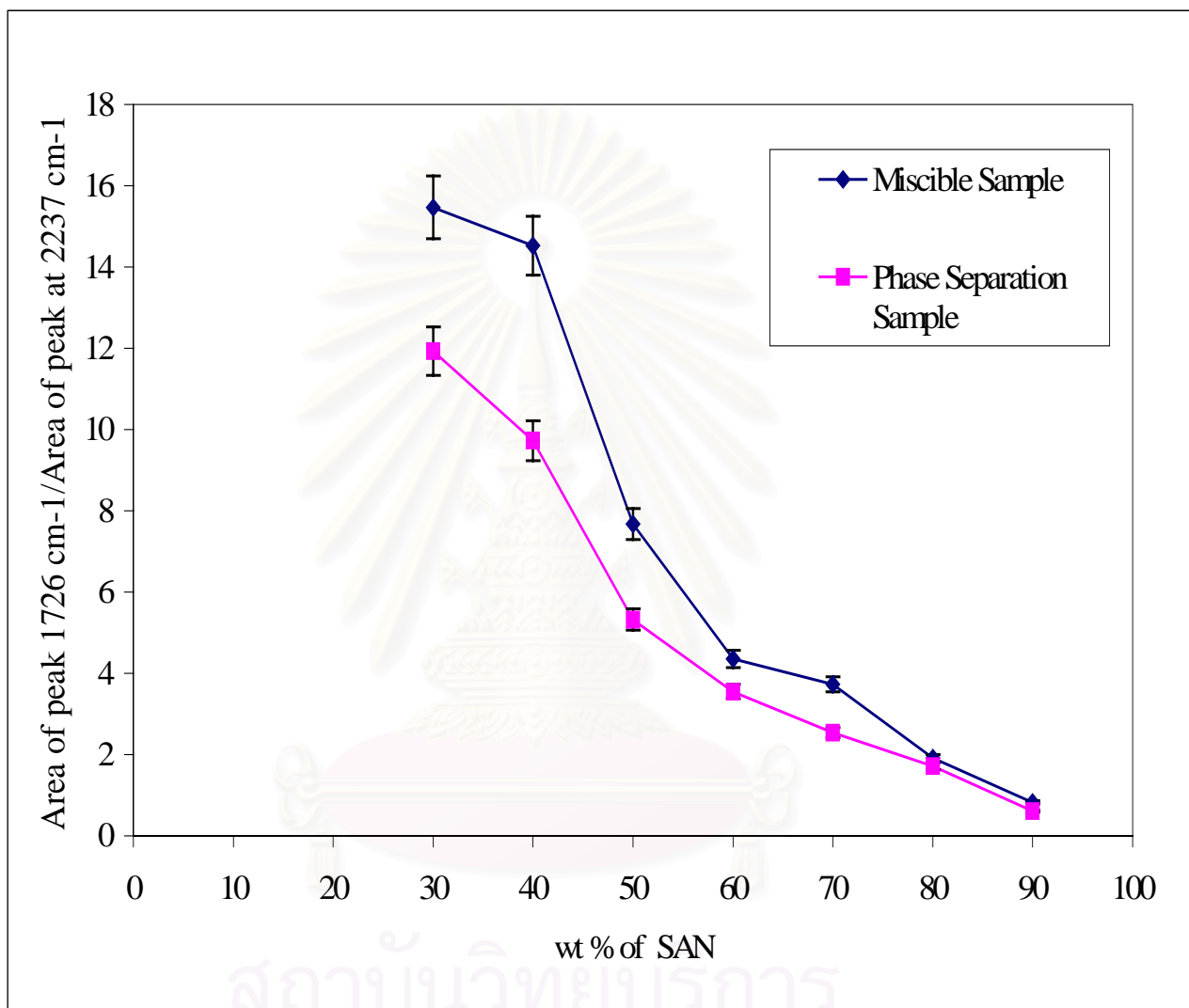


Figure 5.47 Comparing ratio of area under peak 1726 cm⁻¹ and area under peak 2237 cm⁻¹ with %weight of SAN

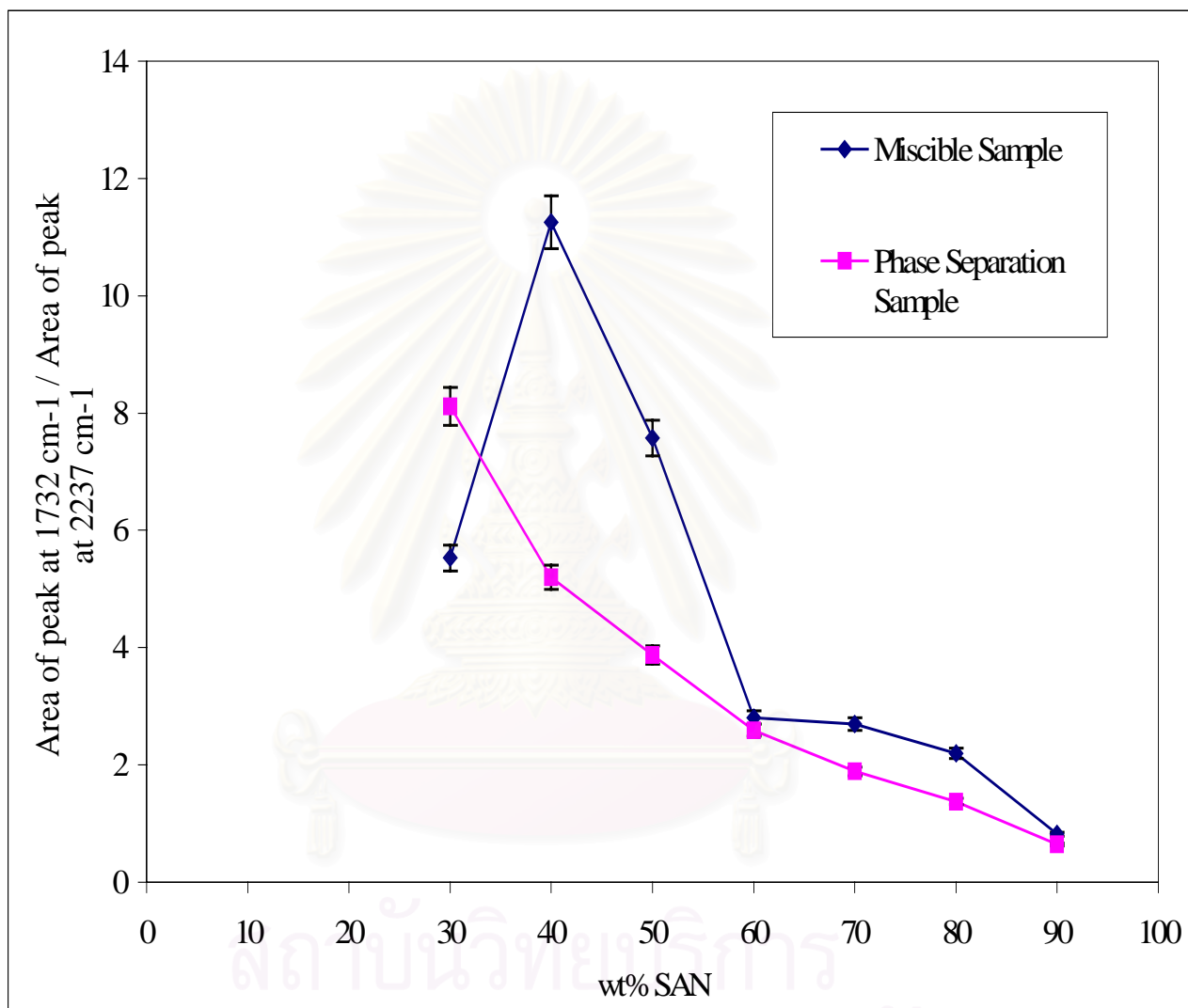


Figure 5.48 Comparing ratio of area under peak 1732 cm^{-1} and area under peak 2237 cm^{-1} with % weight of SAN

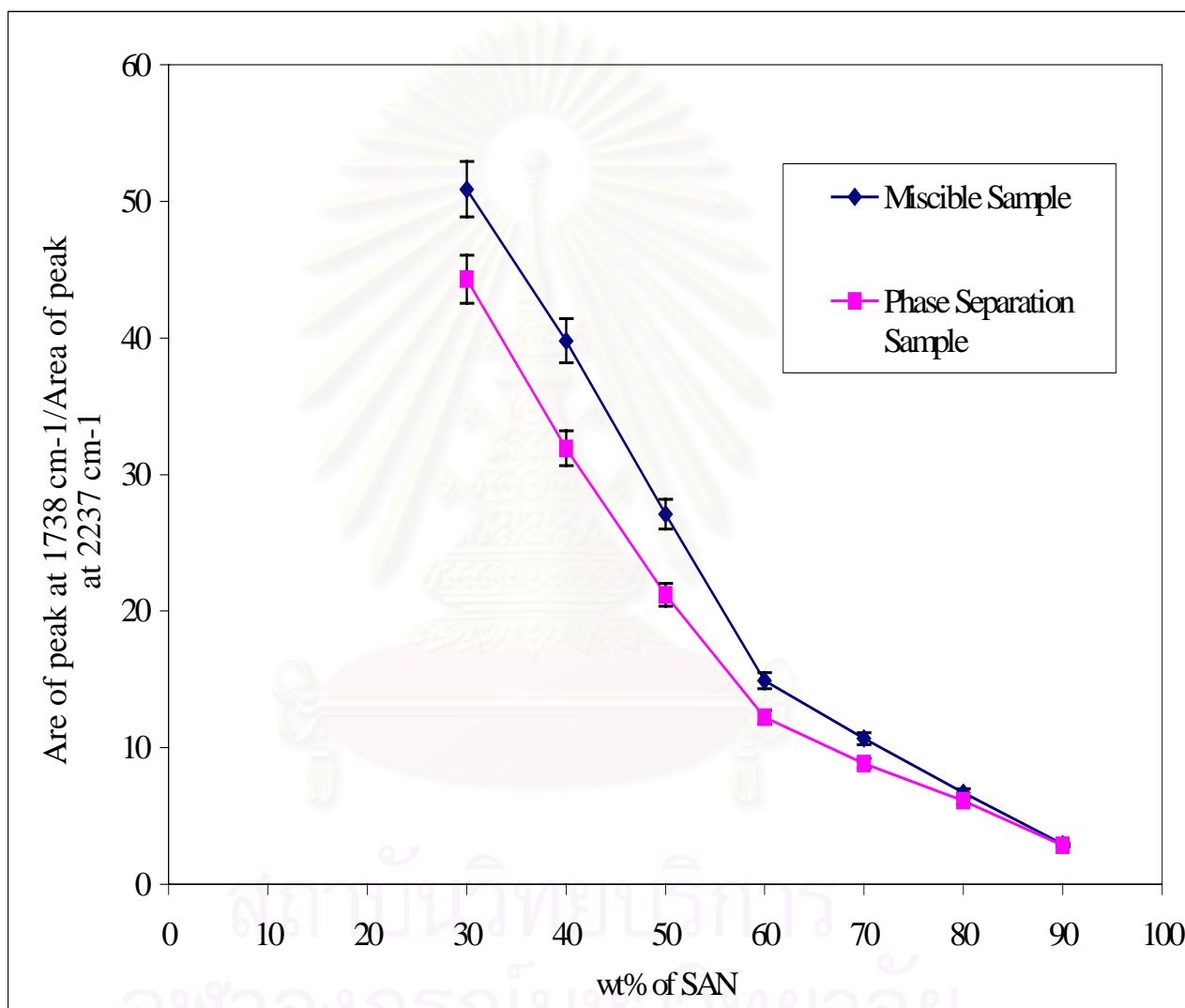


Figure 5.49 Comparing ratio of area under peak 1738 cm^{-1} and area under peak 2237 cm^{-1} with % weight of SAN

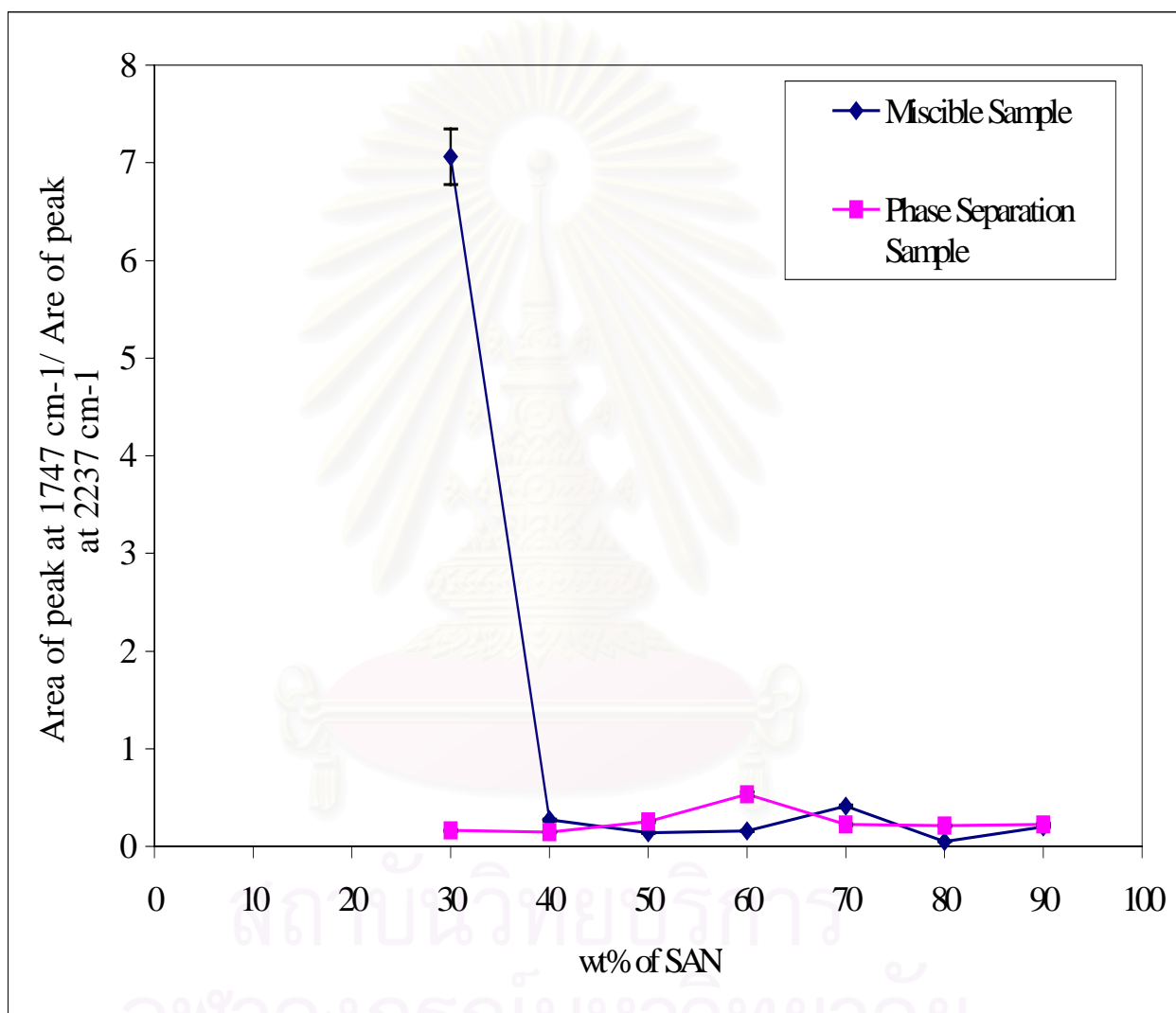


Figure 5.50 Comparing ratio of area under peak 1747 cm⁻¹ and area under peak 2237 cm⁻¹ with % weight of SAN

5.3 The prediction of unknown blend sample of SAN/PMMA

Due to the melting temperature between SAN and PMMA are 105 and 100 °C respectively. The glass transition temperature (T_g) of the blend was in range 100-105 °C. The DSC is not sensitive enough to detect the actual T_g of the blend narrow between these polymer. Thus the standard curve for predicting the unknown composition of this blend needed to be constructed by plotting the ratio of area under carbonyl peak to the area of mono-substitution of aromatic in SAN against weight percent of SAN in blending as shown in figure 5.51. Furthermore, the prediction between miscible and phase separated samples were investigated by plotting the ratio of area under carbonyl peak to the area of cyanide group in SAN as shown in figure 5.52.

5.3.1 Discussion

After the accurate FTIR spectra of miscible and phase separated blends from the suitable preparation method were observed by using OMNIC program. The ratio of carbonyl peak area of PMMA and mono-substitution area of aromatic in SAN at wave number 700 cm^{-1} were investigated at all compositions in order to predict the composition of unknown samples of this polymer blend as shown in figure 5.51. Figure 5.51 showed that the area ratio of carbonyl peak of PMMA to mono-substitution area of aromatic in SAN at wavenumber 702 cm^{-1} is in the range 11-12, 9-8, 6-5, 4-3, 3-2, 2-1, 1-0 correspond to 30, 40, 50, 60, 70, 80, 90 %wt of SAN respectively. Figure 5.52 also showed that the difference between the area ratio under carbonyl peak to cyanide group area in SAN at wavenumber 2237 cm^{-1} of miscible samples and that of phase separation samples.

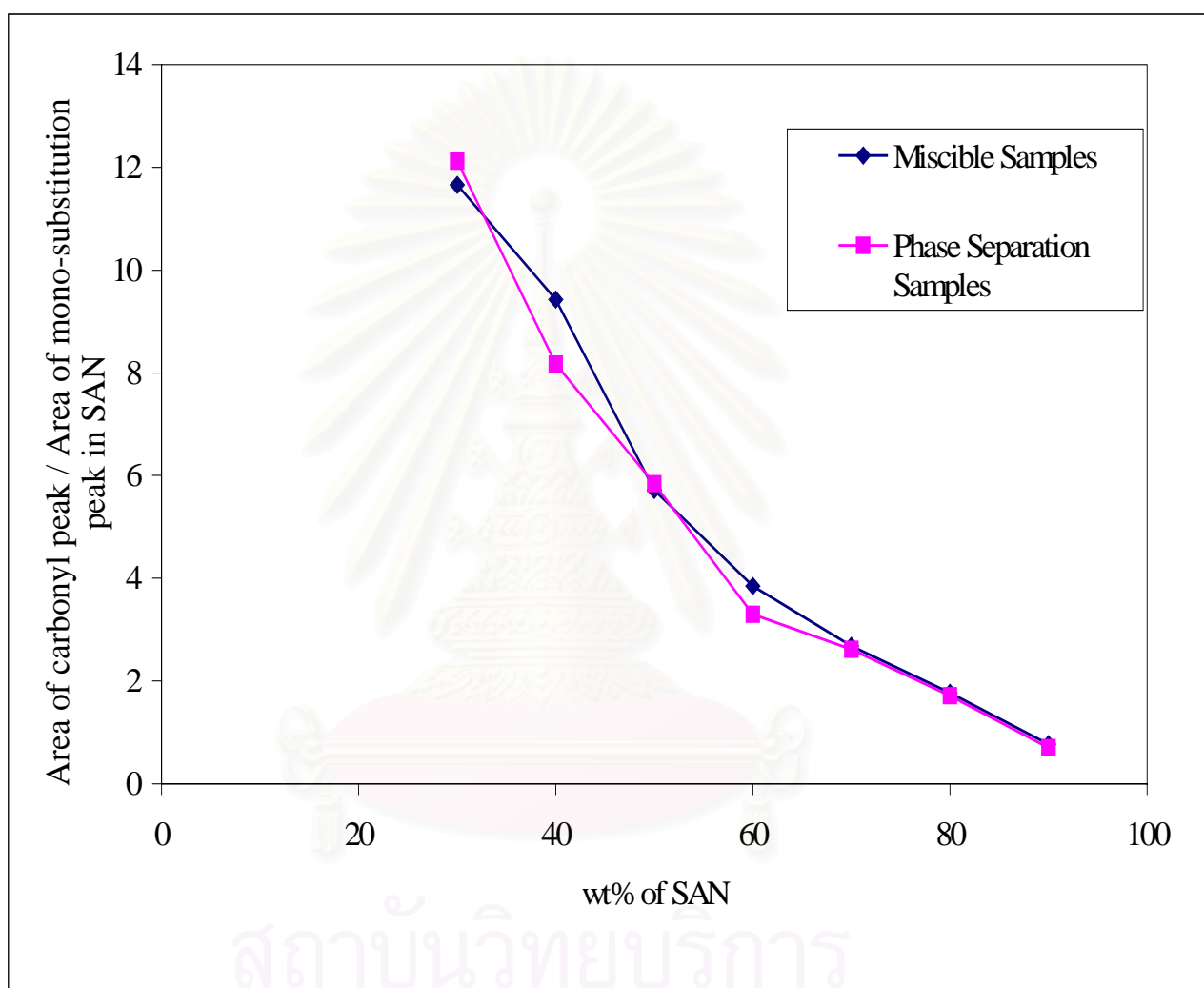


Figure 5.51 Prediction the ratio of unknown blending between SAN/PMMA

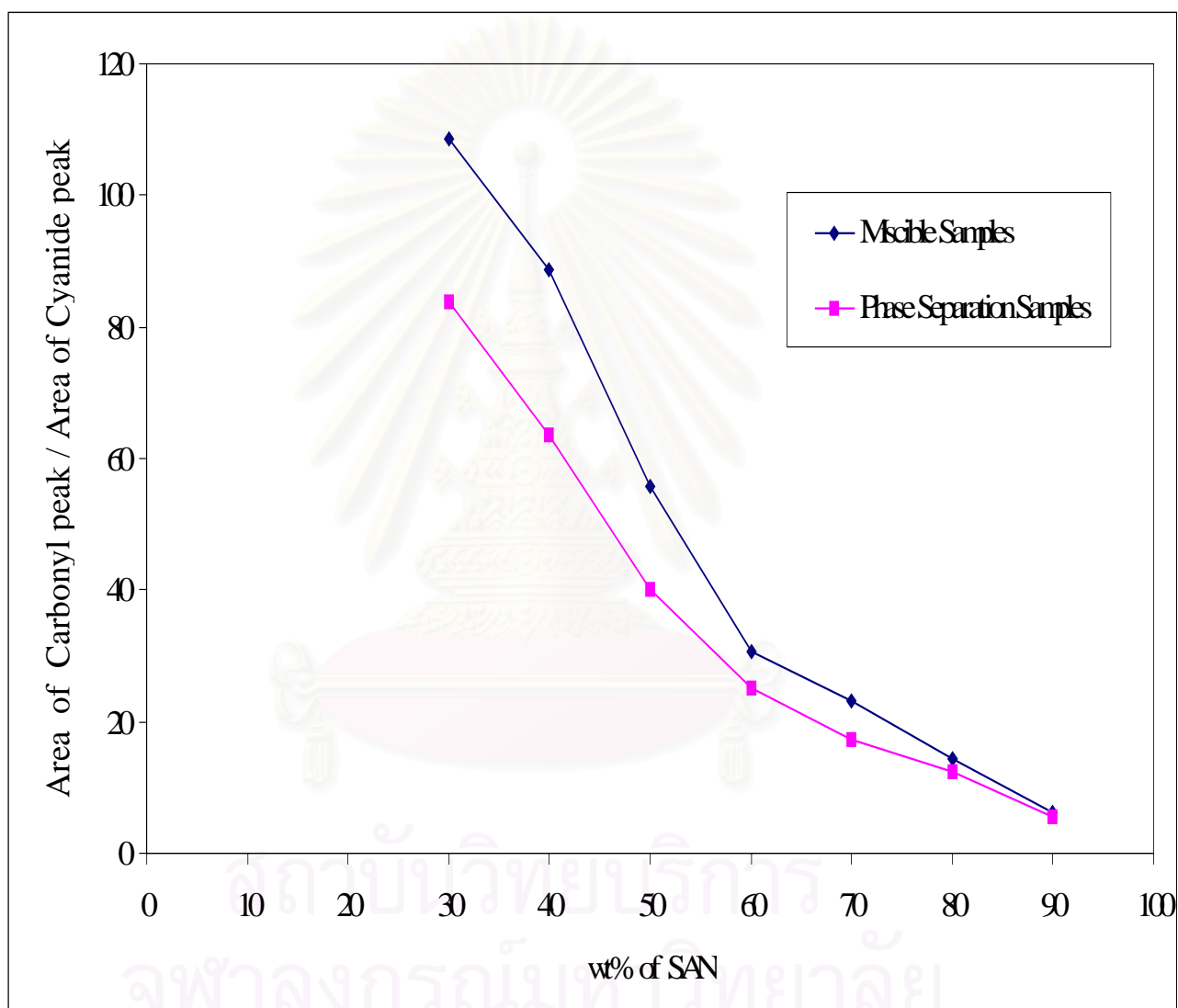


Figure 5.52 Prediction the type of unknown blending between SAN/PMMA.

CHAPTER VI

CONCLUSIONS AND RECOMMENDATIONS

6.1 Conclusions

The present work involved the investigation of the effects of sample preparation methods for quantitative analysis on infrared spectras, the effects of phase separation on the IR spectra of this blend, and the prediction of composition and occurred phase separated of unknown samples of polymer blend between styrene-acrylonitrile copolymer (SAN) and poly (methyl methacrylate) (PMMA) by using Fourier Transform Infrared Spectroscopy (FTIR). The miscible blends at various compositions of SAN and PMMA are prepared from melt mixing method. The infrared spectras of blending were constructed from plotting the absorbance (A) against wavenumber(cm^{-1}). Whereas the comparing area under peak of carbonyl group and the prediction of composition of unknown samples of this polymer pair constructed from plotting the area under interesting peak against blend compositions. The number of conclusions from the results of this work can be summarized as follows:

1. Three preparation methods for quantitative analysis by FTIR are compared in this work : KBr Disc method, KBr cubic method and film preparation method. For the KBr Disc method, there are three main effects that affected the IR spectra, that is the effect of moisture in air, the effect of size of ground samples and the effect of nonlinearity. For KBr cubic method, there are two effects that affected IR spectra, that is the effect of the clearance and smoothness of KBr cubics and the effect of nonlinearity. For film preparation method, there are one effect that affected IR spectra that is the effect of nonlinearity, but this effect can be eliminated by controlling the thickness of

film. From the experimental results, it can conclude that the pressing in film (film preparatin method) is the most suitable method for preparing the infrared spectra for quantitative analysis by FTIR.

2. The results from analyzing the second derivative of IR spectra of miscible samples and phase separated samples. The result showed that the miscible spectra had five hidden peaks that combine to be carbonyl peak, whereas the phase separation had four hidden peaks that combine to be carbonyl peak. In this work, we can not set the resolution of scan lower than four cm^{-1} , because there are effects from the noise of air peaks. So for phase separation samples, the recheck actual number of hidden peaks were occurred by comparing the root mean square error (RMS error) between four hidden peaks and five hidden peaks that were simulated by OPUS program. The results showed that in phase separated sample, there are five hidden peaks under carbonyl peak, which are occurred at wave number 1720, 1726, 1732, 1738 and 1747 cm^{-1} , respectively.

3. The areas of hidden peaks under carbonyl peak of miscible samples and phase separated samples were plotted versus composition of mixture samples. The results are shown that the areas under peaks at wavenumber 1720, 1726, 1738 cm^{-1} have the same trend. When comparing each miscible samples or phase separated samples separately, it showed that the quantities of areas under interesting peak at high concentration of PMMA in mixture samples are more than at low concentration of PMMA. When comparing at the same composition, the areas under peak 1720, 1726, 1738 cm^{-1} of miscible samples are higher than the area under peaks of phase separated samples. So the differences in the peaks at wavenumber 1720, 1726, 1738 cm^{-1} appeared because the phase separated samples have higher internal energy than miscible samples. For this reason, the

phase separated samples absorbed the IR energy less than that absorbed by the miscible samples

4. Compositions of samples between SAN and PMMA can be predicted by plotting ratio of peak area at wave number 1732 cm^{-1} to peak area at wave number 702 cm^{-1} versus composition of mixture sample. Unknown sample of this blend can be predicted by examined the composition from the result of ratio of area under peak at wave number 1732 cm^{-1} to area under peak at wave number 702 cm^{-1} from the calibration curve. Furthermore the prediction of phase separated composition can also be proceeded by plotting the calibration curve of the ratio of area under peak at wave number 1732 cm^{-1} to area under peak at wave number 2237 cm^{-1} versus composition.

6.2 Recommendations for Further Studies.

1. The preparation of blending ratio SAN: PMMA (2:8), (1:9) and pure PMMA can not be succeed for quantitative FTIR. Because of the non-linearity effect problem.
2. The effects of phase separation to number of peaks between miscible samples and phase separation samples should be confirmed in lower resolution of scanning than that of four cm^{-1} in this research and the conformation that occurred in polymer blend should be investigated with other right and precise instruments.
3. SAN or PMMA should be prepared from synthesis in side the laboratory more than commercial grade, because it will give the more accurate result.

REFERENCES

Brysdon, J. A. Plastic Materials., 6th ed. London: Butterworth-Heinemann, 1995.

Brian C. Smith, Fourier Transform Infrared Spectroscopy, New York: CRC Press, 1996

Cesteros, Luis C. Hydrogen bonding in poly(4-vinylpyridine)/poly(vinyl acetate-co-vinyl alcohol) blends. An infrared study. Macromolecules 26(26) (1993): 7256-7262

Charier, J-M. Polymer Materials and Processing. New York: Oxford University, 1991.

Coleman, M. M., Lee, J. Y. FTIR studies of hydrogen bonding in polymer blend. Methacrylic Acid copolymer-polyether blends. Polymer Preprints, American Chemical Society 28(2) (1987): 131-132.

Coleman, Michal M. Hydrogen bonding in polymer blends. FTIR studies of urethane-ether blends. Macromolecules 21(1) (1988): 59-65.

Ha, Chang-Sik. Specific interactions in maleic anhydride grafted PP and sulfonated EPDM ionomer blends by FTIR spectroscopy Polymerpreprints, Division of Polymer Chemistry, American Chemical Society 37(1) (1996): 24-29.

REFERENCES (continued)

- Higgins, G.M.C. and Miller, R.G.J., Insoluble polymers and rubbers, in Laboratory Methods in Infrared Spectroscopy, London, 1972.
- Janathanan, V. Intramolecular interactions in poly(styrene-co-acrylonitrile)/poly (ϵ -caprolactone) blends Journal of Polymer Science, Part B 31(8) (1993): 1013-1017.
- Kroschwitz, J. I. Concise Encyclopedia of Polymer Science and Engineering. 2nd ed. New York: John Wiley&Sons, 1990.
- Lim, Jong-Chul. FTIR investigation of ion-dipole interaction in styrene ionomer/poly (ethylene oxide) blends Journal of Polymer Science, PartB 32(1) (1994): 29-35
- Oiarzabal, L. Miscibility Study of Polyolefin Blends. Doctoral dissertation, Department of Chemical Engineering, Imperial College, 1993.
- Olabishi, O., Robeson, L. M., and Shaw, M. T. Polymer-Polymer Miscibility. San Diego: Academic Press, 1979.
- Patricia B. Coleman, Practical Sampling Techniques for Infrared Analysis. Florida: CRC Press, 1993.

REFERENCES (continued)

- Painter, Paul C., Tang, Wei-long; Graf, John F. Formation of molecular composites through hydrogen-bonding interactions Macromolecules 24(13) (1991): 3929-3936
- Paul, D. R., Newman, S. Polymer Blends. Vol. 1. New York: Academic Press, 1978
Practices for General Techniques of Infrared Quantitative Analysis, ASTM Practice E 168-88, ASTM: Philadelphia, 1991.
- Radmard, B. Dadmun. Accessibility of functional groups to intermolecular hydrogen bonding in polymer blends containing a liquid crystalline polymer Polymer 42(4) (1996): 1591-1600
- Rosato, D. V., Dimattia, D. P., and Rosato, D. V. Designing with Plastics and Compositess a Handbook. New York: Van Nostrand Reinhold, 1991.
- Rudinger Schafer, Jorg Zimmermann, Jorg Kressler and Rolf Mulhaupt, Mprphology and phase behaviour of poly (methyl methacrylate) / poly (styrene co-acrylonitrile) blends monitored by FTIR microscopy, Polymer 38(15) (1996): 3745-3752
- Russell, J. D., Infrared Spectroscopy of Inorganic Compounds, in Laboratory Methods in Vibrational Spectroscopy, New York: John Wiley & Sons, 1987.

REFERENCES (continued)

Silverstein, R.M., Bassler, G. C., Morrill, T. C. Spectrometric Identification of Organic Compounds. New York: John Wiley & Sons Inc, 1991

Smith, A.L., Applied Infrared Spectroscopy: Fundamentals, Techniques and Analytical Problem Solving. New York: John Wiley & Sons, 1979.

Tosi, C. and Ciampelli, F., Applications of Infrared Spectroscopy to ethylene-propylene copolymers, Advances in Polymer Science, 2 (1973) : 87.

Thongyai, S. Determination of Polymer Miscibility by Calorimetry (First Year Report). Doctoral dissertation, Department of Chemical Engineering, Imperial College, 1990.

Utracki, L. A. Polymer Alloys and Blends. New York: Hanser, 1990.

Walsh, D. J., Higgins, J. S., and Maconnachie, A. Polymer Blends and Mixtures. Dordrecht: Martinus Nijhoff, 1985.

William Kemp, Organic Spectroscopy. The Macmillan Press, 1994.

Willis, H.A., Preparation of Polymer Samples for IR Examination, in Laboratory Methods in Vibrational Spectroscopy, New York, 1987.

APPENDIX

(EXPERIMENTAL RESULTS)

A. The area under interesting peak from the studies of phase separation effect.

Table A.1 The area under peak at wavenumber 2237 cm^{-1} (cyanide peak) of miscible samples. The range that observed is settled between wavenumber 2220 to 2254 cm^{-1} .

Sample	Weight % of SAN in Blends						
	30	40	50	60	70	80	90
1A	0.1345	0.1157	0.1235	0.1376	0.1358	0.1358	0.1422
1B	0.1342	0.133	0.1413	0.1488	0.1388	0.1355	0.1409
1C	0.1456	0.1165	0.1189	0.1393	0.1395	0.1356	0.141
2A	0.1302	0.1208	0.1286	0.137	0.1278	0.1255	0.142
2B	0.1534	0.1318	0.1198	0.1372	0.1288	0.1292	0.1351
2C	0.1118	0.1268	0.1213	0.1371	0.1392	0.127	0.122

Table A.2a The area under peak at wavenumber 1720 cm^{-1} of miscible samples. The range that observed is settled between wavenumber 1780 to 1650 cm^{-1} .

Sample	Weight % of SAN in Blends						
	30	40	50	60	70	80	90
1A	3.905	2.716	1.619	1.145	0.767	0.474	0.218
1B	3.916	2.965	1.927	1.265	0.775	0.473	0.225
1C	4.169	2.645	1.556	1.154	0.818	0.478	0.22
2A	4.044	2.738	1.655	1.123	0.7398	0.444	0.22
2B	4.53	3.035	1.623	1.127	0.73	0.455	0.215
2C	3.312	2.829	1.56	1.124	0.798	0.45	0.183

Table A.2b The area ratio between peak at wavenumber 1720 cm^{-1} and peak at wavenumber 2237 cm^{-1} of miscible samples.

% SAN	Weight % of SAN in Blends						
	30	40	50	60	70	80	90
1A	29.0335	23.4745	13.1093	8.32122	5.64801	3.49043	1.53305
1B	29.1803	22.2932	13.6377	8.50134	5.58357	3.49077	1.59688
1C	28.6332	22.7039	13.0866	8.28428	5.8638	3.52507	1.56028
2A	31.0599	22.6656	12.8694	8.19708	5.78873	3.53785	1.5493
2B	29.5306	23.0273	13.5476	8.21429	5.6677	3.52167	1.59141
2C	29.6243	22.3107	12.8607	8.1984	5.73276	3.54331	1.5
Average	29.51032	22.74587	13.1852	8.286101	5.714096	3.518184	1.555154

Table A.3a The area under peak at wavenumber 1726 cm^{-1} of miscible samples. The range that observed is settled between wavenumber 1780 to 1650 cm^{-1} .

Sample	Weight % of SAN in Blends						
	30	40	50	60	70	80	90
1A	2.106	1.712	0.954	0.585	0.501	0.257	0.118
1B	2.073	2.02	1.012	0.657	0.51	0.253	0.115
1C	2.217	1.707	0.869	0.581	0.512	0.263	0.112
2A	1.996	1.695	1.021	0.586	0.483	0.24	0.117
2B	2.415	1.849	0.974	0.611	0.483	0.243	0.111
2C	1.719	1.83	0.945	0.625	0.532	0.2508	0.101

Table A.3b The area ratio between peak at wavenumber 1726 cm^{-1} and peak at wavenumber 2237 cm^{-1} of miscible samples.

% SAN	Weight % of SAN in Blends						
	30	40	50	60	70	80	90
1A	15.658	14.7969	7.7247	4.25145	3.68925	1.89249	0.82982
1B	15.4471	15.188	7.16207	4.41532	3.67435	1.86716	0.81618
1C	15.2266	14.6524	7.30866	4.17085	3.67025	1.93953	0.79433
2A	15.3303	14.0315	7.93935	4.27737	3.77934	1.91235	0.82394
2B	15.7432	14.0288	8.13022	4.45335	3.75	1.8808	0.82161
2C	15.3757	14.4322	7.7906	4.55872	3.82184	1.9748	0.82787
Average	15.4635	14.5216	7.67593	4.35451	3.73084	1.91119	0.81896

Table A.4a The area under peak at wavenumber 1732 cm^{-1} of miscible samples. The range that observed is settled between wavenumber 1780 to 1650 cm^{-1} .

Sample	Weight % of SAN in Blends						
	30	40	50	60	70	80	90
1A	0.762	1.384	0.909	0.385	0.352	0.29	0.128
1B	0.7	1.591	1.202	0.411	0.39	0.334	0.064
1C	0.891	1.283	0.85	0.404	0.36	0.32	0.129
2A	0.691	1.317	0.961	0.371	0.358	0.267	0.131
2B	0.852	1.527	0.812	0.386	0.362	0.264	0.113
2C	0.594	1.281	0.991	0.394	0.358	0.262	0.109

Table A.4b The area ratio between peak at wavenumber 1732 cm^{-1} and peak at wavenumber 2237 cm^{-1} of miscible samples.

% SAN	Weight % of SAN in Blends						
	30	40	50	60	70	80	90
1A	5.66543	11.962	7.36032	2.79797	2.59205	2.13549	0.90014
1B	5.2161	11.9624	8.50672	2.7621	2.8098	2.46494	0.45422
1C	6.11951	11.0129	7.14886	2.90022	2.58065	2.35988	0.91489
2A	5.30722	10.9023	7.47278	2.70803	2.80125	2.12749	0.92254
2B	5.55411	11.5857	6.77796	2.81341	2.81056	2.04334	0.83642
2C	5.31306	10.1025	8.16983	2.87381	2.57184	2.06299	0.89344
Average	5.52924	11.2546	7.57275	2.80926	2.69436	2.19902	0.82028

Table A.5a The area under peak at wavenumber 1738 cm^{-1} of miscible samples. The range that observed is settled between wavenumber 1780 to 1650 cm^{-1} .

Sample	Weight % of SAN in Blends						
	30	40	50	60	70	80	90
1A	6.845	4.407	3.31	2.077	1.474	0.925	0.361
1B	6.974	5.244	3.849	2.227	1.492	0.917	0.456
1C	7.39	4.663	3.334	2.132	1.488	0.885	0.363
2A	6.538	4.941	3.55	2.043	1.339	0.838	0.37
2B	7.816	5.172	3.193	2.005	1.362	0.864	0.433
2C	5.652	5.211	3.187	1.994	1.481	0.861	0.403

Table A.5b The area ratio between peak at wavenumber 1738 cm^{-1} and peak at wavenumber 2237 cm^{-1} of miscible samples.

% SAN	Weight % of SAN in Blends						
	30	40	50	60	70	80	90
1A	50.8922	38.0899	26.8016	15.0945	10.8542	6.81149	2.53868
1B	51.9672	39.4286	27.2399	14.9664	10.7493	6.76753	3.23634
1C	50.7555	40.0258	28.0404	15.3051	10.6667	6.52655	2.57447
2A	50.2151	40.9023	27.605	14.9124	10.4773	6.67729	2.60563
2B	50.9518	39.2413	26.6528	14.6137	10.5745	6.68731	3.20503
2C	50.5546	41.0962	26.2737	14.5441	10.6394	6.77953	3.30328
Average	50.8894	39.7973	27.1022	14.906	10.6602	6.70828	2.91057

Table A.6a The area under peak at wavenumber 1747 cm^{-1} of miscible samples. The range that observed is settled between wavenumber 1780 to 1650 cm^{-1} .

Sample	Weight % of SAN in Blends						
	30	40	50	60	70	80	90
1A	0.9588	0.0331	0.0145	0.0209	0.0622	0.0076	0.0402
1B	0.9158	0.0364	0.01953	0.02159	0.0448	0.0055	0.0446
1C	1.09	0.0337	0.01196	0.02159	0.0547	0.0062	0.0397
2A	0.886	0.0321	0.01337	0.024	0.06135	0.0063	0.0395
2B	1.0711	0.0348	0.0124	0.023	0.047	0.00651	0.0043
2C	0.799	0.0302	0.033	0.0206	0.061	0.00742	0.003

Table A.6b The area ratio between peak at wavenumber 1747 cm^{-1} and peak at wavenumber 2237 cm^{-1} of miscible samples.

% SAN	Weight % of SAN in Blends						
	30	40	50	60	70	80	90
1A	7.12862	0.28608	0.11741	0.15189	0.45803	0.05596	0.2827
1B	6.82414	0.27368	0.13822	0.14509	0.32277	0.04059	0.31654
1C	7.48626	0.28927	0.10059	0.15499	0.39211	0.04572	0.28156
2A	6.80492	0.26573	0.10397	0.17518	0.48005	0.0502	0.27817
2B	6.9824	0.26404	0.10351	0.16764	0.36491	0.05039	0.03183
2C	7.14669	0.23817	0.27205	0.15026	0.43822	0.05843	0.02459
Average	7.06217	0.2695	0.13929	0.15751	0.40935	0.05021	0.20256

Table A.7 The area under peak at wavenumber 2237 cm^{-1} (cyanide peak) of phase separated samples. The range that observed is settled between wavenumber 2220 to 2254 cm^{-1} .

Sample	Weight % of SAN in Blends						
	30	40	50	60	70	80	90
1A	0.1685	0.1352	0.1375	0.1313	0.1718	0.133	0.1281
1B	0.1589	0.1421	0.1497	0.1383	0.1553	0.1455	0.1444
1C	0.1644	0.1374	0.1499	0.1455	0.155	0.1565	0.1462
2A	0.2251	0.163	0.16	0.178	0.1916	0.1641	0.1538
2B	0.1315	0.137	0.1414	0.1607	0.1528	0.1476	0.1442
2C	0.1279	0.1458	0.1671	0.1466	0.1776	0.1627	0.1443

Table A.8a The area under peak at wavenumber 1720 cm^{-1} of phase separated samples. The range that observed is settled between wavenumber 1780 to 1650 cm^{-1} .

Sample	Weight % of SAN in Blends						
	30/70	40/60	50/50	60/40	70/30	80/20	90/10
1A	3.042	2.309	1.582	0.838	0.726	0.474	0.203
1B	3.101	2.255	1.359	0.861	0.746	0.48	0.192
1C	2.984	2.295	1.701	0.753	0.769	0.461	0.15
2A	4.567	2.785	1.473	0.987	0.781	0.438	0.125
2B	2.715	2.306	1.429	0.862	0.653	0.402	0.181
2C	2.677	2.431	1.933	1.01	0.746	0.418	0.175

Table A.8b The area ratio between peak at wavenumber 1720 cm^{-1} and peak at wavenumber 2237 cm^{-1} of phase separated samples.

Sample	Weight % of SAN in Blends						
	30	40	50	60	70	80	90
1A	18.0534	17.0784	11.5055	6.38233	4.22584	3.56391	1.5847
1B	19.5154	15.8691	9.07816	6.2256	4.80361	3.29897	1.32964
1C	18.1509	16.7031	11.3476	5.17526	4.96129	2.94569	1.02599
2A	20.2888	17.0859	9.20625	5.54494	4.0762	2.6691	0.81274
2B	20.6464	16.8321	10.1061	5.36403	4.27356	2.72358	1.2552
2C	20.9304	16.6735	11.5679	6.8895	4.20045	2.56915	1.21275
Average	19.5975	16.707	10.4686	5.93028	4.42349	2.96173	1.2035

Table A.9a The area under peak at wavenumber 1726 cm^{-1} of phase separated samples. The range that observed is settled between wavenumber 1780 to 1650 cm^{-1} .

Sample	Weight % of SAN in Blends						
	30	40	50	60	70	80	90
1A	1.929	1.291	0.789	0.553	0.49	0.213	0.098
1B	1.896	1.397	0.745	0.59	0.369	0.25	0.099
1C	1.913	1.372	0.836	0.574	0.358	0.27	0.073
2A	2.845	1.603	0.9	0.536	0.543	0.308	0.082
2B	1.635	1.358	0.771	0.519	0.401	0.257	0.068
2C	1.562	1.382	0.838	0.497	0.398	0.265	0.102

Table A.9b The area ratio between peak at wavenumber 1726 cm^{-1} and peak at wavenumber 2237 cm^{-1} of phase separated samples.

Sample	Weight % of SAN in Blends						
	30	40	50	60	70	80	90
1A	11.4481	9.54882	5.73818	4.21173	2.85215	1.6015	0.76503
1B	11.932	9.8311	4.97662	4.26609	2.37605	1.71821	0.6856
1C	11.6363	9.98544	5.57705	3.94502	2.30968	1.72524	0.49932
2A	12.6388	9.83436	5.625	3.01124	2.83403	1.8769	0.53316
2B	12.4335	9.91241	5.45262	3.22962	2.62435	1.74119	0.47157
2C	12.2127	9.47874	5.01496	3.39018	2.24099	1.62876	0.70686
Average	12.0502	9.76514	5.39741	3.67564	2.53954	1.7153	0.61025

Table A.10a The area under peak at wavenumber 1732 cm^{-1} of phase separated samples. The range that observed is settled between wavenumber 1780 to 1650 cm^{-1} .

Sample	Weight % of SAN in Blends						
	30	40	50	60	70	80	90
1A	1.419	0.696	0.573	0.366	0.32	0.206	0.068
1B	1.057	0.779	0.62	0.346	0.301	0.207	0.099
1C	1.485	0.69	0.58	0.343	0.29	0.218	0.124
2A	1.4897	0.865	0.52	0.477	0.343	0.224	0.083
2B	1.109	0.712	0.575	0.461	0.3	0.183	0.098
2C	1.124	0.734	0.63	0.346	0.34	0.194	0.085

Table A.10b The area ratio between peak at wavenumber 1732 cm^{-1} and peak at wavenumber 2237 cm^{-1} of phase separated samples.

Sample	Weight % of SAN in Blends						
	30	40	50	60	70	80	90
1A	8.42136	5.14793	4.16727	2.78751	1.86263	1.54887	0.53084
1B	6.65198	5.48205	4.14162	2.50181	1.93818	1.42268	0.6856
1C	9.03285	5.02183	3.86925	2.35739	1.87097	1.39297	0.84815
2A	6.61795	5.30675	3.25	2.67978	1.79019	1.36502	0.53966
2B	8.43346	5.19708	4.06648	2.8687	1.96335	1.23984	0.67961
2C	8.78812	5.03429	3.7702	2.36016	1.91441	1.19238	0.58905
Average	7.99095	5.19832	3.87747	2.59256	1.88996	1.36029	0.64548

Table A.11a The area under peak at wavenumber 1738 cm^{-1} of phase separated samples. The range that observed is settled between wavenumber 1780 to 1650 cm^{-1} .

Sample	Weight % of SAN in Blends						
	30	40	50	60	70	80	90
1A	7.675	4.284	2.688	1.658	1.45	0.909	0.374
1B	7.133	4.503	2.976	1.696	1.195	0.993	0.428
1C	7.519	4.437	2.912	1.848	1.351	0.994	0.352
2A	9.934	4.991	3.357	2.261	1.714	0.875	0.351
2B	5.574	4.417	3.097	1.998	1.423	0.895	0.412
2C	5.374	4.647	3.111	1.672	1.251	0.895	0.434

Table A.11b The area ratio between peak at wavenumber 1738 cm^{-1} and peak at wavenumber 2237 cm^{-1} of phase separated samples.

Sample	Weight % of SAN in Blends						
	30	40	50	60	70	80	90
1A	45.549	31.6864	19.5491	12.6276	8.44005	6.83459	2.91959
1B	44.8899	31.689	19.8798	12.2632	7.69478	6.82474	2.96399
1C	45.736	32.2926	19.4263	12.701	8.71613	6.35144	2.40766
2A	44.1315	30.6196	20.9813	12.7022	8.94572	5.33211	2.28218
2B	42.3878	32.2409	21.9024	12.4331	9.31283	6.06369	2.85714
2C	42.0172	31.8724	18.6176	11.4052	7.04392	5.50092	3.00762
Average	44.1186	31.7335	20.0594	12.3554	8.3589	6.15125	2.7397

Table A.12a The area under peak at wavenumber 1747 cm^{-1} of phase separated samples. The range that observed is settled between wavenumber 1780 to 1650 cm^{-1} .

Sample	Weight % of SAN in Blends						
	30	40	50	60	70	80	90
1A	0.02413	0.02622	0.02393	0.03756	0.00613	0.03894	0.0025
1B	0.02541	0.0238	0.0604	0.0388	0.0336	0.0124	0.0039
1C	0.0233	0.0157	0.04264	0.0338	0.0339	0.0122	0.0219
2A	0.02298	0.1443	0.0122	0.0372	0.0193	0.0628	0.0844
2B	0.03049	0.01552	0.02324	0.01358	0.02134	0.0367	0.068
2C	0.018	0.0608	0.113	0.309	0.11	0.029	0.02

Table A.12b The area ratio between peak at wavenumber 1747 cm^{-1} and peak at wavenumber 2237 cm^{-1} of phase separated samples.

Sample	Weight % of SAN in Blends						
	30	40	50	60	70	80	90
1A	0.1432	0.19393	0.17404	0.28606	0.03568	0.29278	0.01952
1B	0.15991	0.16749	0.40347	0.28055	0.21636	0.08522	0.02701
1C	0.14173	0.11426	0.28446	0.2323	0.21871	0.07796	0.14979
2A	0.10209	0.88528	0.07625	0.20899	0.10073	0.38269	0.54876
2B	0.23186	0.11328	0.16436	0.08451	0.13966	0.24864	0.47157
2C	0.14073	0.41701	0.67624	2.10778	0.61937	0.17824	0.1386
Average	0.15326	0.31521	0.29647	0.53336	0.22175	0.21092	0.22588

B. The area ratio for concentration prediction of unknown blend between SAN/PMMA.

Table B.1 The area under carbonyl peak of miscible samples. The range that observed is settled between wavenumber 1780 to 1650 cm^{-1} .

%SAN	Weight % of SAN in Blends						
	30	40	50	60	70	80	90
1A	14.5768	10.2521	6.8065	4.2129	3.1562	1.9536	0.8652
1B	14.5788	11.8564	8.00953	4.58159	3.2118	1.9825	0.9046
1C	15.757	10.3317	6.62096	4.29259	3.2327	1.9522	0.8637
2A	14.155	10.7231	7.20037	4.147	2.98115	1.7953	0.8775
2B	16.6841	11.6178	6.6144	4.152	2.984	1.83251	0.8763
2C	12.076	11.1812	6.716	4.1576	3.23	1.83122	0.799

Table B.2 The area under carbonyl peak of phase separated samples. The range that observed is settled between wavenumber 1780 to 1650 cm^{-1} .

%SAN	Weight % of SAN in Blends						
	30	40	50	60	70	80	90
1A	14.0891	8.60622	5.65593	3.45256	2.99213	1.84094	0.7455
1B	13.2124	8.9578	5.7604	3.5318	2.6446	1.9424	0.8219
1C	13.9243	8.8097	6.07164	3.5518	2.8019	1.9552	0.7209
2A	18.8587	10.3883	6.2622	4.2982	3.4003	1.9078	0.7254
2B	11.0635	8.80852	5.89524	3.85358	2.79834	1.7737	0.827
2C	10.755	9.2548	6.625	3.834	2.845	1.801	0.816

Table B.3 The area under mono-substitution of aromatic in SAN of miscible samples. The range that observed is settled between wavenumber 725 to 675 cm^{-1} .

%SAN	Weight % of SAN in Blends						
	30	40	50	60	70	80	90
1A	1.299	1.084	1.185	1.083	1.163	1.100	1.188
1B	1.264	1.255	1.452	1.205	1.140	1.116	1.241
1C	1.341	1.089	1.126	1.143	1.137	1.066	1.174
2A	1.240	1.150	1.254	1.066	1.155	1.010	1.141
2B	1.406	1.216	1.181	1.068	1.139	0.991	1.001
2C	0.993	1.208	1.155	1.069	1.294	1.120	0.999

Table B.4 The area under mono-substitution of aromatic in SAN of phase separated samples. The range that observed is settled between wavenumber 725 to 675 cm^{-1} .

%SAN	Weight % of SAN in Blends						
	30	40	50	60	70	80	90
1A	1.147	1.032	0.934	1.041	1.231	1.124	0.994
1B	1.079	1.105	0.975	1.099	1.079	1.189	1.214
1C	1.146	1.087	1.044	1.082	1.038	1.147	1.071
2A	1.607	1.282	1.121	1.333	1.226	1.083	1.029
2B	0.913	1.083	0.993	1.196	1.048	1.003	1.155
2C	0.884	1.122	1.158	1.086	1.062	1.016	1.144

Table B.5 The area ratio between carbonyl peak and mono-substituted aromatic in SAN at wavenumber 700 cm^{-1} of miscible samples.

%SAN	Weight % of SAN in Blends						
	30	40	50	60	70	80	90
1A	11.223	9.457	5.743	3.89	2.713	1.776	0.728
1B	11.5366	9.446	5.5157	3.802	2.817	1.777	0.729
1C	11.753	9.487	5.88	3.755	2.843	1.831	0.736
2A	11.411	9.327	5.741	3.891	2.582	1.778	0.769
2B	11.865	9.558	5.603	3.886	2.619	1.85	0.875
2C	12.156	9.257	5.815	3.889	2.497	1.635	0.8
Average	11.6574	9.422	5.71628	3.85217	2.6785	1.7745	0.77283

Table B.6 The area ratio between carbonyl peak and mono-substituted aromatic in SAN at wavenumber 700 cm^{-1} of phase separated samples.

%SAN	Weight % of SAN in Blends						
	30	40	50	60	70	80	90
1A	12.287	8.342	6.055	3.318	2.43	1.638	0.75
1B	12.249	8.109	5.906	3.215	2.45	1.633	0.677
1C	12.15	8.101	5.814	3.282	2.699	1.705	0.673
2A	11.738	8.104	5.588	3.225	2.773	1.762	0.705
2B	12.113	8.134	5.935	3.223	2.671	1.769	0.716
2C	12.166	8.245	5.722	3.529	2.679	1.772	0.713
Average	12.11716	8.1725	5.836666	3.298667	2.617	1.713167	0.705667

Table B.7 The area ratio between carbonyl peak and cyanide peak at wavenumber 2237 cm^{-1} of miscible samples.

%SAN	Weight % of SAN in Blends						
	30	40	50	60	70	80	90
1A	108.378	88.6093	55.1134	30.617	23.2415	14.3859	6.08439
1B	108.635	89.1459	56.6846	30.7903	23.1398	14.631	6.42016
1C	108.221	88.6841	55.6851	30.8154	23.1735	14.3968	6.12553
2A	108.717	88.7674	55.9904	30.2701	23.3267	14.3052	6.17958
2B	108.762	88.1472	55.212	30.2624	23.1677	14.1835	6.48631
2C	108.014	88.1798	55.3669	30.3253	23.204	14.4191	6.54918
Average	108.455	88.589	55.6754	30.5134	23.2089	14.3869	6.30752

Table B.8 The area ratio between carbonyl peak and cyanide peak at wavenumber 2237 cm^{-1} of phase separated samples.

%SAN	Weight % of SAN in Blends						
	30	40	50	60	70	80	90
1A	83.615	63.6555	41.134	26.2952	17.4164	13.8417	5.81967
1B	83.1492	63.0387	38.4796	25.5372	17.029	13.3498	5.69183
1C	84.6977	64.1172	40.5046	24.411	18.0768	12.4933	4.93092
2A	83.7791	63.7319	39.1388	24.1472	17.7469	11.6258	4.71651
2B	84.133	64.2958	41.6919	23.98	18.3137	12.0169	5.73509
2C	84.0891	63.476	39.6469	26.1528	16.0191	11.0695	5.65489
Average	83.9105	63.7192	40.0993	25.0872	17.4336	12.3995	5.42482

C. Error Analysis

Most experimental data in this thesis are reported with the error bar of 95 % confidence. It should be noted that 95% confidence interval or 0.95 confidence coefficient in fact mean if it is assumed that the distribution is the normal probability distribution, 95% of data fall within this region. The value can be defined as,

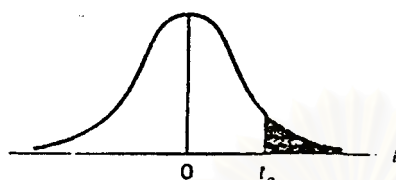
$$t_{0.25} \frac{(\sigma)}{\sqrt{n}} \quad (C-1)$$

where $t_{0.25}$ is the standard normal value of $t_{0.25}$ at the degree of freedom of $(n-1)$, as can be seen in figure C-1

σ is standard deviation

n is number of data

สถาบันวิทยบริการ
จุฬาลงกรณ์มหาวิทยาลัย

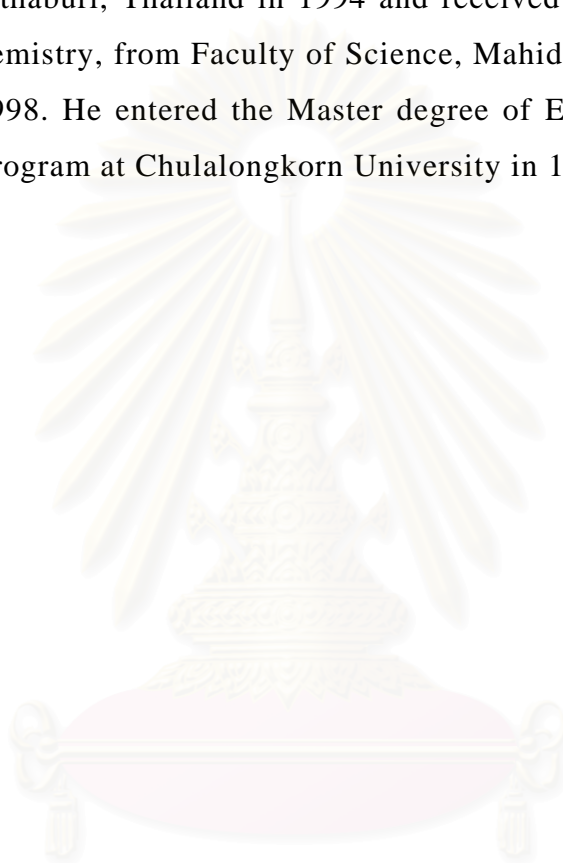


ν	$t_{.975}$	$t_{.950}$	$t_{.925}$	$t_{.900}$	$t_{.875}$	$t_{.850}$	$t_{.825}$
1	3.078	6.314	12.706	31.821	63.657	318.31	636.62
2	1.886	2.920	4.303	6.965	9.925	22.326	31.599
3	1.638	2.353	3.182	4.541	5.841	10.213	12.924
4	1.533	2.132	2.776	3.747	4.604	7.173	8.610
5	1.476	2.015	2.571	3.365	4.032	5.893	6.869
6	1.440	1.943	2.447	3.143	3.707	5.208	5.959
7	1.415	1.895	2.365	2.998	3.499	4.785	5.408
8	1.397	1.860	2.306	2.896	3.355	4.501	5.041
9	1.383	1.833	2.262	2.821	3.250	4.297	4.781
10	1.372	1.812	2.228	2.764	3.169	4.144	4.587
11	1.363	1.796	2.201	2.718	3.106	4.025	4.437
12	1.356	1.782	2.179	2.681	3.055	3.930	4.318
13	1.350	1.771	2.160	2.650	3.012	3.852	4.221
14	1.345	1.761	2.145	2.624	2.977	3.787	4.140
15	1.341	1.753	2.131	2.602	2.947	3.733	4.073
16	1.337	1.746	2.120	2.583	2.921	3.686	4.015
17	1.333	1.740	2.110	2.567	2.898	3.646	3.965
18	1.330	1.734	2.101	2.552	2.878	3.610	3.922
19	1.328	1.729	2.093	2.539	2.861	3.579	3.883
20	1.325	1.725	2.086	2.528	2.845	3.552	3.850
21	1.323	1.721	2.080	2.518	2.831	3.527	3.819
22	1.321	1.717	2.074	2.508	2.819	3.505	3.792
23	1.319	1.714	2.069	2.500	2.807	3.485	3.767
24	1.318	1.711	2.064	2.492	2.797	3.467	3.745
25	1.316	1.708	2.060	2.485	2.787	3.450	3.725
26	1.315	1.706	2.056	2.479	2.779	3.435	3.707
27	1.314	1.703	2.052	2.473	2.771	3.421	3.690
28	1.313	1.701	2.048	2.467	2.763	3.408	3.674
29	1.311	1.699	2.045	2.462	2.756	3.396	3.659
30	1.310	1.697	2.042	2.457	2.750	3.385	3.646
40	1.303	1.684	2.021	2.423	2.704	3.307	3.551
60	1.296	1.671	2.000	2.390	2.660	3.232	3.460
120	1.289	1.658	1.980	2.358	2.617	3.160	3.373
∞	1.282	1.645	1.960	2.326	2.576	3.090	3.291

Figure C-1 Critical value for student's t. From Mendenhall, W. and Sincich, T., "A second Course in Statistics: Regression Analysis", 5th edition, Prentice-Hall International, New Jersey, 1996

CURRICULUM VITAE

Mister Songkroh Pasuknirant was born in Bangkok, Thailand in June 30, 1977. He finished high school from Suankularb Wittayalai Nonthaburi School at Nonthaburi, Thailand in 1994 and received the Bachelor degree of Science in Chemistry, from Faculty of Science, Mahidol University, Bangkok, Thailand in 1998. He entered the Master degree of Engineering in Chemical Engineering program at Chulalongkorn University in 1999.



สถาบันวิทยบริการ
จุฬาลงกรณ์มหาวิทยาลัย